NASA/CR—2003-212525

Ultra-High Bypass Engine Aeroacoustic Study

Philip R. Gliebe and Bangalore A. Janardan
GE Aircraft Engines, Cincinnati, Ohio

October 2003

The NASA STI Program Office . . . in Profile

Since its founding, NASA has been dedicated to the advancement of aeronautics and space science. The NASA Scientific and Technical Information (STI) Program Office plays a key part in helping NASA maintain this important role.

The NASA STI Program Office is operated by Langley Research Center, the Lead Center for NASA's scientific and technical information. The NASA STI Program Office provides access to the NASA STI Database, the largest collection of aeronautical and space science STI in the world. The Program Office is also NASA's institutional mechanism for disseminating the results of its research and development activities. These results are published by NASA in the NASA STI Report Series, which includes the following report types:

- TECHNICAL PUBLICATION. Reports of completed research or a major significant phase of research that present the results of NASA programs and include extensive data or theoretical analysis. Includes compilations of significant scientific and technical data and information deemed to be of continuing reference value. NASA's counterpart of peer-reviewed formal professional papers but has less stringent limitations on manuscript length and extent of graphic presentations.

- TECHNICAL MEMORANDUM. Scientific and technical findings that are preliminary or of specialized interest, e.g., quick release reports, working papers, and bibliographies that contain minimal annotation. Does not contain extensive analysis.

- CONTRACTOR REPORT. Scientific and technical findings by NASA-sponsored contractors and grantees.

- CONFERENCE PUBLICATION. Collected papers from scientific and technical conferences, symposia, seminars, or other meetings sponsored or cosponsored by NASA.

- SPECIAL PUBLICATION. Scientific, technical, or historical information from NASA programs, projects, and missions, often concerned with subjects having substantial public interest.

- TECHNICAL TRANSLATION. English-language translations of foreign scientific and technical material pertinent to NASA's mission.

Specialized services that complement the STI Program Office's diverse offerings include creating custom thesauri, building customized databases, organizing and publishing research results . . . even providing videos.

For more information about the NASA STI Program Office, see the following:

- Access the NASA STI Program Home Page at ***http://www.sti.nasa.gov***

- E-mail your question via the Internet to help@sti.nasa.gov

- Fax your question to the NASA Access Help Desk at 301–621–0134

- Telephone the NASA Access Help Desk at 301–621–0390

- Write to:
  NASA Access Help Desk
  NASA Center for AeroSpace Information
  7121 Standard Drive
  Hanover, MD 21076

NASA/CR—2003-212525

Ultra-High Bypass Engine Aeroacoustic Study

Philip R. Gliebe and Bangalore A. Janardan
GE Aircraft Engines, Cincinnati, Ohio

Prepared under Contract NAS3–25269, Task Order 4

National Aeronautics and
Space Administration

Glenn Research Center

October 2003

Acknowledgments

The following people contributed substantially to the study reported herein. Christopher J. Smith provided integration of the cycle analysis, flowpath design, mission analysis, and carried out the DOC analyses. Paul Feig and Valerie McKay provided the mission analysis. Larry Dunbar and Michael Salay carried out the engine flowpath designs. Rick Donaldson, Mark Wagner, and Charlotte Salay provided the engine cycle analyses. Dr. Bangalore Janardan and George Kontos provided the engine system noise predictions.

Available from

NASA Center for Aerospace Information
7121 Standard Drive
Hanover, MD 21076

National Technical Information Service
5285 Port Royal Road
Springfield, VA 22100

Available electronically at http://gltrs.grc.nasa.gov

Preface

This report was delivered to NASA as an informal document. There were three engine noise studies done by the Allison Engine Company (now Rolls Royce), General Electric Aircraft Engines and Pratt & Whitney in preparation for the Advanced Subsonic Technology (AST) Noise Reduction Program. The objectives of the studies were to identify engine noise reduction technologies to help prioritize the research that was subsequently done by the AST Program. The reports also summarize the predicted performance and economic impact of the noise reduction technologies.

The emphasis of commercial turbofan research during the early 1990's was on higher bypass ratio engines. While the technology insertion into service has been slower than expected, many of the results from these studies will remain valid for a long period of time and should not be forgotten by the aerospace community. In 2003, NASA decided to publish all three studies as Contractor Reports to provide references for future work. The quality of the reproduction of the original report may be poor in some sections.

Dennis L. Huff
Chief, Acoustics Branch
NASA Glenn Research Center

ULTRA-HIGH BYPASS ENGINE AEROACOUSTIC STUDY

Final Report Prepared for

National Aeronautics and Space Administration
Lewis Research Center
Contract NAS3 25269
Task Order 4

by

Philip R. Gliebe
and
Bangalore A. Janardan

GE Aircraft Engines
Advanced Engineering Programs Department

July 8, 1993

ABSTRACT

A system study was carried out to identify potential advanced aircraft engine concepts and cycles which would be capable of achieving a 5 to 10 EPNdB reduction in community noise level relative to current FAR36 Stage 3 limits for a typical large-capacity commercial transport aircraft. The study was directed toward large twin-engine aircraft applications in the 400,000 to 500,000 pound take-off gross weight class.

Four single-rotation fan engine designs were evaluated, over a range of fan pressure ratios from 1.3 to 1.75. An advanced core design technology was assumed, compatible with what can probably be demonstrated by year 2005, in terms of overall cycle pressure ratio and turbine inlet temperature. In addition, two counter-rotating (CR) fan engine configurations were studied. One of these employed a front-drive, geared fan, and the other was configured with an aft-mounted, turbine-driven (direct-drive) fan, similar in concept to the GEAE-developed UDF Engine. Utilizing GEAE design methods, models and computer codes, the engine performance, weight, manufacturing cost, maintenance cost, direct operating cost (DOC) and community noise levels were estimated for these advanced, ultra-high bypass engine designs.

The results obtained from this study suggest that significant noise level reductions can potentially be achieved by designing an engine with a fan pressure ratio of 1.5 or less. Selecting fan pressure ratio significantly less than 1.5, however, while yielding greater sideline noise reductions, provides only small noise reductions at reduced power (cutback and approach), while adding significantly to the weight and DOC of the system. Significant noise reductions were also forecast for the counter-rotating fan engines. The front-drive, gear-driven CR fan engine, designed for a fan pressure ratio of 1.3, had significant weight and D.O.C. penalties relative to the single-rotation (SR) fan counterpart, although the noise levels were 1 to 2 EPNdB lower. The rear-drive, turbine-driven CR fan, however, was forecast

to have lower DOC as well as lower noise levels relative to its single-rotation (1.6 fan pressure ratio) counterpart, with very small weight penalty.

In summary, several aircraft engine configurations were identified which, with further technology development, could achieve the objective of 5 to 10 EPNdB reduction relative to FAR36 Stage 3 community noise certification limits. Optimum design fan pressure ratio is concluded to be in the range of 1.4 to 1.55 for best noise reduction with acceptable weight and DOC penalties. Further in-depth studies in this pressure ratio range are recommended to define the best engine architecture in terms of single- vs. counter-rotation, geared vs. direct drive fan, and separate flow vs. mixed flow exhaust.

ULTRA-HIGH BYPASS ENGINE AEROACOUSTIC STUDY

INTRODUCTION

The projected growth of commercial aircraft operations suggests that air traffic and passenger-miles will increase significantly in the coming decades. Many airport operators and rule-making organizations feel that the current FAR36 Stage 3 community noise limits may not be sufficiently stringent to preclude significant community annoyance around airports. Several rule-tightening scenarios have been proposed, including reducing the current FAR36 Stage 3 limits by anywhere from 3 to as much as 10 EPNdB at each monitoring point.

Local airports have already imposed their own restrictions to implement noise abatement in surrounding communities. These include night-time curfews, night-time operating limits based on certificated noise levels, frequency-of-operation restrictions based on noise levels, and landing fees based on noise levels.

These local airport noise restrictions are usually more stringent than the FAR Stage 3 limits in terms of equivalent EPNL, although they may be based on other metrics such as dBA (Washington National Airport), SENEL (Orange County John Wayne Airport), and contour area (London Heathrow and Gatwick Airports). These local airport restrictions are typically 3 to 7 dB more stringent when cast in terms of equivalent FAR36 EPNL.

Given the current climate for increasing rule stringency and the projected growth in commercial air traffic, it is reasonable to expect that noise level limits will become significantly lower in the next 10 to 20 years. The current technology available to accomplish significant reductions in engine noise will impose serious performance and/or weight penalties to the engine/aircraft system, since all of the known practical methods for reducing engine noise have been incorporated in modern high bypass engine designs, at least to the extent possible within the guidelines of practicality and economic viability.

Engine configurations being considered for future large civil transport aircraft include so-called Ultra-High Bypass (UHB) engine cycles, with bypass ratios exceeding 10 to 15:1. The advantage of a UHB cycle is the significant improvement in propulsive efficiency and corresponding specific fuel consumption that can potentially be attained. A significant factor in assessing the potential benefit of a UHB engine is the achievable core technology that can be incorporated, specifically the overall pressure ratio (OPR), the compressor exit temperature (T3) and the turbine inlet temperature (T41).

An important factor in the selection of a new engine cycle and architecture is the noise reduction potential, and how much of any identified noise goal needs to be achieved by advances in noise reduction and suppression technology vs. the "natural" noise reduction which might be achieved from the proper cycle selection. A proper study is therefore required to assess the potential improvements in engine performance, weight, cost, complexity, mission

economics and environmental emissions, including noise. The focus of the present study was to address noise reduction, but to provide realistic engine concept architectures with reasonable performance and economic assessments, so that potential low-noise engine concepts could be identified that hold promise.

OBJECTIVES

The major objective of the present study was to identify candidate Ultra-High Bypass (UHB) engine concepts which provide the best noise reduction opportunities with the least economic penalties. A second objective was to quantify the effect of bypass ratio (BPR) selection on the acoustics and economics of advanced UHB engine concepts. A final objective was to identify the noise reduction technology improvements required for the best of the configurations studied, and recommend a follow-up study and experimental development program.

The community noise goal selected for assessing the relative merits of the study engines was that the community noise levels should be at least 5 to 10 EPNdB lower than the current FAR36 Stage 3 limits.

SCOPE OF STUDY

The present study focused on a large twin-engine civil aircraft application, with a 3000 nautical mile mission range and a 250 to 300 passenger capacity, similar to the current Boeing B767-300 and Airbus A300-600 aircraft in service today. Several advanced engine cycle concepts were selected for evaluation. Four single rotation fan engine designs were selected, with design fan pressure ratios (FPR) of 1.3, 1.45, 1.6 and 1.75. These engines were assumed to all have the same core technology, i.e., they all had the same overall pressure ratio, compressor exit temperature and high-pressure turbine inlet temperature design points.
Two counter-rotating fan configurations were also studied. The first was a front-mounted, gear-driven CR fan with a design fan pressure ratio of 1.3. This engine concept is a Counter-rotating alternative to the 1.3 FPR single-rotation fan. A second CR fan engine was evaluated which had an aft-mounted, direct, CR turbine-driven fan, similar in concept to the GEAE-developed Unducted fan engine or UDF. It was configured with a design fan pressure ratio of 1.6, and served as the CR alternative to the 1.6 FPR single-rotation fan engine.

For these six engines, a preliminary design analysis was carried out, consisting of the following steps:

1. Cycle and Engine Architecture Selection
2. Engine Flowpath Design
3. Engine Cycle Performance Mapping
4. Engine/Aircraft Mission Analysis

5. Community Noise Analysis

6. Noise Reduction Feature Assessment

Step 6 consisted of, for each of the basic advanced engines studied, identifying design changes which would reduce the noise, and then evaluating the performance, weight, and economic impact of these changes and the resulting noise reduction benefit. For all engines studied, the aircraft was assumed fixed in size and weight, and no advanced aircraft performance improvements were assumed.

The baseline selected for referencing all performance, weight, economic and noise benefits was an updated version of the Energy Efficient Engine (EEE) developed by GEAE under NASA contract in the early 1980's, reference 1. This engine, considered to be a current technology state-of-the-art demonstrated design, was also used as a reference baseline for advanced concept engine studies reported in reference 2.

TECHNOLOGY LEVEL ASSUMPTIONS

The guideline for establishing technology levels for this study was to select what could potentially be available for year 2005 entry into service. Based on GEAE experience and expertise, the following engine technology level assumptions were made:

- Compressor Exit Temperature (T3) - 1390 deg.F
- HP Turbine Inlet Temperature (T41) - 2800 deg.F
- Maximum Overall Pressure Ratio (OPR) - 55:1
  - High Pressure Compressor (HPC) - 27:1
  - Fan + Booster (LPC) - 2.04:1
- Component efficiencies - based on a 5 percent reduction in losses relative to current technology.

As mentioned in the previous section, current state-of-the-art aircraft performance was assumed.

ENGINE CYCLE SELECTION PHILOSOPHY

As discussed in the introduction, it was the intent of this study to evaluate the effect of increasing bypass ratio on community noise. From the standpoint of engine cycle selection, for a given thrust requirement, the bypass ratio is a product of the fan pressure ratio selected and the core technology level (OPR and T41) assumed. Also, from a noise reduction point-of-view, the exhaust jet mixing noise, a primary contributor at full power for current high bypass engines, is dictated to a great extent by the fan pressure ratio. The FPR selected sets the fan jet exhaust velocity, which in turn sets the jet exhaust noise level, since jet noise is roughly proportional to the sixth power of the jet velocity for a given thrust.

Fan pressure ratio was therefore selected as the major independent variable to be studied, and the bypass ratio was considered as a computed result based on the core technology assumed and the thrust requirement. FPR was varied from 1.75, typical of current high bypass engines (but now with an advanced core), down to 1.3. FPR values less than 1.3 were felt to be impractical in that the resulting fan and nacelle size would not be compatible with an under-the-wing installation on a typical B767/A300 type aircraft. The study resources limited the number of FPR values to four cycles: 1.3, 1.45 ,1.6, and 1.75.

From previous preliminary design studies (reference 2, for example), it was concluded that the imcompatibility between fan and Low Pressure Turbine (LPT) speed for achieving good component efficiencies and low number of LPT stages as FPR is reduced implies that a geared fan should be used for FPR values significantly less than about 1.5. The FPR=1.45 and 1.3 engine cycle architectures were therefore designed as gear-driven fan engines.

A mixed flow exhaust system architecture was assumed for all study engines with FPR of 1.45 and higher. It was felt that this would result in better Specific Fuel Consumption (SFC), and lower noise. Separate Flow exhaust system architecture was assumed for the FPR = 1.3 engines, because it was felt that the large nacelle size required at this low fan pressure ratio would make a mixed flow system much too heavy and yield high nacelle drag because of the much larger wetted area.

It was of interest to evaluate whether a counter-rotating fan offered a noise reduction advantage relative to a single-rotation fan. Conceptually, having two rotors produce the same total FPR as one rotor would allow the two rotors to run at lower tip speeds, and therefore potentially produce less total noise than one rotor producing the same FPR at a significantly higher tip speed.

For low FPR, a gear-driven CR fan seemed the best approach. For reasons to be discussed later, the use of a gearbox for counter-rotation imposed severe restrictions on the speed ratio, torque ratio and fan exit swirl, and the maximum reasonable FPR that gave a sensible engine was found to be 1.3. A 1.3 FPR engine with a CR gear-driven fan was therefore selected for evaluation.

A direct-drive CR fan was also evaluated. To avoid having to fit two fan shafts through the middle of a two-spool core, with all the conflicting requirements for bearings, shaft sizes, and core flow path constraints, a rear-mounted fan was selected. A higher FPR of 1.6 was selected, to take advantage of the reduced tip speed requirement at higher FPR, and potentially provide a quieter engine at a smaller fan diameter. This engine is similar in concept to the GEAE-developed UDF engine, as discussed in reference 3, but with a ducted CR fan and much lower bypass ratio.

Table 1 lists the primary cycle and geometry parameters for the engine configurations selected for study. The selection in some cases involved some iterations to arrive at an engine cycle and engine architecture that was reasonable, in the sense that there were no known barrier problems that needed to be overcome to make the engine viable. Table 2 summarizes the component efficiencies that were assumed for each configuration.

It should be understood that the decisions for which engines should be gear-driven vs. direct drive and which engines should be mixed flow vs. separate flow were based on prior experience with preliminary design study

results, and probably need verification if a final engine design concept were to be pursued. A thorough design optimization study would be required to more carefully weigh the trades between performance, noise, weight, cost, complexity, maintainability and customer acceptance, before deciding on the fan drive and exhaust system architecture.

FLOW PATH DESIGN SUMMARY

SINGLE-ROTATION FAN ENGINE DESIGNS:

The advanced engine preliminary designs were generated using a GEAE computer code called **FLOWPATH**. This code utilizes GEAE modelling experience for component aerodynamic performance, mechanical design, and manufacturing (material selection, costs, etc.). For a given cycle, the code **FLOWPATH** will define an entire engine, using appropriate mission requirement data for each component. The engine overall and component dimensions are estimated, and all part weights are determined, including blade and vane airfoils, disks, frame structures, bearings, seals, shafts, and controls and accessories. A typical subsonic mission engine **FLOWPATH** output is shown in figure 1.

The advanced engine designs selected for study were generated using the **FLOWPATH** code. Figure 2 shows the **FLOWPATH** generated engine cross-section for the baseline updated EEE engine. This engine, described in references 1 and 2, serves as the reference for the performance, noise, weight and D.O.C. assessments for the advanced engines. In its original form (reference 1), it was built and tested, and GEAE has evaluated its performance and noise characteristics.

The engine **FLOWPATH** cross-sections for the two direct-drive single-rotation engines, Engine 1 (FPR=1.75) and Engine 2 (FPR=1.6), are shown in figure 3. The **FLOWPATH** cross-sections for the two gear-driven single-rotation engines, Engine 3 (FPR=1.45) and Engine 4 (FPR=1.3), are shown in figure 4. Note that Engines 1, 2, and 3 all have mixed-flow exhaust systems. It is also noteworthy that the HP compressor has fewer stages (8 vs. 10) for the geared engines, and one HP turbine stage for the geared engines vs. two for the direct-drive engines. The gear-driven fan engines are therefore shorter from fan rotor exit to turbine rear frame exit. These single-rotation fan engines are sometimes labelled as S75, S60, S45, and S30 for Engines 1, 2, 3, and 4, respectively.

It can be seen from figures 3 and 4 that all of the advanced study engines employ an integral vane/frame outlet guide vane (OGV) design for the fan. This provides a larger axial spacing between the fan rotor and the OGV, which helps keep the fan interaction-generated tone noise lower than would be the case with a separate OGV row in front of the fan frame struts.

FRONT-MOUNTED COUNTER-ROTATION FAN DESIGNS:

As discussed in the previous section on Engine Cycle Selection, two counter-rotation fan engine designs were studied. The front mounted, gear-driven fan engine was designed for a fan pressure ratio of 1.3. This was found to be the about the highest fan pressure ratio that would still result in a reasonable engine configuration.

For a very high bypass ratio engine, the bore size of the core engine becomes quite small, and there is insufficient room for two counter-rotating shafts for driving the fans directly by an LP counter-rotating turbine. Thus, a single shaft LP turbine was selected with a gearbox to drive the two counter-rotating fan rotors. A planetary gearbox design was studied, and the gearbox constraints dictated the selection of the fan pressure ratio.

The first constraint to be addressed is that of keeping the rotor inlet relative Mach number at or below unity. This is desirable from the standpoint of mimimizing noise. As long as the fan pressure ratio is low enough, this constraint is easily satisfied on the front fan rotor. Because of the swirl added by the first rotor and the counter-rotating wheel speed of the second rotor, the second rotor will have a higher relative Mach number than the first, especially at the hub. The selection then involves an iterative process of choosing an overall fan pressure ratio, selecting the forward/aft rotor pressure ratio split and evaluating the implied rotor tip speeds, torque ratios, and inlet relative Mach numbers. Figure 5 shows a typical design curve used for selecting fan tip speeds as a function of fan pressure ratio.

A second constraint involved keeping the second rotor exit swirl as small as possible, in order to reap the "inherent advantage" of Counter-rotation that no OGV row is needed. This constraint implies keeping the rotor torque ratio as close to unity as possible. This also helps keep the number of planet gears required to a minimum. Figure 6 shows the design trends for dependency of exit swirl and number of planet gears on fan (front-to-rear) torque ratio. However, for a CR output shaft, having torque ratio close to unity requires a much higher gear ratio, so that, for a given fan speed, the LP turbine must run at a much higher speed. Figure 7 shows the required gear ratio as a function of torque ratio.

An additional constraint to consider is that of LP turbine exit flow area and speed combined. Figure 8 shows the turbine exit flow area required as a function of fan pressure ratio. Higher Bypass ratios require greater LP turbine expansion and greater exit area to pass the flow. The parameter combination AN2 or (Exit Area)*(RPM-squared) is a measure of the LP turbine last stage blade root stress. Design limits on this parameter therefore add a constraint to the selection of fan pressure ratio and torque ratio, as shown in figure 9. A limit on "AN2" of 45 was selected as being as high as possible without significantly exceeding best available technology and experience.

The trends shown in figures 5 through 9 were employed to arrive at a fan overall pressure ratio of 1.3, a speed ratio of 0.8 (aft/forward), and a torque ratio of 1.5. This kept the exit swirl down to 7 or 8 degrees, the number of planet gears down to eight, and the gear ratio down to about 5:1. A separate flow exhaust system was also selected for this engine, because the bypass ratio was high enough (BPR=15.75) that a mixed flow system would offer no significant performance advantage. Also, the mixed flow benefit on jet noise would be very small, and, as will be discussed later, the jet noise contribution itself is small at any rate for this engine cycle.

Figure 10 shows the resulting engine cross-sections as generated by the **FLOWPATH** program for the front-mounted, gear-driven, counter-rotating fan engine. Four versions are shown in figure 10, corresponding to four different

combinations of fan blade numbers and rotor-to-rotor axial spacings. These four variants were selected to evaluate the influence of blade number selection and axial spacing on community noise, and to determine the economic sensitivities to these changes. This engine configuration is referred to as engine 5, and the four variants are labelled 5A, 5B, 5C, and 5D, as summarized in table 3. This engine is also sometimes referred to as CF30.

Engine 5B is the baseline from which the other variants (5A, 5C, and 5D) were selected. Figure 10a shows a comparison of Engine 5A (top) with the baseline 5B (bottom). The difference is the increase in forward-to-aft rotor axial spacing-to-chord ratio from 1.2 (5B) to 2.5 (5A). The advantage of 5A over 5B was expected to be a reduction in interaction noise, but at the expense of engine length and weight.

Figure 10b shows a comparision of Engine 5C (top) with 5B (bottom). The difference is the change in rotor blade numbers from 19 forward rotor blades and 15 aft rotor blades (5B) to 15 forward rotor blades and 19 aft rotor blades (5C). The intent of this variant was to produce negative-spinning interaction modes, which would have greater transmission loss through the forward rotor, thus reducing the forward-radiated interaction tone levels. In addition, the number of frame vane/struts was increased from 36 to 46, in order to preserve cut-off of the aft rotor BPF (blade-passing frequency) tone produced by aft rotor wake-strut interactions.

Figure 10c shows a comparision of Engine 5D (top) with 5B (bottom). This Engine is a variant of Engine 5C with the rotor-to-rotor axial spacing increased from 1.2 to 2.5 projected chords. This engine is the longest and heaviest of the four.

Aft-Mounted Counter-Rotating Fan Design:

The final Engine configuration studied is an aft-mounted, counter-rotating fan engine design. The **FLOWPATH**-generated engine cross-section is shown in figure 11. This configuration is similar in concept to the Unducted Fan Engine, reference 3, which has a two-spool gas generator core which drives a free-wheeling, counter-rotating turbine, which in turn powers the two, counter-rotating fan stages. In selecting the cycle for this engine concept, gearbox constraints were not a consideration, and the fan shafts do not have to pass through the core. It was therefore decided to take advantage of the two fan stages and select a fan pressure ratio which was reasonably high, so as to provide a compact engine, but not so high as to produce high jet noise. A fan <u>total</u> pressure ratio of 1.6 was selected as being comparable to Engine S60, its single-rotation counterpart, and potentially would have a propulsive efficiency and noise advantage as well.

The fan nacelle designed for this engine, as shown in figure 11, requires support struts both forward of and behind the fan. The forward struts potentially could shed wakes into the fan rotors, producing additional noise, so a large axial spacing of 3 strut chords was selected to minimize this effect. Further, the forward strut and first rotor blade numbers were selected to provide a high spinning mode number (28 - 4 = 24) so that the nacelle treatment between the struts and rotor would have better attenuation

performance. In addition, the rotor-to-rotor axial spacing criterion of 2.5 forward rotor projected chords was easily accommodated because the forward-to-aft fan power frame spacing was also needed to fit in the required number of turbine rotor stages.

Engine Weight and Cost Estimates:

Engine weight and cost estimates were made for all of the engine configurations described in the above paragraphs, using the **FLOWPATH** code. Figure 12 summarizes the engine-plus-nacelle weights, manufacturing costs, and maintenance costs for the four single-rotation and two counter-rotation fan engines, in terms of percent changes from the baseline EEE values. The component contributions of the fan, booster, HP compressor, HP turbine, and LP turbine systems to the total changes in engine weight, manufacturing cost, and maintenance cost are shown in figures 13, 14, and 15, respectively.

The front-driven, counter-rotating fan engine had four variants, as shown in figures 10a-c. The corresponding variations in weight, manufacturing cost, and maintenance cost are shown in figure 16. In general, the significant discriminator is the axial spacing difference, as shown by the fact that engines 5A and 5D have similar weights and costs, and engines 5B and 5C have similar weights and costs, with engines 5B and 5C being slightly lighter and cheaper.

For each of the engine cross-sections shown in figures 3 and 4, axial spacing and inlet length were evaluated from an acoustic design viewpoint. The axial spacings and inlet lengths were then modified, if necessary, to provide acoustically prudent axial spacing/chord ratios of 2.6 or greater and inlet treatment effective length/diameter ratios of 0.35. An example of the engine cross-section changes is shown in figure 17, for Engine 3, the S45 configuration. The first-iteration cross-section is shown at the bottom of the figure, labeled "Aero", and the modified cross-section, reflecting the above spacing and inlet length criteria, is shown at the top of the figure, labeled "Acoustic". The corresponding impacts on weight and cost are shown in figure 18 for S45 or Engine 3. It can be seen from figure 17 that the additional axial spacing incorporated between the fan rotor and OGV adds considerable "empty" space to the engine between the booster compressor exit and the fan frame.

ENGINE/AIRCRAFT SYSTEM PERFORMANCE AND COST COMPARISIONS

A mission analysis was carried out for all of the engine configurations described in the previous section. A reference mission was selected, which consisted of a 3000 nautical-mile range mission for a medium-size twin engine aircraft with 407,000 lb Maximum takeoff gross weight (MTOGW) carrying 210 passengers. The aircraft geometry was fixed, i.e., it was not adjusted in size to reflect differences in fuel burn among the engines studied. Typical current-technology aircraft performance characteristics were used in the mission analysis. The engines were sized to provide the same takeoff (M=0.25/Sea-Level) and top-of-climb thrusts (M=0.85/35000 ft.). The mission profile is illustrated in figure 19.

In order to account for the influence of fan pressure ratio and subsequent fan/nacelle diameter changes on aircraft performance, the landing gear length was adjusted to accommodate increasing nacelle diameter, using the guideline that nacelle/wing channel height is kept constant, so that interference drag is minimized. Also, nacelle-to-ground clearance was maintained constant, to prevent contact in the event of nose-wheel collapse. Since the nacelle/pylon drag is a function of wetted surface area of the nacelle and pylon relative to the wing area, adjustments were made to these drag components based on airframe manufacturers recommended procedures for estimating the change of profile drag with change in wetted area/wing area. The resulting nacelle-plus-pylon (strut) wetted areas for the various engine configurations studied are shown in figure 20.

The primary objective of the mission analysis for this study was to evaluate the fuel burn and the Direct Operating Cost (DOC) for each of the advanced engines, in order to provide an approximate assessment of the economic performance of each engine. Results were evaluated in terms of changes from the baseline (modified Energy-Efficient Engine) values, as the methods used are better at forecasting trends than forecasting absolute levels.

The trends for fuel burn are shown in figure 21, for the six advanced engines studied. Percent change in mission fuel burn, the reference value being for the baseline EEE, is plotted vs. Fan Pressure Ratio (FPR). The trend for the single-rotation fans is that fuel burn decreases as fan pressure ratio decreases (note that the pressure ratio scale decrease from left to right). The front-drive CR fan has about 2 percent higher fuel burn than its SR counterpart, while the rear-drive CR fan is about 1.6 percent lower in fuel burn than its SR counterpart. In fact, the rear-drive CR fan engine (CR60 or engine no. 6) has the lowest fuel burn of any of the advanced engines studied. The results shown in figure 21 can be related directly to the changes in engine weight (figure 12), cruise Specific Fuel Consumption (SFC), and Nacelle-plus-pylon drag (figure 22).

An approximate estimate of the relative changes in DOC are shown in figure 23, for an assumed fuel price of $1.00 per gallon. These estimates take into account the manufacturing cost, the maintenance costs, and mission fuel burn (figure 21). For the purposes of estimating the engine-to-engine changes in DOC, the estimated maintenance costs employ the assumption that the high pressure components (HP compressor, combustor, HP turbine) have approximately the same maintenance costs for all the engines studied, so that the differences are those due to differences in LP system maintenance costs (fan, LP turbine, booster compressor, nacelle, etc.). **The predicted changes in HP system maintenance costs shown in figure 15 were not used in the DOC estimates, the** rationale being that any HP system introduced into service would be developed to provide the same or better reliability and maintenance costs as today's engines.

It can be seen from figure 23 that most all of the advanced engine concepts studied offer a substantial improvement in DOC over the baseline EEE configuration, on the order of 4 to 5 percent improvement. The exceptions are the front-drive, counter-rotating fan configurations, 5A, 5B, 5C, and 5D, which offer only about 1.5 to 2.0 percent improvement. Apparently the SFC advantage of these configurations is off-set by the significant increase in weight, nacelle size and attendant manufacturing and maintenance costs.

It is also surprising that the rear-drive, counter-rotating fan configuration engine 6, is the best from the DOC standpoint, even though it is a much more complicated configuration than engines 1 and 2, and perhaps even engines 3 and 4. This result apparently stems from this configuration having a substantially lower nacelle drag, and hence the lowest fuel burn, due to its much smaller nacelle size, which can be seen from comparing figure 11 with figures 3 and 4. This fuel burn advantage off-sets the higher maintenance costs, and the manufacturing cost is estimated to be comparable to the direct-drive single-rotation fan engines.

Finally, the impact of adding inlet treatment length and fan rotor-to-stator axial spacing to conform to current acoustic design practice was estimated, and these results are summarized in figure 24. These results in general show a small fuel burn and performance penalty, less than 0.5 percent in most cases. Hence it can be argued that any new technology approach to noise reduction being contemplated must not impose more than a 0.5 percent penalty on the system fuel burn or DOC, or it may not be worth the cost of the time and resources required for development. This, of course, depends upon the noise reductions achieved, which must be weighed against the penalties. This is discussed further in the next section on noise analysis trends.

COMMUNITY NOISE PREDICTION RESULTS

Noise Estimation Procedure:

Community noise predictions were made for the baseline and advanced study engine configurations described in the previous sections using a GEAE estimation system called **FAST**, **F**lyover **A**coustic **S**ysthesis **T**echnique. This system consists of a suite of computer programs which synthesize total flyover noise characteristics by superimposing individual component noise spectra (fan inlet, fan exhaust, turbine, combustor/core, jet, airframe, etc.), adjusting for flight conditions and aircraft motion effects on each component. The component noise spectra can be computed from built-in empirical correlation methods, or scaled from an existing component database.

For the present study, a database decomposition and synthesis approach was employed, using EEE prototype engine acoustic test results (reference 1). The engine test data was decomposed into jet, fan inlet and fan exhaust components, and this component database was then used to estimate the target engine component noise levels at each flight condition. GEAE standardized data scaling and adjustment procedures, part of the **FAST** system, were employed to correct the database component noise levels for differences in cycle conditions, tip speeds, blade numbers, axial spacings, etc., between the database conditions and the target engine geometry and conditions.

A schematic of the database decomposition process is shown in figure 25. An empirical jet noise prediction model is used to assist in subtracting the jet mixing noise from the measured engine noise spectrum, by basically "fitting" the predicted spectrum to the measured data. Once the jet mixing noise portion of the spectrum has been extracted, the remaining spectrum is further decomposed into forward-radiated and aft-radiated noise turbomachinery

spectra, using least-squares curve-fitting techniques for the directivity patterns at each frequency. Since most of the resulting inlet and exhaust turbomachinery noise is produced by the fan, it is called fan noise. The component data is then edited for LP compressor tones and LP turbine tones.

For the advanced study engines, a cut-off LP turbine and compressor design was assumed, so no component noise estimates for these components were included in the system noise predictions. Core or combustor noise was computed using an existing GEAE empirical model which is built into the **FAST** system. Jet mixing noise, fan inlet noise, and fan exhaust noise component spectra were all estimated from the EEE database decomposition (figure 25). As discussed above, The database point used in the estimate is selected based on the key cycle parameters which most closely match the target engine condition. Parameters considered include jet exhaust velocity, fan pressure ratio, and fan tip speed.

The fan inlet and fan exhaust spectra are corrected to the target engine conditions based on the differences in airflow, tip speed, and pressure ratio. Corrections are also made for differences in blade and vane numbers and rotor-stator axial spacing relative to rotor projected (axial) chord. The procedure has the option to correct the database spectra for the differences in broadband noise due to differences in fan rotor incidence angle, using correlations similar to those described in reference 4. This option was not used for this study, because it was felt that any significant incidence angle differences would imply a new blade shape, so that the blades would run at similar incidence angles. However, it is possible that low pressure ratio fans may exhibit a significantly different change in rotor incidence angle in going from high power to approach power, compared to the change exhibited by the database (EEE) engine. This was neglected in this study, but should be considered as a possible refinement for any follow-on studies.

The EEE database used for estimating the advanced engine noise had acoustic treatment in the inlet and fan duct. The fan noise suppression due to the treatment was assumed preserved in the advanced study engines. No attempt was made to change the suppression characteristics based on differences on treatment length, depth, characteristic frequency, treatment surface area, flow area,etc.; i.e., the treatment suppression (delta dB) inherent in the data base was maintained. A possible refinement of this study for the future would be to extract the treatment suppression from the data base and adjust the suppression spectra to acount for differences between the data base geometry and tuning frequency and the target engine geometry and tuning frequency, and then recombine the treatment suppression spectra with the hardwall target engine spectra.

The EEE database used for this study was acquired from engine ground static tests that did not have an inflow control device (ICD). Hence the fan inlet component was contaminated to some extent by ground/test-stand-generated inflow turbulence and distortion-induced noise. This contamination manifests itself primarily as a blade-passing frequency phenomenon. Both enhanced waveform-averaging techniques and empirical corrections (developed from tests of other engines with and without an ICD) were used to estimate the

corrections to be applied to achieve "clean" inflow conditions experienced in flight. Both of these approaches gave similar corrections, within a fraction of a decibel. These corrections were applied to the component database spectra before scaling to the target engine conditions.

The EEE fan has a cut-on vane/blade ratio (34 vanes and 32 blades), and the advanced engine configurations were designed for cut-off V/B ratio. Hence there is some realism lost in simulation of the fan tone harmonic spectral content and directivity. However, correlations of EEE data (normalized for thrust, size, airflow, etc.) against CF6 and CFM56 engine data showed similar Perceived Noise Level (PNL) trends, so it was concluded that the EEE fan noise levels were not untypical of modern high bypass engine levels. No adjustments were made for this cut-on vs. cut-off design difference. However, this could be pursued in further follow-on studies.

Finally, all baseline EEE and advanced study engine Effective Perceived Noise Level (EPNL) predictions were adjusted based on calibrations of the FAST methodology with actual certification data from various GEAE CF6-80C2-powered aircraft applications. It was felt important to do this because a primary goal of this study is identification of engine architectures potentially capable of achieving noise levels 5 to 10 EPNdB below current FAR36 Stage 3 limits. This is an absolute prediction level goal, and therefore the predicted levels must be as realistic as possible, and relative changes only are not sufficient.

Noise Level Results - Single-Rotation Fan Engines:

Community noise predictions were made for all of the study engines listed in table 1. For the single-rotation engines, the procedure was a straightforward application of the process described in the previous subsection. The noise levels, in terms of EPNL, were estimated for sideline or lateral conditions, takeoff or community conditions, and approach or landing conditions. Both full-power takeoff and takeoff with cutback noise levels were estimated for all engines in table 1. The fan tip speeds and fan pressure ratios at each community noise point for each engine configuration are listed in table 4. For reference, the fan blade and vane numbers for each engine are also listed in table 5. Aircraft flight conditions used for these estimates correspond to a typical large twin-engine aircraft in the 400,000 lb takeoff gross weight class. These flight conditions, including cutback altitudes, were maintained constant for all engine configurations. Therefore the estimates do not include any effects of changing aircraft weight or thrust requirements due to differences in required fuel load for the 3000 nautical mile mission.

A summary of the predicted EPNL values for the single-rotation engine configurations (Engines 1-4) are shown in figure 26, along with the baseline EEE predictions, for comparison. The striking trend to be noted is that the sideline and full-power takeoff levels drop dramatically from Engine 1 (FPR=1.75) to Engine 4 (FPR=1.3). It is also noted that the approach noise levels are nearly the same for all the engine types, within 1 or 2 EPNdB.

The component contributions of the combustor, jet, fan inlet and fan exhaust noise to the EPNL values are shown in figures 27 through 30. The nomenclature for these and subsequent figures is as follows:

AFN	Airframe noise component level
COM	Combustor noise component level
FEX	Fan exhaust noise component level
FIN	Fan inlet noise component level
JET	Jet exhaust noise component level (either CNJ or SFJ)
CNJ	Conical nozzle (mixed flow) jet noise component level
SFJ	Separate flow jet noise component level

These figures show that the combustor/core noise varies monotonically with fan pressure ratio, reflecting the progressively smaller core mass flow and larger LP turbine pressure and temperature drop as fan pressure ratio is decreased or bypass ratio is increased. The jet noise also drops monotonically with decreasing fan pressure ratio, reflecting the corresponding drop in jet exhaust velocities in both fan and core streams. However, at the approach power setting, the differences in jet noise are small, but are still well below the total system levels.

Figure 29 shows that the fan exhaust noise decreases substantially with decreasing fan pressure ratio at sideline and takeoff, but also becomes relatively insensitive to fan pressure ratio at approach power. Figure 30 shows that the fan inlet noise is not very sensitive to decreasing fan pressure ratio at any power setting except approach. Note also that the fan inlet (FIN) and fan exhaust (FEX) components become the dominant engine noise source components at approach power. Evidently the intuitively-expected drop in fan noise as fan tip speed and pressure ratio are reduced (at a given thrust) is, to a varying extent, offset by the noise increase due to increase in airflow attendant with maintaining constant thrust.

The relative contributions of each engine component to the total for each configuration are given in Appendix A for reference. Appendix A also shows the (Tone-corrected) Perceived Noise Level directivity patterns (but corrected to a constant 150 ft. radial distance) for each configuration, at sideline and approach conditions.

As discussed in the section on Mission Analysis, initial engine cross-section layouts were made which resulted in substantially smaller axial spacings than the baseline EEE fan value of 2.6 projected (axial) chords. The noise predictions discussed above were made using these smaller than desired axial spacings, the database levels having been adjusted to reflect smaller spacing to chord ratios. A follow-up calculation was then made to determine the effect on noise of increasing the axial spacing to the EEE baseline value of 2.6. The impact of axial spacing on fan inlet (FIN) and fan exhaust (FEX) contributions to EPNL are shown in figure 31. The impact on exhaust EPNL is seen to be much greater than on inlet EPNL.

Combining these results with the impact on System EPNL and economic parameters (figure 24), an approximate set of noise vs. weight, fuel burn, and DOC derivatives can be derived. This has been done is and summarized in Table 6, for the four single-rotation fan engine configurations.

Noise Level Results - Counter-Rotation Fan Engines:

Community noise level estimates were made for the front-drive, gear-driven, counter-rotating fan engine configurations shown in figures 10a through 10c, and summarized in table 3. A modification of the conventional estimating procedure was made to account for the effects of counter-rotation in an approximate fashion. The Counter-rotating Ducted Fan (CDF) noise characteristics were synthesized by superimposing the characteristics of two fan stages, the forward fan stage consisting of rotor 1 plus rotor 2, and the aft fan stage consisting of rotor 2 plus a stator or outlet guide vane (OGV). In this approximate model, the forward fan stage "stator" rotation (i.e., rotor 2) effects are neglected, and sum tones are neglected. Also, any rotor 1 - OGV interactions are neglected.

For the simulated forward fan stage, there is additional transmission loss through the aft fan stage OGV, and additional treatment length for aft duct suppression, as shown in figure 32. The aft fan stage, on the other hand, has additional transmission loss through the forward fan stage rotor 1, as well as additional treatment length for forward duct suppression, also shown in figure 32. These additional transmission losses and increased suppressions were assumed to result in a total of 3 dB in additional suppression to the forward fan stage aft-radiated noise and aft fan stage forward-radiated noise, respectively. A schematic of the computation process for a CDF engine is shown in figure 33.

Using the procedure described in the above paragraphs and shown in figures 32 and 33, the community noise levels were estimated for engines 5A, 5B, 5C, and 5D (see figures 10a-10c and table 3). The resulting system noise levels are summarized in figure 34, and the results are shown for engine 4 (same FPR = 1.3) for comparison. Note that all four variants of Engine 5 are significantly quieter than Engine 4 at sideline, full-power takeoff, and takeoff with cutback, but all have about the same noise level as Engine 4 at approach. The corresponding fan inlet and fan exhaust (FIN and FEX) component levels are shown in figures 35 and 36, respectively.

The fan inlet noise (FIN) component levels for Engines 5 vs. Engine 4 shown in figure 35 indicate that the rotor-stator axial spacing effect on FIN EPNL is negligible, comparing 5A and 5D vs. 5B and 5C. Further, the effect of decreasing the number of front rotor blades from 19 to 15 is to increase the FIN EPNL by about 1 EPNdB, comparing 5A and 5B vs. 5C and 5D. Except at approach, the net FIN noise (sum of forward and aft fan stages) for the Engine 5 variants is about 2 to 3 EPNdB lower than the single-stage version, Engine 4. Recall that the CDF rotors operate at lower tip speeds and pressure ratios than does the single fan rotor of Engine 4, as can be seen from the operating conditions listed in table 4.

It should be noted that the rear rotor runs at 80 percent of the front rotor speed, so that having blade counts of 19 front/15 rear results in a spreading out of the tone frequencies in the spectrum. In contrast, with blade counts of 15 front/19 rear, the two rotor blade-passing frequencies are almost coincident. Thus the difference in blade count arrangement affects the noise spectrum harmonic content and the consequent NOY-weighting that determines Perceived Noise Level (PNL, PNLT, EPNL).

The fan exhaust noise (FEX) component levels for Engines 5 vs. Engine 4 shown in figure 36 indicate that the rotor-stator axial spacing effect on FEX EPNL is significant, being about 1 to 2.5 EPNdB, depending on the operating condition. The effect of reducing front rotor blade number, or alternatively, increasing rear rotor blade number, is small and inconsistent. All variants of Engine 5 are predicted to have lower FEX levels than the single-rotation equivalent Engine 4.

A similar procedure was used to estimate the noise of Engine 6, the aft-mounted, counter-rotating, direct-drive fan engine shown in figure 11. This configuration has a design fan pressure ratio of 1.6, and so is comparable to the single-rotation version Engine 2. The estimated community noise levels for this engine are shown in figure 37, along with those of Engine 2. It is seen that the CDF Engine 6 is substantially quieter than Engine 2 at all conditions.

The fan inlet noise (FIN) component levels for Engine 6 vs. Engine 2 are shown in figure 38. It is seen that the CDF FIN levels are anywhere from 3 to 8 EPNdB lower than the SR fan levels, depending on the operating condition. This range of benefit reflects the lower tip speed that the CDF rotors operate at relative to the equivalent SR fan (see table 4), as well as the changes in sensitivity of FIN noise to tip speed at each operating condition.

The fan exhaust noise (FEX) component levels for Engine 6 vs. Engine 2 are shown in figure 39. It is seen that the CDF FEX levels are anywhere from 3 to 11 EPNdB lower than the SR fan, but the effect is large (8 dB or greater) at all but the approach power conditions. The benefits shown primarily reflect the reductions in rotor pressure ratio and the strong sensitivity of FEX noise to fan pressure ratio.

The substantial noise improvements obtained for engine 6 (figures 37, 38, 39) should be viewed with caution, because they do not account for sum tones, and they reflect approximating the rotor-rotor interaction tones by rotor-stator tones. The modelling of the excess blade row transmission and duct liner suppression effects is also quite crude. These results can therefore be looked upon as "best possible outcome" results.

For the cycle selected, the system noise reductions due to counter-rotation for this engine were much smaller than the reductions in the fan noise (FIN and FEX) components. This is because the jet mixing noise component is substantially higher than the fan noise components at full power and cutback power, and so the benefit (system/component) is not one for one. This is readily seen by comparing the differences in figures 38 and 39 with those of figure 37. It does suggest, however, that perhaps a somewhat smaller fan pressure ratio selection, say 1.5 or so, would result in a greater system noise benefit, because the jet mixing noise would not be as large a contributor to the total system noise. This is suggested as a possible refinement for further study.

Summary of Noise Prediction Results:

A summary of all component and total EPNL levels for all of the study engines discussed above is tabulated in tables 7 through 13, along with the corresponding fan speeds and pressure ratios at each community noise certification condition.

A comparison of the PNLT directivity patterns, projected on a 150-ft. arc, for all the engines studied, are shown in figure 40, for the sideline condition (full power). The corresponding results at approach power are shown in figure 41. At full power, the directivity more or less shifts from an aft-dominated, jet noise controlled pattern to a "saddle-shaped" fan noise controlled pattern as the design FPR decreases from 1.75 to 1.3. The baseline EEE pattern is similar to Engine 2, having approximately the same FPR. The front drive CDF, Engine 5, has the lowest PNLT pattern, and the rear-drive CDF, Engine 6, has PNLT levels comparable to the lowest FPR single-rotation fan, Engine 4.

At approach power, there is very little difference among all the engines (figure 41) in the aft arc PNLT patterns, the largest variation being in the forward arc where the fan inlet-radiated noise dominates the spectrum. Here the total spread is about 5 PNdB in the 30 to 50 degree angle range, with Engine 1 (S75) being the highest and Engine 5 (CF30) being the lowest. This figure suggests that below a design FPR of about 1.6, approach noise reductions with decreasing FPR will be negligible, and this was observed in the EPNL comparisons shown in figure 26. The directivity patterns shown in figure 41 also suggest that **further reductions in approach noise will require reductions in both inlet and exhaust radiated fan noise, since they have about the same peak PNLT for design FPR of 1.6 and lower.**

A summary of the EPNL margins (FAR36 Stage 3 Limit EPNL minus predicted EPNL) for all the engines studied, at the three community noise conditions, is given in figure 42. EPNL margins are plotted vs. Fan Pressure Ratio, with FPR decreasing to the right, which is also in the direction of increasing Bypass Ratio and fan diameter. It is seen that decreasing design FPR produces an almost linear increase in sideline margin, and that both CDF engines have margins 2 to 3 dB greater than the SR counterparts. A similar trend is shown in figure 42 for full-power takeoff.

With cutback, however, there seems to be a "flattening of the curve" for design FPR less than 1.45, so that very little increase in margin is realized in going from FPR of 1.45 down to 1.3. Further, the CDF advantage is significantly smaller (about 1 EPNdB) at FPR = 1.3, compared to about 3 EPNdB at FPR = 1.6.

At approach, figure 42 indicates that EPNL margin is nearly independent of design FPR, and further that the CDF benefit is rather small, on the order of 1 EPNdB or less. This is due in part to the fact that airframe noise is a significant contributor to the total system noise at approach, and hence the system noise impact due to reductions in engine noise is not one for one. Further, as pointed out in figure 41, only the forward-arc portion of the engine noise directivity pattern is significantly reduced by reducing FPR, so the total engine noise reduction is small at any rate.

A commonly used "one number" figure of merit for aircraft system community noise is cummulative margin, which is the sum of the individual margins at sideline, takeoff (with or without cutback), and approach. The cummulative margins for all the engines studied are summarized in figure 43. Results for both "with cutback" and "Full-Power Takeoff" are shown. Considering the primary objective of this study, i.e., to identify engine design concepts capable of achieving 5 to 10 EPNdB margin relative to FAR36 Stage 3, we could say that cummulative margins of 15 to 30 EPNdB would be acceptable. This acceptability criterion suggests that a design FPR between 1.5 and 1.6 would be the maximum acceptable for single-rotation fan engines, depending on whether cutback or full power takeoff was required.

If we consider future increases in rule stringency on the order of 5 to 7 EPNdB as a possibility, then figures 42 and 43 imply that a design FPR of 1.5 or so would be acceptable at sideline and takeoff. Further noise reduction technology advances would be needed to reduce approach noise, for both the engine and the airframe, irrespective of the design FPR chosen.

CONCLUSIONS

A major conclusion of this study is that achieving the goal of community noise levels that are 5 to 10 EPNdB below the current FAR36 Stage 3 limits is feasible for advanced high bypass turbofan engine concepts. The results also lead to the conclusion that increasing the engine cycle design bypass ratio will also result in improvements in aircraft operating economics, as measured by mission fuel burn and direct operating cost. In principle, engine cycle selection for improved economics and for lower noise need not be incompatible.

Considering single-rotation fan engine concepts, this study showed that the best engine cycle for economics should have a fan pressure ratio between 1.4 and 1.6, and a bypass ratio between 8:1 and 10:1. This "optimum" range reflects a tradeoff between improved propulsive efficiency with increasing bypass ratio on the one hand, and increasing weight, cost, nacelle drag and installation penalties on the other hand.

From a community noise point of view, the noise level improves with increasing bypass ratio, but the rate of improvement begins to diminish beyond a bypass ratio of 10:1 or so. In particular, the design bypass ratio selection has very minimal effect on approach noise, and the approach noise condition becomes the limiting point for achieving reductions relative to FAR36 Stage 3 limits. Also, when a cutback procedure is used for the takeoff community point, very little noise reduction is realized beyond a design bypass ratio of 10:1. The chief benefit of going to bypass ratios greater than 10:1 is in reducing full-power takeoff noise.

It was concluded from the results of this study that a counter-rotating fan engine provides a substantial noise benefit relative to an equivalent design bypass ratio single-rotation fan engine. The benefit decreases as bypass ratio increases. This benefit is associated with the individual fan rotors operating at substantially lower tip speeds and pressure ratios relative to the equivalent single rotor fan, and the sensitivity of noise to tip speed and fan pressure ratio decreases as tip speed decreases.

The economic consequences of counter rotation fans relative to single rotation fans depends on the drive system type selected. If a front-mounted, gear-driven fan is used, the mechanical design constraints imposed by the counter-rotating gearbox limit the practical engine cycles to fan pressure ratios of 1.3 or less, corresponding to bypass ratios greater than 15:1, where the noise benefit is small, and the weight and DOC penalties are substantial. The aft-mounted, direct-drive counter-rotating fan concept, however, appears to have both substantial noise reduction benefits and DOC improvements relative to its single-rotation counterpart, when designed for a bypass ratio of 10:1 or so.

RECOMMENDATIONS

The results of this study produced some unexpected conclusions, and inspired ideas for further study to clarify certain issues regarding the best engine cycle selection from both a noise and performance point-of-view. Additionally, an objective of this study was to provide guidance and recommendations for an experimental investigation that would provide needed verification and additional technology for shaping the engine architecture for future products. Hence the following recommendations are divided into two categories, the first addressing additional study model refinements and extensions to the current study, and the second addressing potential scale model fan test programs that would provide additional technology data.

STUDY METHODOLOGY IMPROVEMENTS AND EXTENSIONS:

The following improvements in acoustic modeling are recommended to enhance the realism of the predicted trends for future cycle selection studies:

1. Refine the fan (FIN and FEX) component noise predictions to reflect differences in incidence angle at part speed between different fan pressure ratio design points, so as to account for the influence of changes in fan broadband noise with incidence angle and how this effect changes with fan design pressure ratio.

2. Refine the fan (FIN and FEX) component noise predictions to reflect differences in inlet and exhaust duct liner suppression as inlet L/D, exhaust L/H, liner depth, tuning frequency, etc. are changed with design fan pressure ratio.

3. Refine the fan (FIN and FEX) component noise prediction correlations to extend the correlation database to lower tip speeds, specifically to tip speeds as low as 300 ft/sec. The current database correlations are only accurate down to about 600 ft/sec.

4. Refine the jet component noise prediction correlations to extend the correlation database to lower jet velocities, specifically to jet velocities as low as 300 ft/sec. The current database correlations are only accurate down to about 800 ft/sec.

5. Refine the fan (FIN and FEX) component noise predictions for counter-rotating fans to include better representations of:

   a. transmission and reflection effects for forward and aft rotor sources
   b. forward and aft rotor liner suppression adjustments for effective inlet and exhaust treatment lengths
   c. sum tone frequency contributions

   It is recommended that a hybrid model for counter-rotating fans be developed that combines the current empirical "two-fan superposition" concept with a simplified, 2D strip theory model of counter-rotating fan noise (a model developed by GE under an IR&D program). This hybrid model would combine the realism of data-based fan noise characteristics inherent in the empirical model with the multiple-blade-row coupling, transmission, and reflection characteristics of the 2D analytical model, and thus provide a more realistic model of counter-rotating fan noise.

Because the results of this study showed such a dramatic (and unexpected) benefit in both performance and noise for the aft-mounted, counter-rotating fan engine (Engine 6), it is highly recommended that the model improvements of item 5 above be carried out, and that the acoustic analysis for Engine 6 be repeated with the hybrid fan noise model, to substantiate the results obtained in the present study. It is also recommended that the same analysis be carried out with the hybrid fan noise model for a variant of engine 6 having a design fan pressure ratio of 1.45, since the benefits obtained for Engine 6 with a fan pressure ratio of 1.6 were somewhat offset by the jet noise contributions at high power.

Several possible extensions to the present parametric study are recommended. These include the following:

1. Evaluate both direct-drive and geared fans over the design fan pressure ratio range of 1.4 to 1.6. It is not clear from the sparce matrix of the present study where the change should be made from a direct-drive to a gear-driven fan, and what the relative benefits/penalties are at a given fan pressure ratio.

2. Evaluate both separate-flow and mixed-flow exhaust systems over the design fan pressure ratio range of 1.4 to 1.6. Again, the limited matrix of the present study did not permit an evaluation of the benefits and penalties of separate vs. mixed flow at a given fan pressure ratio.

3. Evaluate the impact of core technology improvements (e.g., increasing design OPR, T41, T3, etc.) on the resulting noise levels for selected design fan pressure ratios. For example, a design FPR=1.6 engine could achieve significantly lower takeoff noise levels if the jet noise component were reduced by reducing core size and increasing core energy extraction (and hence bypass ratio). This would result in a smaller, lighter engine than would be obtained from increasing fan size to increase bypass ratio.

Scale Model Experimental Programs:

The results of this study have indicated that the best engine cycle design, considering both economics and noise, should have a design FPR somewhere in the range of 1.4 to 1.6, irrespective of fan drive type and core type. The issues of separate vs. mixed, geared vs. direct, etc., have acoustic consequences and implications which basically boil down to the following:

> **"How do the noise characteristics of a fan change as a function of design tip speed and pressure ratio, and what are the dominant mechanisms and most effective reduction/suppression techniques as design tip speed and pressure ratio are varied?"**

If we focus on a design fan pressure ratio range of interest of 1.4 to 1.6, and expand our thinking to consider "off-optimum" tip speeds at a given design FPR, we can postulate the following probing questions:

> If we select higher or lower than optimum design tip speed, what is the trade between noise, efficiency and stall margin?
>
> Is high tip speed (greater than 1200 ft/sec) necessarily "bad" for a fan pressure ratio of 1.4?
>
> Is low tip speed (less than 1200 ft/sec) necessarily "bad" for a fan pressure ratio of 1.6?
>
> What is the trade-off between subsonic tip speed with a gearbox vs. supersonic tip speed with direct drive on fan noise and performance?
>
> Can we separate tip speed effects from pressure ratio effects on fan noise?

The following scale model test program is recommended that would address these questions. It would consist of designing, building, and testing a series of fan rotors at selected values of fan tip speeds and pressure ratios. The proposed design point matrix is shown in figure 44. The test vehicle recommended is the GEAE Universal Propulsion Simulator (UPS), described in reference 5, which would allow evaluation of noise, fan performance, and stall margin. There would be two design fan pressure ratio families, 1.4 and 1.6. For each family, three different tip speed designs would be tested. It is also recommended that, for selected design points in the matrix of figure 44, swept blade versions of the rotors be designed and tested. Testing could be carried out in the NASA Lewis 9 by 15 ft. wind tunnel, or in any suitable anechoic free jet facility.

With the proposed fan design point matrix shown in figure 44, the following acoustics issues could be addressed:

> Changes in Tone vs. Broadband noise contributions as design tip speed is varied
>
> High camber vs. Low camber blade effects on part-power noise
>
> Buzz-saw noise contribution vs. design tip speed

Liner suppression potential vs. design tip speed

Sweep benefits vs. design tip speed and design FPR

Axial spacing effects (and effectiveness) on noise vs. design tip speed and FPR

Vane/Blade number ratio effects (and effectiveness) on noise vs. design tip speed and FPR.

Based on initial results of the above proposed test program, additional noise reduction development ideas could be addressed for selected rotor designs which show promise. Examples include the following:

Integrated vane-plus-strut fan frame design vs. separate vane and frame design - to obtain maximum axial spacing benefit in smallest axial length

Alternate treatment panel tuning concepts - tuning for buzz-saw (Multiple Pure Tone or MPT) noise, tuning for approach noise, tuning for high frequency (important for London Airport noise limits)

Wide Chord fan blade vs. conventional shrouded fan blade - evaluate whether spacing/chord benefit by increasing spacing is the same as the benefit by reducing chord.

The proposed program would therefore consist of two phases, the first phase being the design, fabrication and testing of the recommended six rotor designs with a common nacelle and fan frame/vane assembly. A different fan inner wall duct and Outlet Guide Vane (OGV) may be needed for 1.4 FPR designs vs. the 1.6 FPR designs. Utilizing results of the first phase of testing, noise reduction concepts can be developed and quantified in the second phase which reflect the increased knowledge gained on the important noise source contributions and controlling parameters from the first phase.

The proposed program as described above would provide basic technology information that is not tied to a specific engine architecture, but can be used to help select the engine architecture and predict the performance and noise trades of one type of engine vs. another, weighing the benefits and penalties of noise reduction through cycle selection vs. noise reduction by component design features.

It is further recommended that, pending an encouraging outcome of the enhanced and improved counter-rotating fan Engine 6 study recommended in the previous subsection, a "proof-of-concept" test be run of a Model Propulsion Simulator (MPS) scale model Unducted Fan, as described in reference 6, suitably modified to incorporate a shroud or nacelle. The objective of this test would be to further verify the study results, and identify whether or not a counter-rotating fan can indeed be quieter than its single-rotation counterpart. If this "proof-of-concept" test shows that a counter-rotating fan can be substantially quieter than a single-rotation fan at the same fan total pressure ratio, then a more extensive test and analysis program could be undertaken to develop the concept.

ACKNOWLEDGEMENTS

The following people contributed substantially to the study reported herein. Christopher J. Smith provided integration of the cycle analysis, flowpath design, mission analysis, and carried out the DOC analyses. Paul Feig and Valerie McKay provided the mission analysis. Larry Dunbar and Michael Salay carried out the engine flowpath designs. Rick Donaldson, Mark Wagner and Charlotte Salay provided the engine cycle analyses. Dr. Bangalore Janardan and George Kontos provided the engine system noise predictions.

REFERENCES

1. Lavin, S.P., Ho, P.Y., and Chamberlin, R.:"Measurements and Predictions of Energy Efficient Engine Noise" - AIAA 9th Aeroacoustics Conference paper AIAA 84-2284, Williamsburg, Va., October 15-17, 1984.

2. Unique Systems Analysis Program Task 2 Final Oral Report "Subsonic UBE Studies" NASA Lewis Research Center Contract NAS3-25460, GE Aircraft Engines Advanced Technology Operation Staff, February 16, 1990.

3. Nichols, H.E., "UDF Engine/MD80 Flight Test Program" AIAA/SAE/ASME/ASEE 24th Joint Propulsion Conference paper AIAA 88-2805, Boston, Mass., July 11-13, 1988.

4. Gliebe, P.R., "The Effect of Throttling on Forward Radiated Fan Noise" AIAA 5th Aeroacoustics Conference paper AIAA 79-0640, Seattle, Wash., March 12-14, 1979.

5. Balan, C., and Hoff, G.E., "Propulsion Simulator for High Bypass Turbofan Performance Evaluation" SAE Technical Paper no. 931410, April 20, 1993.

6. Delaney, B.R., Balan, C., West, H., Humenik, F.M., and Craig, G., "A Model Propulsion simulator For Evaluating Counterrotating Blade Characteristics" SAE paper 861715, Warrendale, Pa., October 1986.

Table 1.

NASA/GE UBE ACOUSTIC STUDY

ENGINE CYCLE PARAMETERS

(61,500 Lbs T/O Thrust Size, Year 2000+ Technology)

Aerodynamic Design Point Cruise .8M 35000 Ft

	Updated E^3 Base	Study Configurations					
		Single Rotating				Counter Rotating	
						Front Fan	Rear Fan
FPR	1.62	1.75	1.60	1.45	1.30	1.30	1.60
BPR	5.8	5.94	7.75	9.81	15.75	15.75	7.73
OPR	38.5	55	55	55	55	55	55
HP Comp PR	22.6	27.0	27.0	8.0	8.0	8.0	8.0
$T_{41\ max}$ (°F)	2504	2800	2800	2800	2800	2800	2800
Flow	Mixed	Mixed	Mixed	Mixed	Separate	Separate	Mixed
Fan Drive	Direct	Direct	Direct	Geared	Geared	Geared	Direct
Fan Inlet $\frac{H}{T}$	0.342	0.30	0.30	0.30	0.30	0.30	0.45
Fan Tip Dia	99.5	89	96	106	130	130	97.2
Fan Tip Speed	1272	1480	1354	1030	984	655/525	960/770

Table 2.

NASA/GE UBE ACOUSTIC STUDY

COMPONENT EFFICIENCES

η AD AT AERO DESIGN POINT DATA 0.8M 35000 FT STD DAY

COMPONENT	ENGINE					
	E^3	1.75	1.60	1.45	1.30	1.60CR
FAN TIP	.893	.905	.915	.930	.940	.915
ROOT BOOSTER	.909	.900	.900	.881	.881	.881
HPC	.843	.857	.856	.868	.868	.868
HPT	.925	.935	.934	.919	.919	.919
IPT	--	--	--	--	--	.911
LPT	.923	.940	.940	.936	.936	.921
GEARBOX CR	--	--	--	.982	.985	--
T/O	--	--	--	.993	.993	--
MIXER EFF	.85	.85	.85	.85	--	.85
BURNER	.999	.999	.999	.999	.999	.999

Table 3.

Counterrotation fan concepts

- Engine 5 (CF30 CDF)
  - Front drive
  - Gear–driven
  - FPR = 1.3
  - Compares to engine 4
- Engine 6 (CR60 CDF)
  - Rear drive
  - Turbine–driven
  - FPR = 1.6
  - Compares to engine 2

Four Versions:

Config	NB–R1	NB–R2	S/C_{ax}
5A	19	15	2.5
5B	19	15	1.2
5C	15	19	1.2
5D	15	19	2.5

Table 4.

UHB AEROACOUSTIC STUDY ENGINE FAN PARAMETERS

ENGINE		S75	S60	S45	S30	CF30	CR60
FAN DIAM., IN.		88.9	96.3	105.7	129.7	129.7	97.2
M_o=0.8 35K STD. DAY	FPR	1.75	1.60	1.45	1.30	1.30	1.60
	BPR	5.94	7.75	9.81	15.75	15.75	7.73
	UTC	1480	1354	1030	984	655/525	960/770
APP	UTC	935	850	653	566	376/302	592/475
	FPR	1.220	1.178	1.143	1.096	1.095	1.177
C/B	UTC	1340	1222	932	859	571/458	862/691
	FPR	1.579	1.465	1.365	1.240	1.239	1.475
T/O	UTC	1511	1364	1052	955	635/509	953/764
	FPR	1.790	1.625	1.496	1.300	1.300	1.615
S/L	UTC	1496	1353	1038	947	631/505	949/760
	FPR	1.777	1.615	1.484	1.295	1.295	1.609

Table 5.

UHB AEROACOUSTIC STUDY ENGINES

FAN BLADE AND VANE COUNTS

ENGINE	NO. OF BLADES	NO. OF VANES	
S75	24	56	(48 V + 8 STRUTS)
S60	24	56	(48 V + 8 STRUTS)
S45	22	56	(48 V + 8 STRUTS)
S30	22	56	(48 V + 8 STRUTS)
CF30	19+15	36	
CR60	28+22	8	(STRUTS ONLY)

T A B L E 6

WEIGHT AND PERFORMANCE SENSITIVITY FACTORS (Pct. Change per Decibel Reduction) DUE TO ENGINE LENGTH INCREASES FOR SPACING AND TREATMENT

ENGINE	S75	S60	S45	S30
DESIGN FAN PR	1.75	1.60	1.45	1.30
Change in L/D	0.225	0.271	0.212	0.262
Change in Weight (%)	1.77	2.43	1.2	2.29
Change in Drag (%)	0.22	0.328	0.222	0.524
Fuel Burn Change (%)	0.313	0.47	0.292	0.686
Change in Cost (%)	1.12	1.447	0.9	1.308
Change in D.O.C. (%)	0.197	0.274	0.089	0.328
EPNL Change (S/L)	0.3	0.5	1.0	2.0
EPNL Change (C/B)	0.6	0.9	1.0	2.0
EPNL Change (APP)	1.4	1.3	1.0	1.1
EPNL Change (Cum)	2.3	2.7	3.0	5.1
SENSITIVITIES:				
Weight/EPNL (%/dB)	0.770	0.900	0.400	0.449
Fuel Burn/EPNL(%/dB)	0.136	0.174	0.097	0.135
D.O.C./EPNL (%/dB)	0.086	0.101	0.030	0.064

Table 7.

NASA NAS3-25269 TASK-4 E3-TYPE BASELINE NOISE ESTIMATE

TOGW = 407 Klb; LGW = 320 Klb
ENGINE = E3 TYPE BASELINE
ENGINES = 2

		SIDELINE	TAKEOFF	CUTBACK	APPROACH
	RPM	2828	2846	2569	1769
	Tip Speed (fps)	1228	1236	1115	768
	Pressure Ratio	1.576	1.584	1.432	1.163
	NOISE COMPONENT	EPNL, dB			
FAST PREDICTION	COM	84.2	83.6	82.0	82.1
	FEX	91.3	90.8	88.3	89.8
	FIN	84.2	82.9	83.5	92.3
	CNJ	92.5	91.8	88.1	83.5
	AFN	---	---	---	94.0
	SUM	97.2	96.6	94.2	98.7
FAST CALIBRATION		1.6	1.6	1.6	1.8
(PREDICTION-CALIBRATION)		95.6	95.0	92.6	96.9
FAR-36 RULE		100.1	96.8	96.8	103.6
MARGIN (RULE-ESTIMATE)		4.5	1.8	4.2	6.7

George Kontos 6/16/93 9:36 AM
GME3B.XLS/gck508(orig.kc's me3bxls.xls/baj#3)

Table 8.

NASA NAS3-25269 TASK-4 ENGINE #1 (S75)

TOGW = 407 Klb; LGW = 320 Klb
ENGINE = ENGINE #1 (S75)
ENGINES = 2

	SIDELINE	TAKEOFF	CUTBACK	APPROACH
RPM	3856	3895	3454	2411
Tip Speed (fps)	1496	1511	1340	935
Pressure Ratio	1.777	1.790	1.579	1.220

	NOISE COMPONENT	EPNL, dB			
FAST PREDICTION	COM	84.6	83.6	81.1	81.0
	FEX	94.7	93.8	91.0	92.3
	FIN	83.4	81.4	82.2	95.3
	CNJ	96.6	95.7	90.5	85.3
	AFN	---	---	---	94.0
	SUM	100.4	99.6	95.8	100.4
FAST CALIBRATION		1.6	1.6	1.6	1.8
(PREDICTION-CALIBRATION)		98.8	98.0	94.2	98.6
FAR-36 RULE		100.1	96.8	96.8	103.6
MARGIN (RULE-ESTIMATE)		1.3	-1.2	2.6	5.0

George Kontos 6/16/93 9:31 AM
GNASA1.XLS/gck508 (orig. kc's nasa1.xls/baj#3)

Table 9.

NASA NAS3-25269 TASK-4 ENGINE #2 (S60)

TOGW = 407 Klb; LGW = 320 Klb
ENGINE = ENGINE #2 (S60)
ENGINES = 2

	SIDELINE	TAKEOFF	CUTBACK	APPROACH
RPM	3219	3246	2907	2023
Tip Speed (fps)	1353	1364	1222	850
Pressure Ratio	1.615	1.625	1.465	1.178

	NOISE COMPONENT	EPNL, dB			
FAST PREDICTION	COM	83.9	82.9	80.5	80.5
	FEX	93.1	92.2	90.9	91.0
	FIN	84.5	82.5	83.3	95.1
	CNJ	92.9	91.9	87.3	83.4
	AFN	---	---	---	94.0
	SUM	98.0	97.0	94.7	99.7
FAST CALIBRATION		1.6	1.6	1.6	1.8
(PREDICTION-CALIBRATION)		96.4	95.4	93.1	97.9
FAR-36 RULE		100.1	96.8	96.8	103.6
MARGIN (RULE-ESTIMATE)		3.7	1.4	3.7	5.7

George Kontos 6/16/93 9:42 AM
GNASA2.XLS/gck508 (orig. kc's nasa2/baj#3)

Table 10.

NASA NAS3-25269 TASK-4 ENGINE #3 (S45)

TOGW = 407 Klb; LGW = 320 Klb
ENGINE = ENGINE #3 (S45)
ENGINES= 2

	SIDELINE	TAKEOFF	CUTBACK	APPROACH
RPM	2251	2280	2020	1417
Tip Speed (fps)	1038	1052	932	653
Pressure Ratio	1.484	1.496	1.365	1.143

	NOISE COMPONENT	EPNL, dB			
FAST PREDICTION	COM	83.7	82.8	80.1	80.3
	FEX	91.2	90.0	85.6	92.8
	FIN	84.0	81.7	79.5	93.9
	CNJ	89.2	88.2	83.6	83.4
	AFN	---	---	---	94.0
	SUM	95.8	94.4	90.2	99.8
FAST CALIBRATION		1.6	1.6	1.6	1.8
(PREDICTION-CALIBRATION)		94.2	92.8	88.6	98.0
FAR-36 RULE		100.1	96.8	96.8	103.6
MARGIN (RULE-ESTIMATE)		5.9	4.0	8.2	5.6

George Kontos 6/16/93 9:54 AM
GNASA3.XLS/gck508 (orig. kc's nasa3.xls/baj#3)

Table 11.

NASA NAS3-25269 TASK-4 ENGINE #4 (S30)

TOGW = 407 Klb; LGW = 320 Klb
ENGINE = ENGINE #4 (S30)
ENGINES = 2

		SIDELINE	TAKEOFF	CUTBACK	APPROACH
	RPM	1678	1691	1521	1002
	Tip Speed (fps)	947	955	859	566
	Pressure Ratio	1.295	1.300	1.240	1.096
	NOISE COMPONENT	EPNL, dB			
FAST PREDICTION	COM	82.3	81.4	79.3	79.6
	FEX	88.4	87.7	86.4	92.2
	FIN	83.7	81.3	79.1	90.7
	CNJ	85.4	84.3	81.5	83.3
	AFN	---	---	---	94.0
	SUM	93.1	91.9	89.9	98.4
FAST CALIBRATION		1.6	1.6	1.6	1.8
PREDICTION-CALIBRATION		91.5	90.3	88.3	96.6
FAR-36 RULE		100.1	96.8	96.8	103.6
MARGIN (RULE-ESTIMATE)		8.6	6.6	8.5	7.0

George Kontos 6/16/93 10:02 AM
GNASA4.XLS/gck508 (orig. kc's nasa4.xls/baj#3)

Table 12.

BOEING-767/NASA TASK-4 ENGINE #5 (S30/CDF) NOISE ESTIMATE

AIRCRAFT = BOEING 767
TOGW = 407 Klb; LGW = 320 Klb
ENGINE = ENGINE #5 (S30/CDF)
ENGINES = 2

	NOISE COMPONENT	EPNL, dB															
		ENGINE "5A"				*ENGINE "5B"*				*ENGINE "5C"*				*ENGINE "5D"*			
		SL	TO	CB	APP	SL	TO	CB	APP	SL	TO	CB	APP	SL	TO	CB	APP
FAST PREDICTION	COM	82.3	81.4	79.3	79.6	82.3	81.4	79.3	79.6	82.3	81.4	79.3	79.6	82.3	81.4	79.3	79.6
	FEX	84.9	83.9	82.7	90.6	87.7	86.8	83.9	92.8	88.4	87.5	87.3	93.0	85.0	84.1	81.8	90.3
	FIN	81.3	78.7	76.8	91.7	81.3	78.7	77.0	91.7	81.6	78.9	77.5	91.5	81.6	78.8	77.1	91.5
	SFJ	85.4	84.3	81.5	88.8	85.4	84.3	81.5	88.8	85.4	84.3	81.5	88.8	85.4	84.3	81.5	88.8
	AFN	---	---	---	94.0	---	---	---	94.0	---	---	---	94.0	---	---	---	94.0
	SUM	91.1	89.7	87.6	98.5	92.1	90.6	88.0	99.1	92.4	91.2	87.8	99.0	91.2	89.8	87.3	98.4
FAST CALIBRATION		1.6	1.6	1.6	1.8	1.6	1.6	1.6	1.8	1.6	1.6	1.6	1.8	1.6	1.6	1.6	1.8
(PREDICTION-CALIBRATION)		89.5	88.1	86.0	96.7	90.5	89.0	86.4	97.3	90.8	89.6	86.2	97.2	89.6	88.2	85.7	96.6
FAR-36 RULE		100.1	96.8	96.8	103.6	100.1	96.8	96.8	103.6	100.1	96.8	96.8	103.6	100.1	96.8	96.8	103.6
MARGIN (RULE-ESTIMATE)		10.6	8.7	10.8	6.9	9.6	7.8	10.4	6.3	9.3	7.2	10.6	6.4	10.5	8.6	11.1	7.0

George Kontos 6/16/93 11:29 AM
GNASA5.XLS/gck508 (orig. kc's nasa5.xls/baj#3)

Table 13.

BOEING-767/NASA TASK-4 ENGINE #6 (S60/CDF) NOISE ESTIMATE

AIRCRAFT = BOEING 767
TOGW = 407 Klb; LGW = 320 Klb
ENGINE = ENGINE #6 (S60/CDF)
ENGINES = 2

	NOISE COMPONENT	EPNL, dB *ENGINE "6"*			
		SL	TO	CB	APP
FAST PREDICTION	COM	83.5	82.5	80.5	80.7
	FEX	83.2	83.5	82.0	89.1
	FIN	82.1	78.7	76.9	91.1
	CNJ	92.3	91.1	87.3	85.6
	AFN	---	---	---	94.0
	SUM	94.6	93.5	90.1	98.1
FAST CALIBRATION		1.6	1.6	1.6	1.8
(PREDICTION-CALIBRATION)		93.0	91.9	88.5	96.3
FAR-36 RULE		100.1	96.8	96.8	103.6
MARGIN (RULE-ESTIMATE)		7.1	4.9	8.3	7.3

George Kontos 6/16/93 11:37 AM
GNASA6.XLS/gck508 (orig. kc's nasa6.xls/baj83)

LIST OF FIGURES

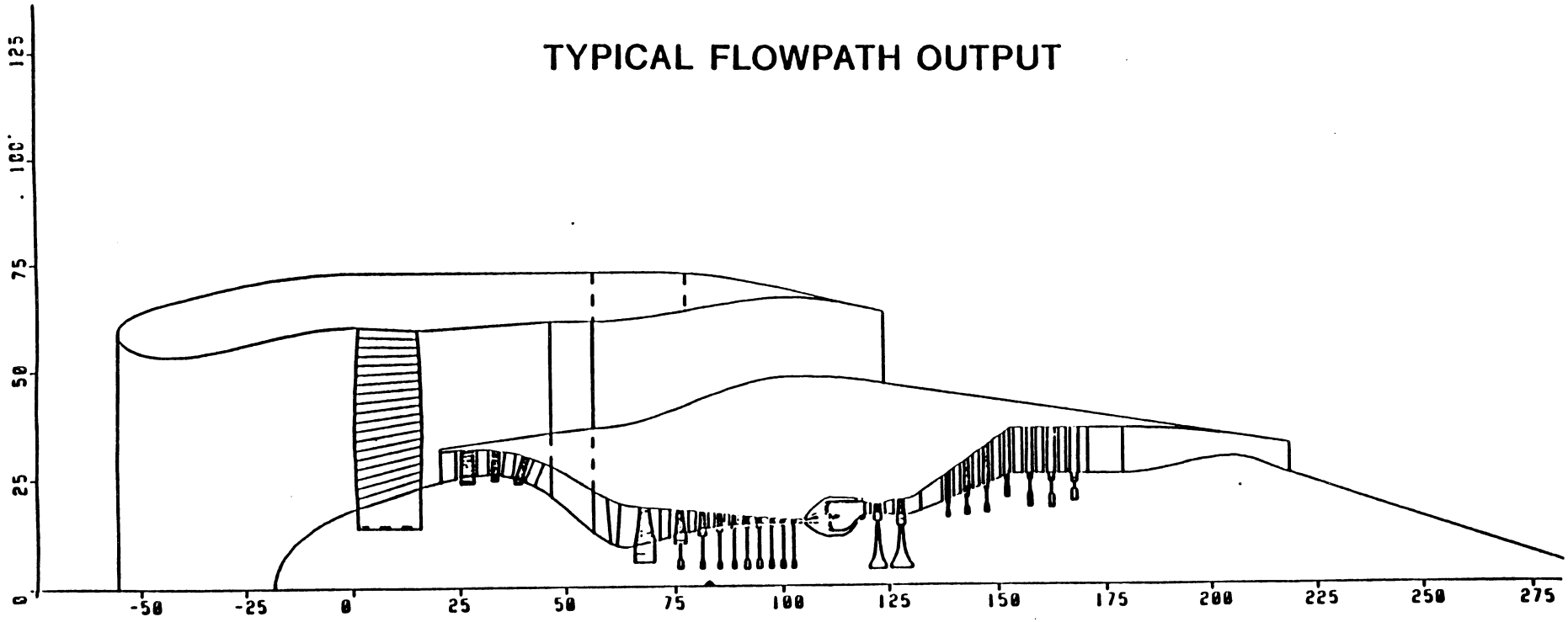

WEIGHT SUMMARY

STUDY : CFX N25 CYCLE
DATE : 04/05/90

B-NOSE	=	45.44
FAN ROTOR	=	1272.57
FAN STATOR	=	1611.30
BOOSTER ROTOR	=	289.24
BOOSTER STATOR	=	506.80
MAIN FRAME	=	2147.10
COMPRESSOR ROTOR	=	835.75
COMPRESSOR STATOR	=	986.20
DIFFSR	=	413.22
HP TURB ROTOR	=	837.89
HP TURB STATOR	=	468.38
LP TURB ROTOR	=	2252.64
LP TURB STATOR	=	1437.71
REAR FH	=	837.64
NACELLE	=	6783.64
C & A	=	679.47
TOTAL ENGINE WEIGHT=		20144.89
Z OF ENGINE C G.=		82.57

INPUT COST BASE YEAR =1989

MANUFACTURING COST SUMMARY

1989 DOLLARS - 25KLB ENGINE

STUDY : CFX N25 CYCLE
DATE : 04/05/90

B-NOSE	=	23.93
FAN ROTOR	=	390.26
FAN STATOR	=	105.30
BOOSTER ROTOR	=	44.10
BOOSTER STATOR	=	122.35
MAIN FRAME	=	656.80
COMPRESSOR ROTOR	=	186.69
COMPRESSOR STATOR	=	240.94
DIFFSR	=	177.89
HP TURB ROTOR	=	464.35
HP TURB STATOR	=	337.31
LP TURB ROTOR	=	335.03
LP TURB STATOR	=	273.06
REAR FH	=	122.22
NACELLE	=	1813.70
C & A	=	276.69

TOTAL MANUFACTURING COST/$1000 5569.62

MAINTENANCE COST SUMMARY

1989 DOLLARS PER SHOP VISIT

STUDY : CFX N25 CYCLE
DATE : 04/05/90

	MATL	SHOP LABOR		MI - TECH	
	1000$	MR	1000$	MR	1000$
B-NOSE=	0.34	6.76	0.21	0.	0.
FAN=	6.61	464.60	14.51	9.25	0.51
BOOSTER=	23.67	276.20	8.63	41.12	2.27
MAIN FRAME=	13.80	88.92	2.78	5.78	0.32
COMPRESSOR=	152.90	276.33	8.63	45.00	2.49
DIFFSR=	56.15	825.39	25.78	150.60	8.33
HP TURB=	431.11	217.12	6.78	568.62	31.43
LP TURB=	10.38	76.05	2.38	14.06	0.78
REAR FH=	23.76	87.32	2.73	26.32	1.45
NACELLE=	0	0		0	0.
C & A=	93.62	225.78	7.05	0.	0.
TOT/SHOP VST	811.03	2544.36	79.48	860.75	47.50
TOTAL COST/SHOP VISIT =		938.10			

Figure 1 Typical Engine Preliminary Design FLOWPATH Code Output

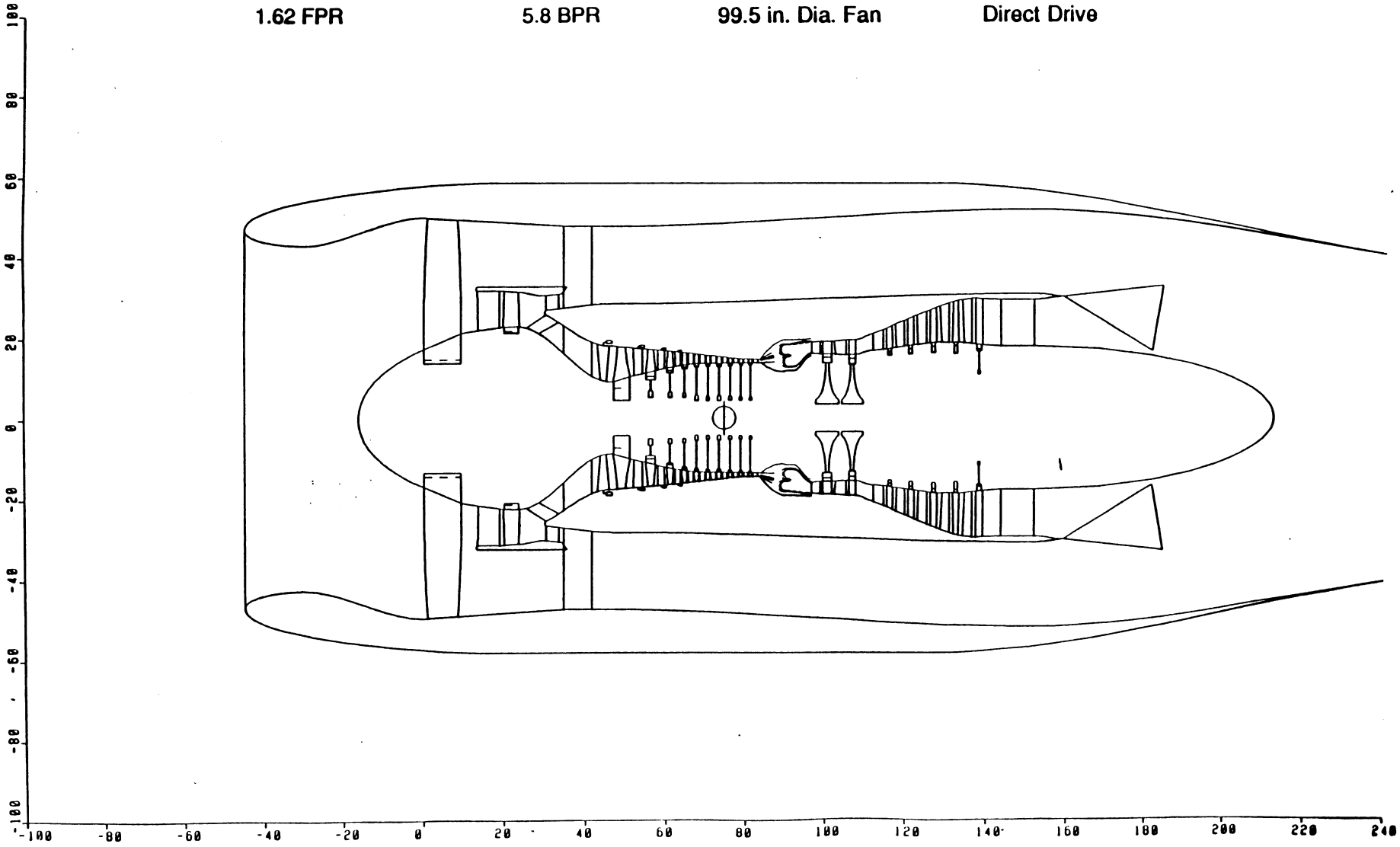

Figure 2 Baseline Updated Energy-Efficient Engine Cross-section

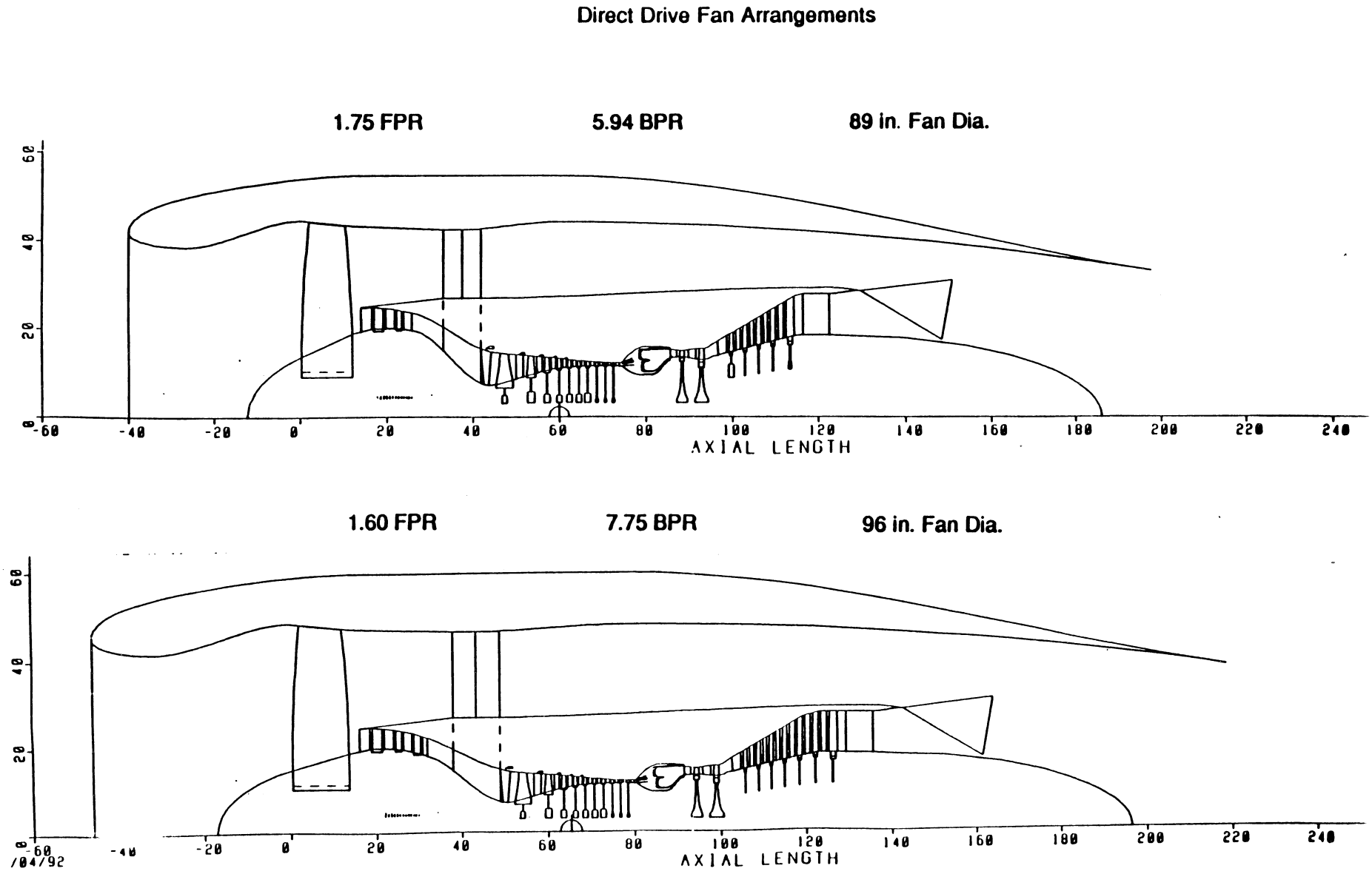

Figure 3 Direct Drive Advanced Engine Cross-Sections (Engines 1 and 2)

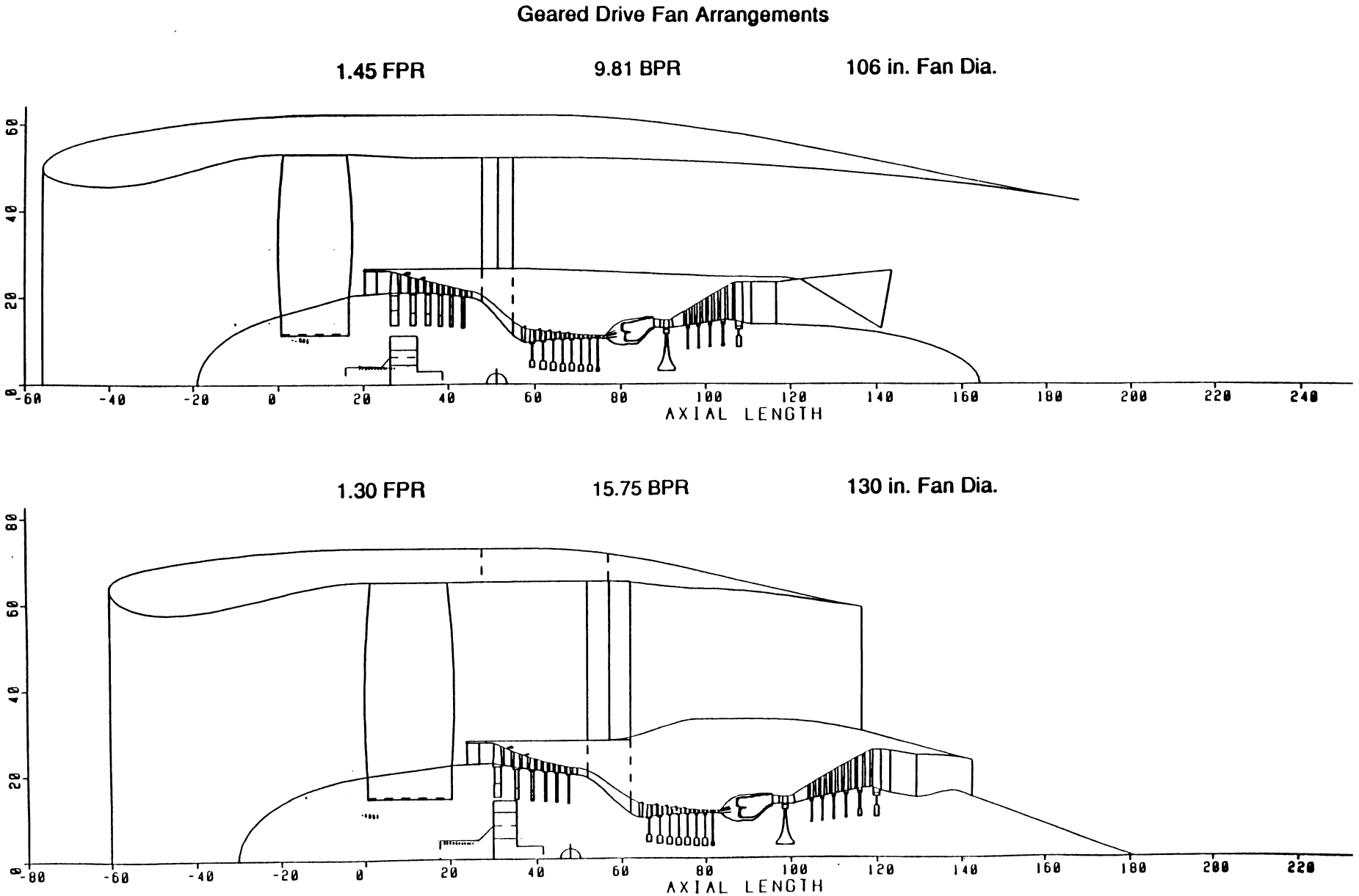

Figure 4 Geared-Fan Advanced Engine Cross-Sections (Engines 3 and 4)

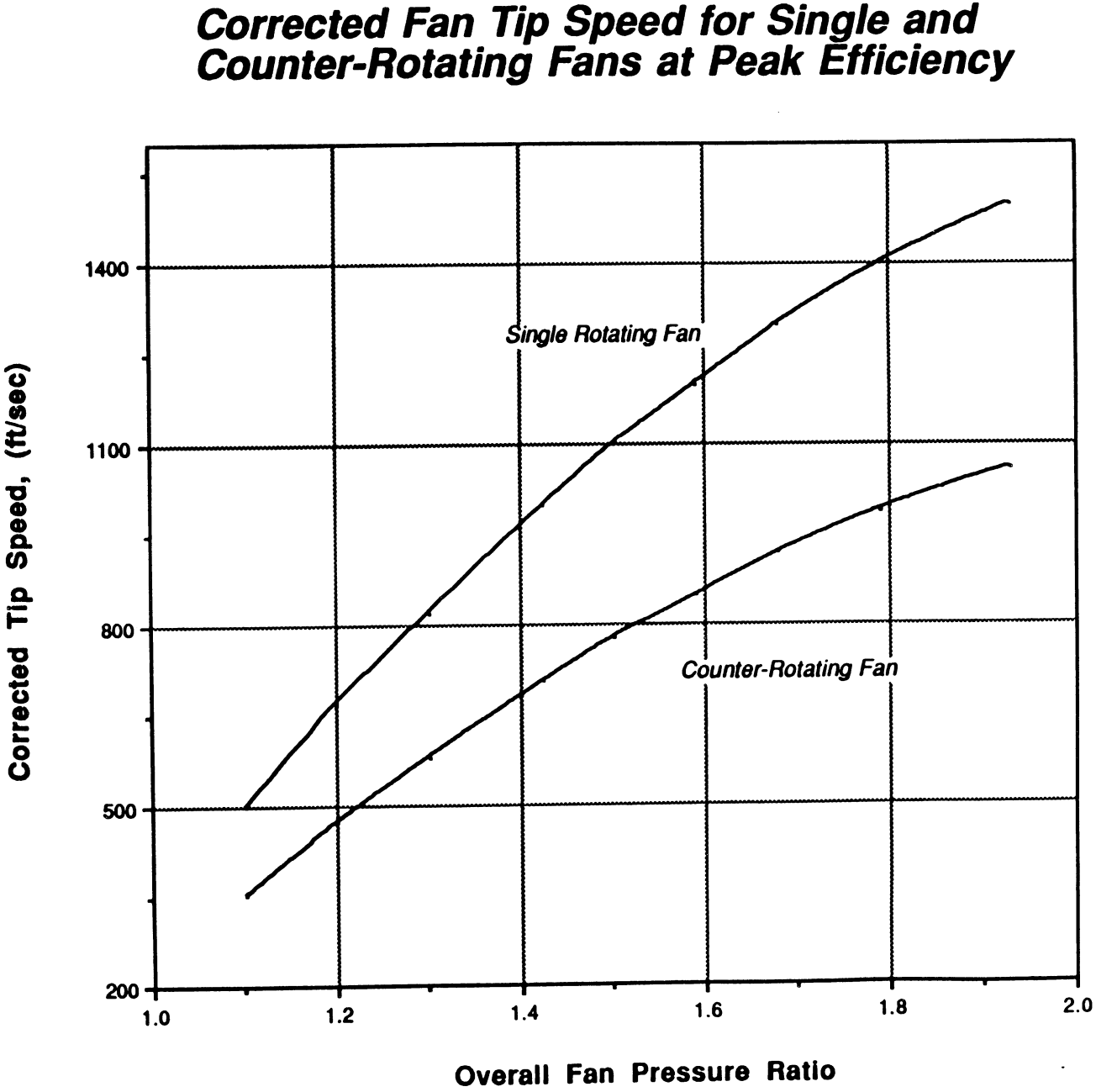

Figure 5 Design Point Fan Tip Speed Selection Trend Curve

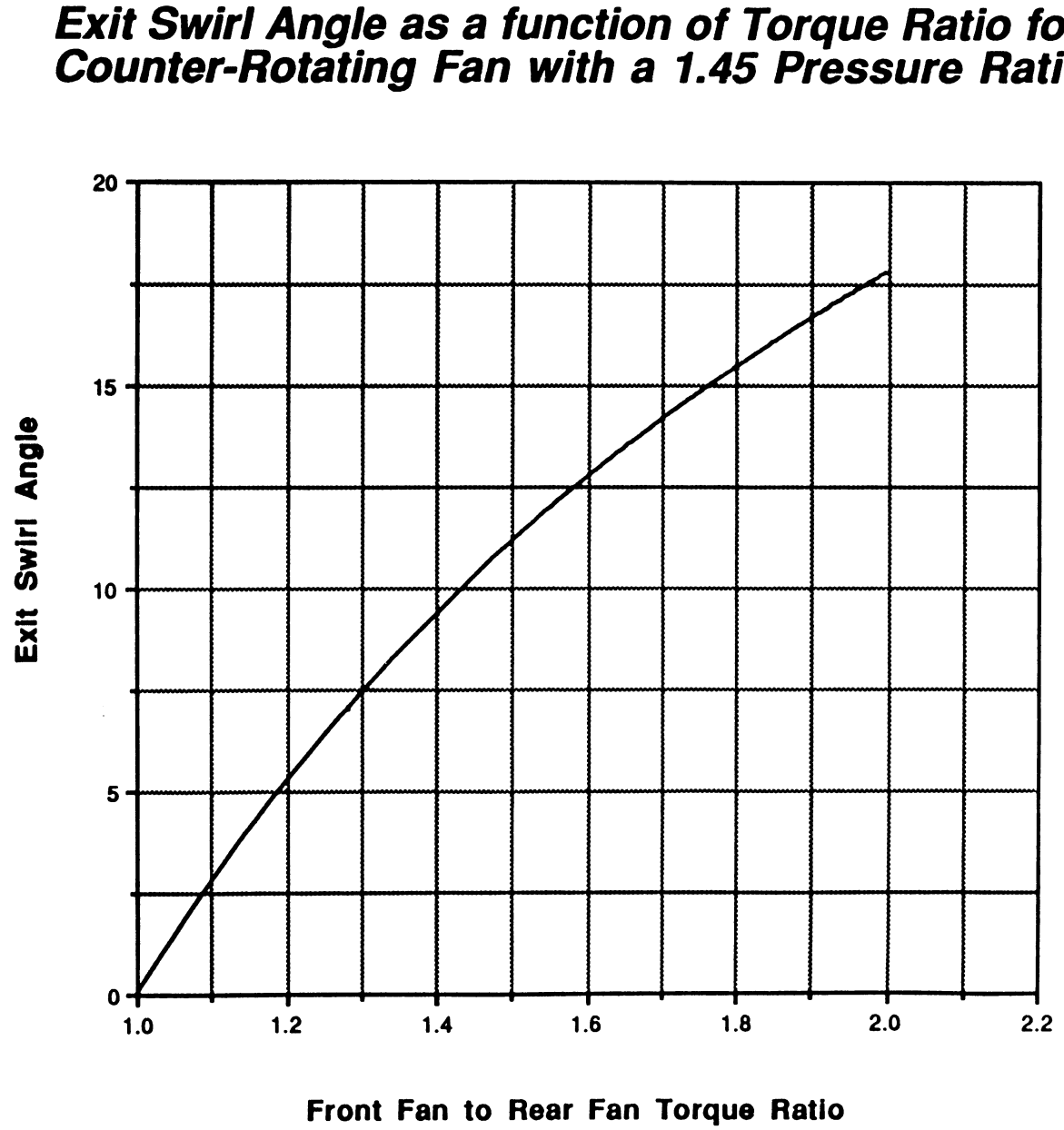

Figure 6a Counter-rotating Fan Swirl vs. Torque Ratio Trend Curve

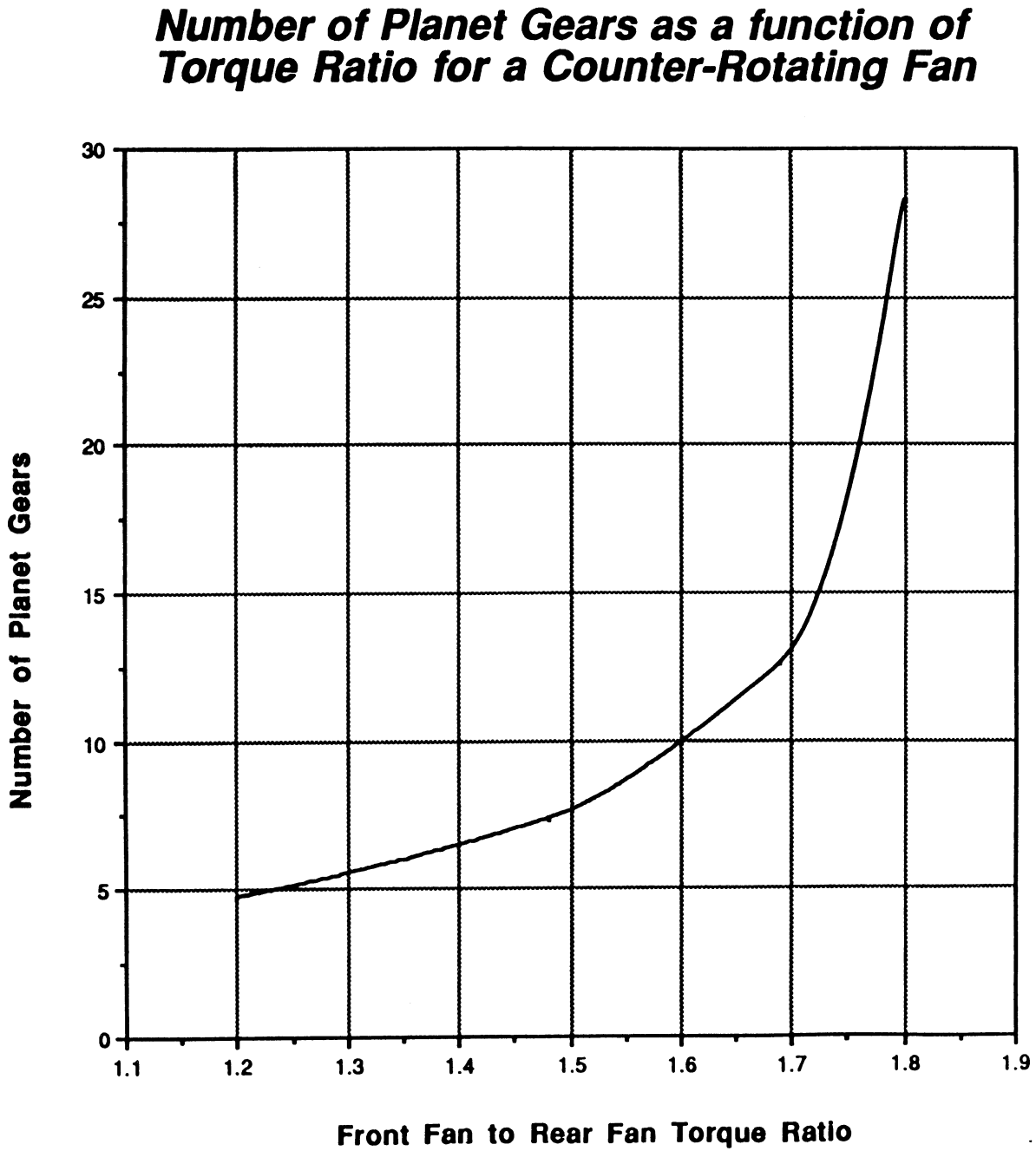

Figure 6b Counter-rotating Fan Gearbox Planet Gear Number Selection

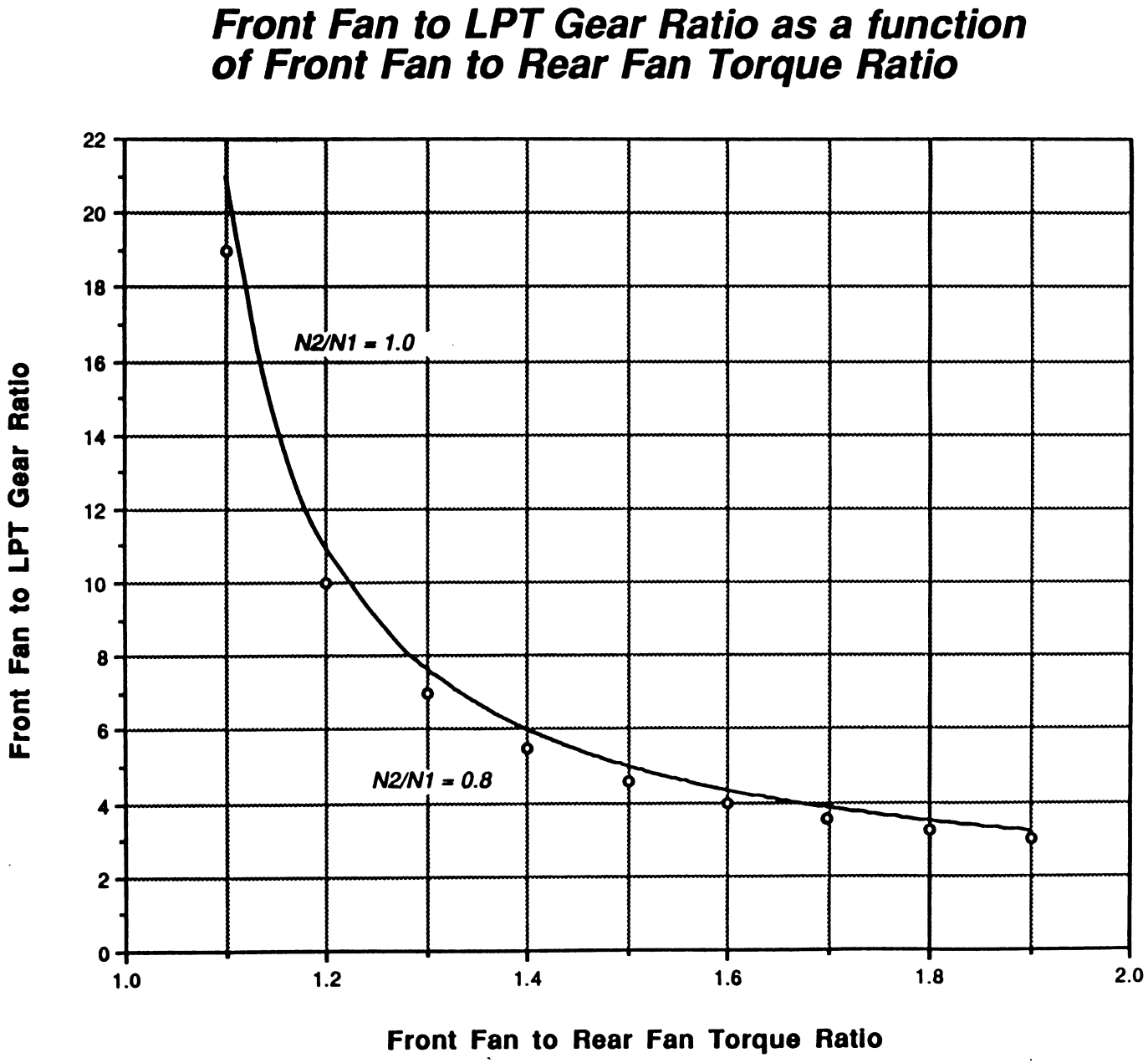

Figure 7 Counter-rotating Fan Gearbox Fan/Turbine Gear Ratio Trend

LP Turbine Exit Area as a function of Overall Fan Pressure Ratio

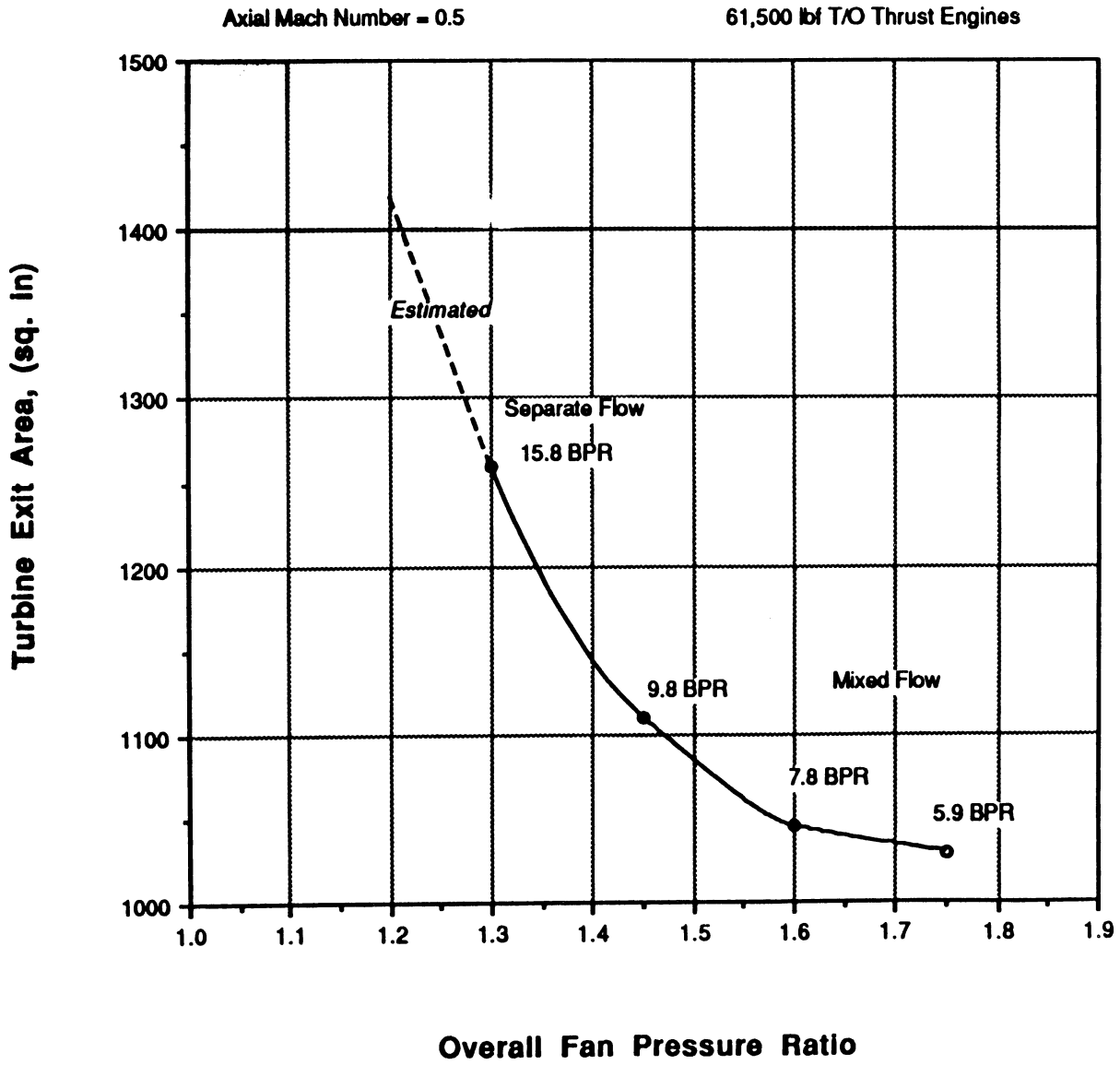

Figure 8 LP Turbine Exit Area Requirements vs. Fan Pressure Ratio

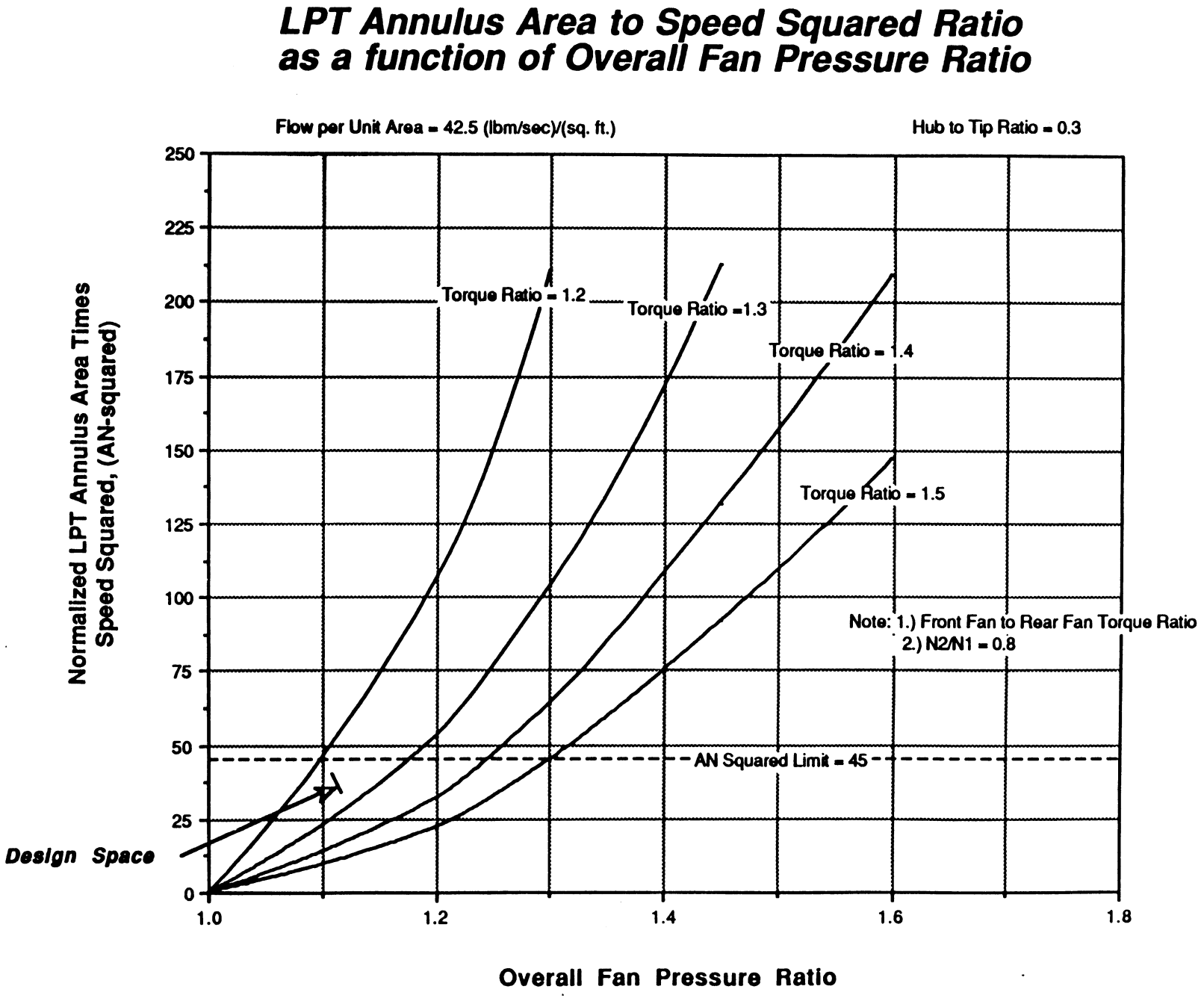

Figure 9 Counter-rotating Fan LPT AN2 Trend Curves and Limits

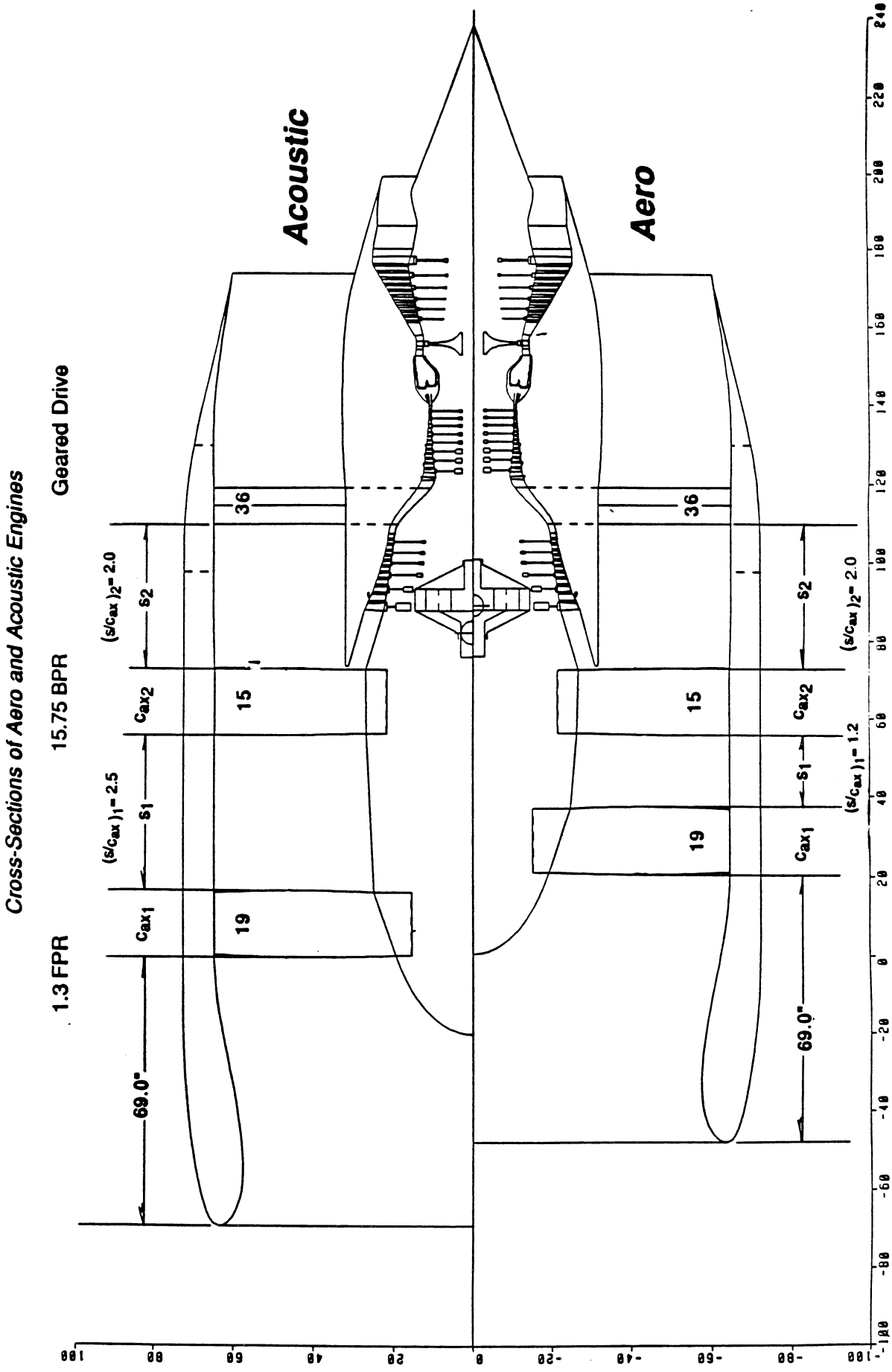

Figure 10a Geared Counter-rotating Fan Engines 5A and 5B Cross-sections

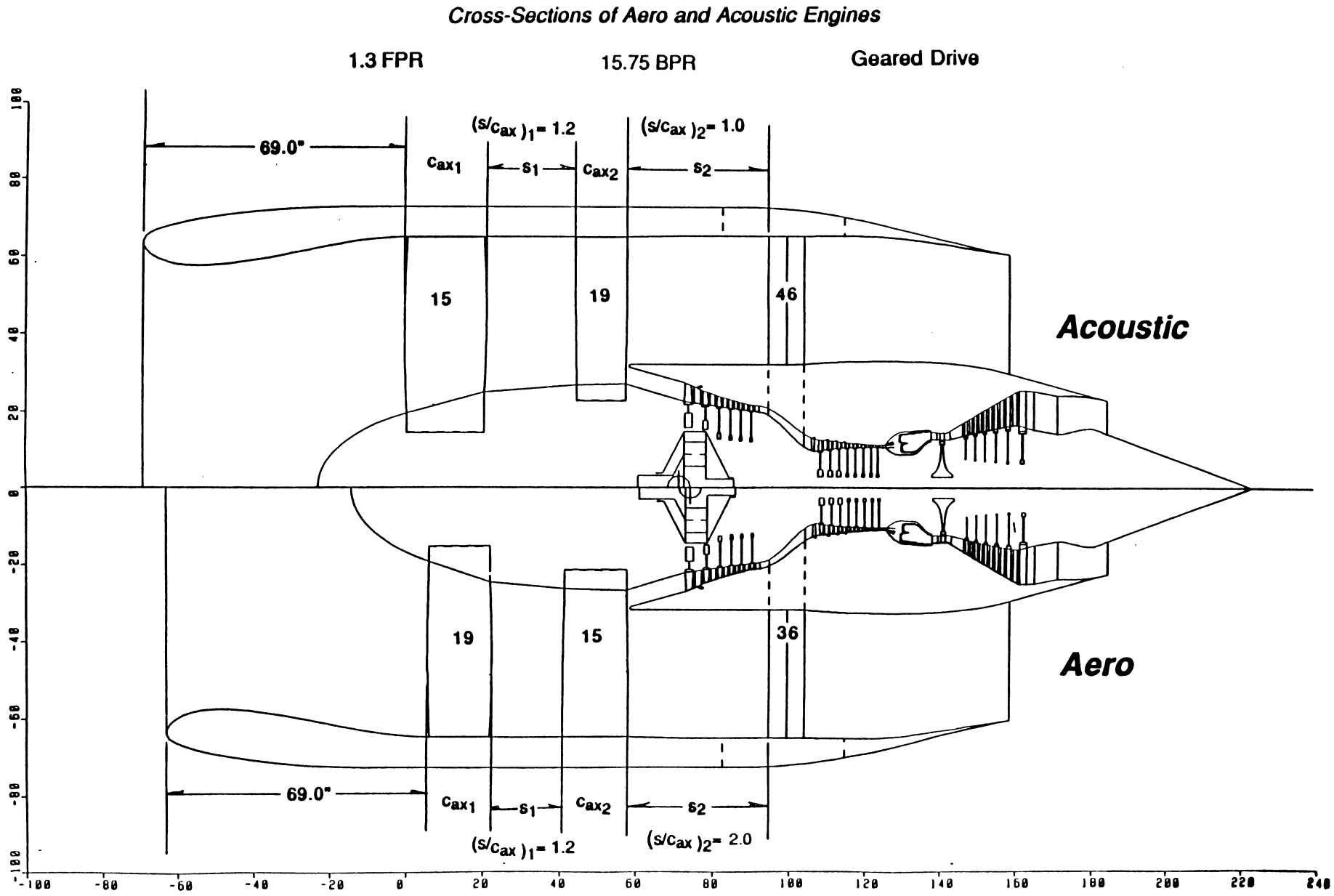

Figure 10b Geared Counter-rotating Fan Engines 5C and 5B Cross-sections

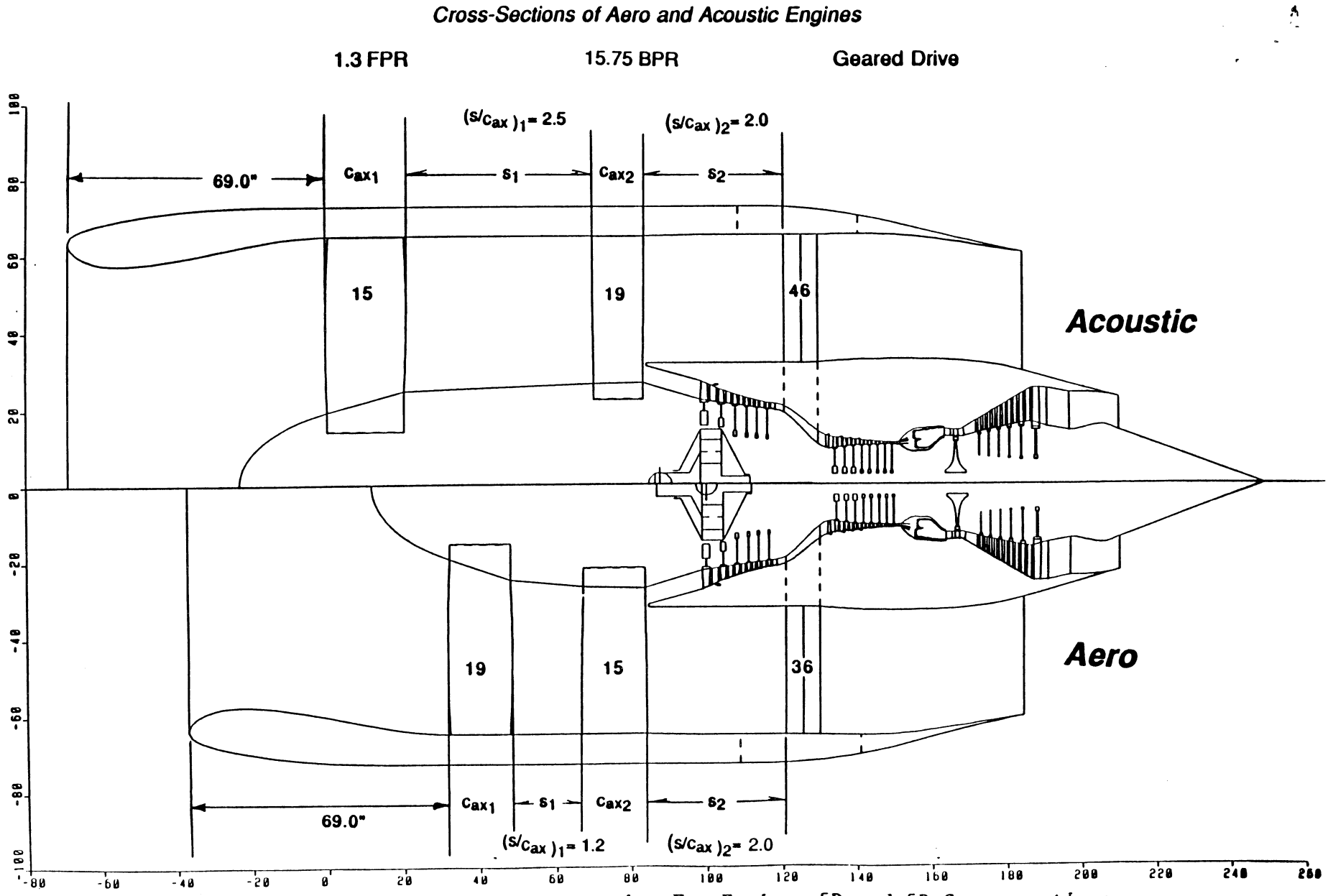

Figure 10c. Geared Counter-rotating Fan Engines 5D and 5B Cross-sections

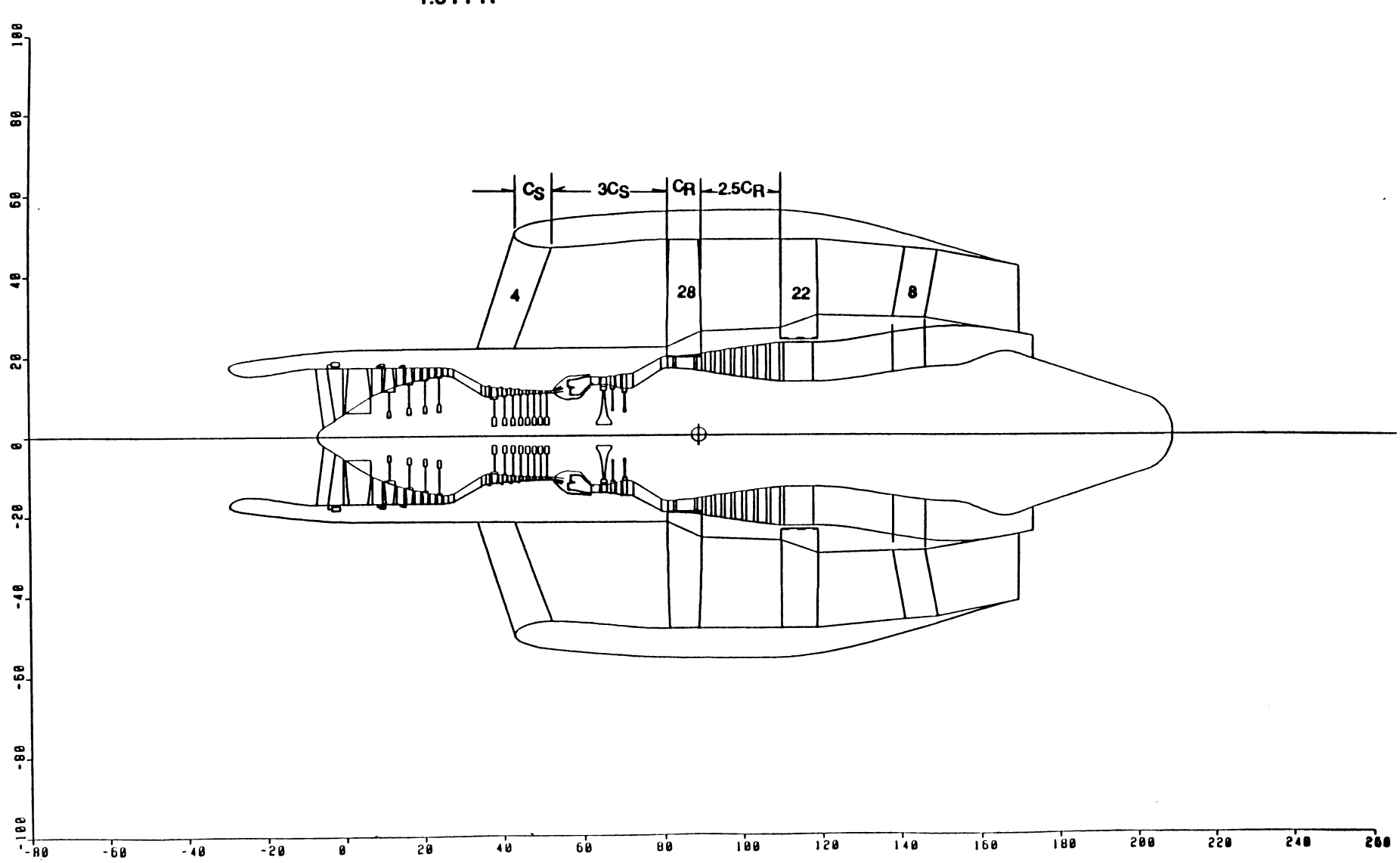

Figure 11 Aft Direct-Drive Counter-rotating Fan Engine 6 Cross-section

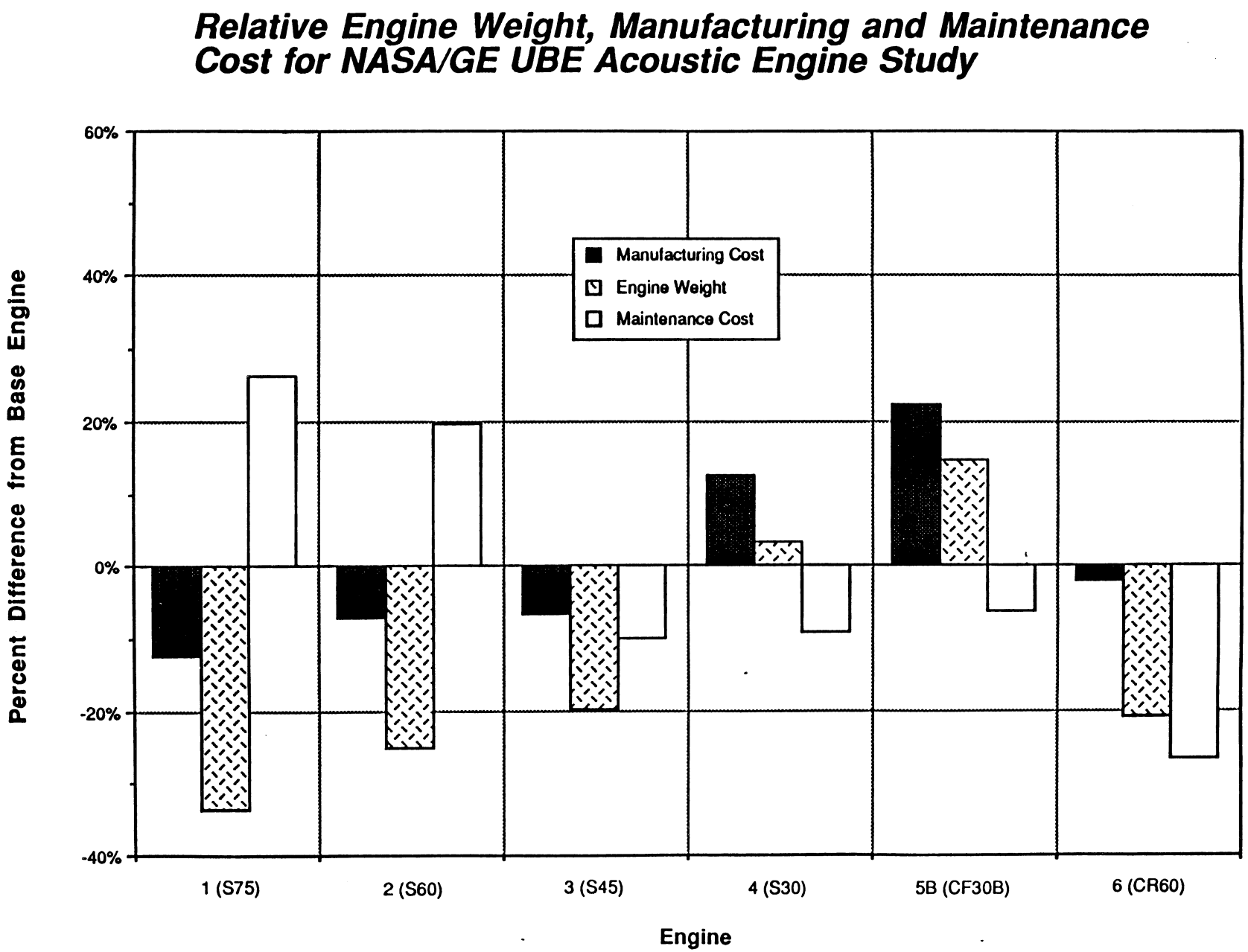

Figure 12 Weight, Manufacturing, and Maintenance Cost Trends

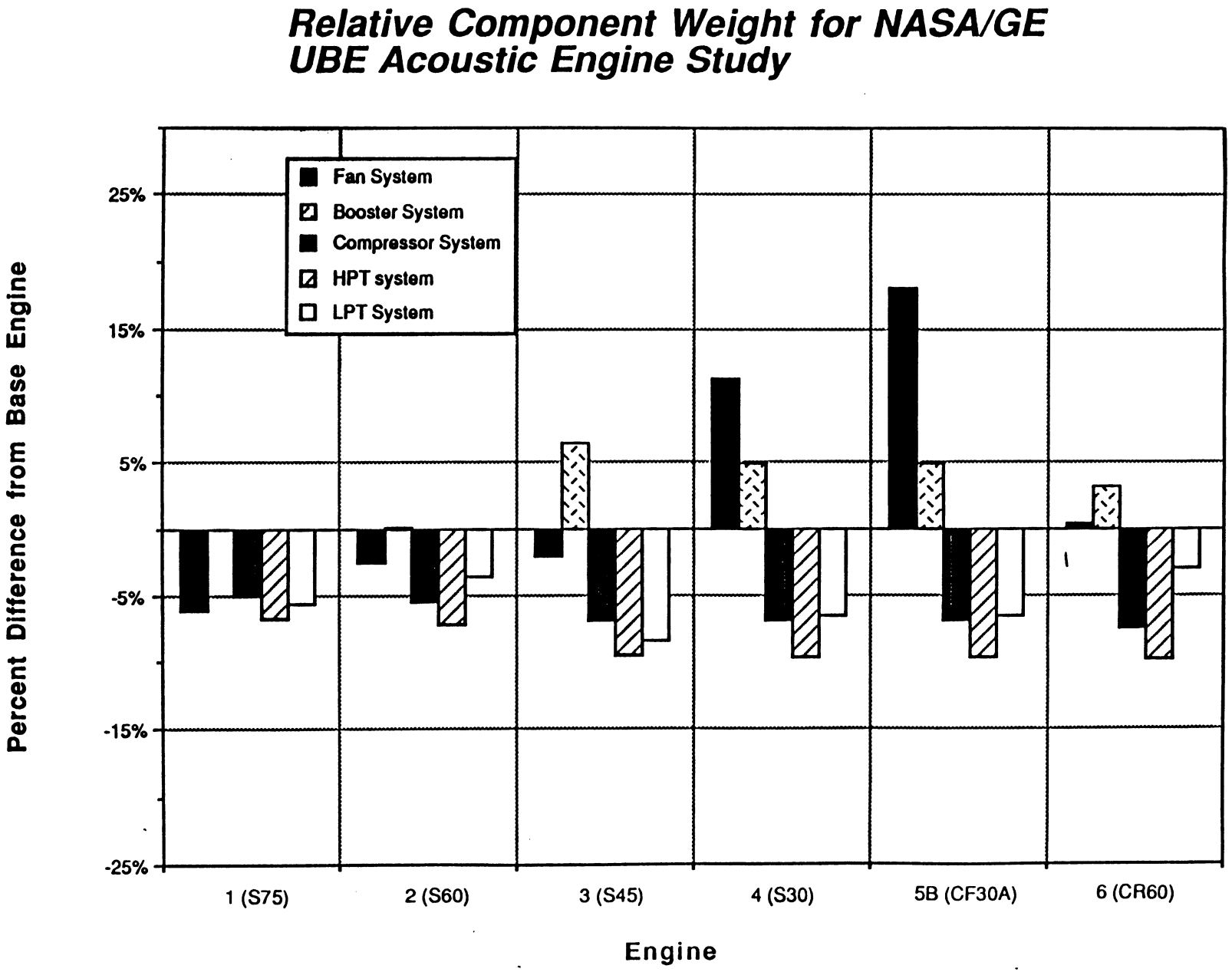

Figure 13 Relative Component Weight Breakdown for Engines 1 through 6

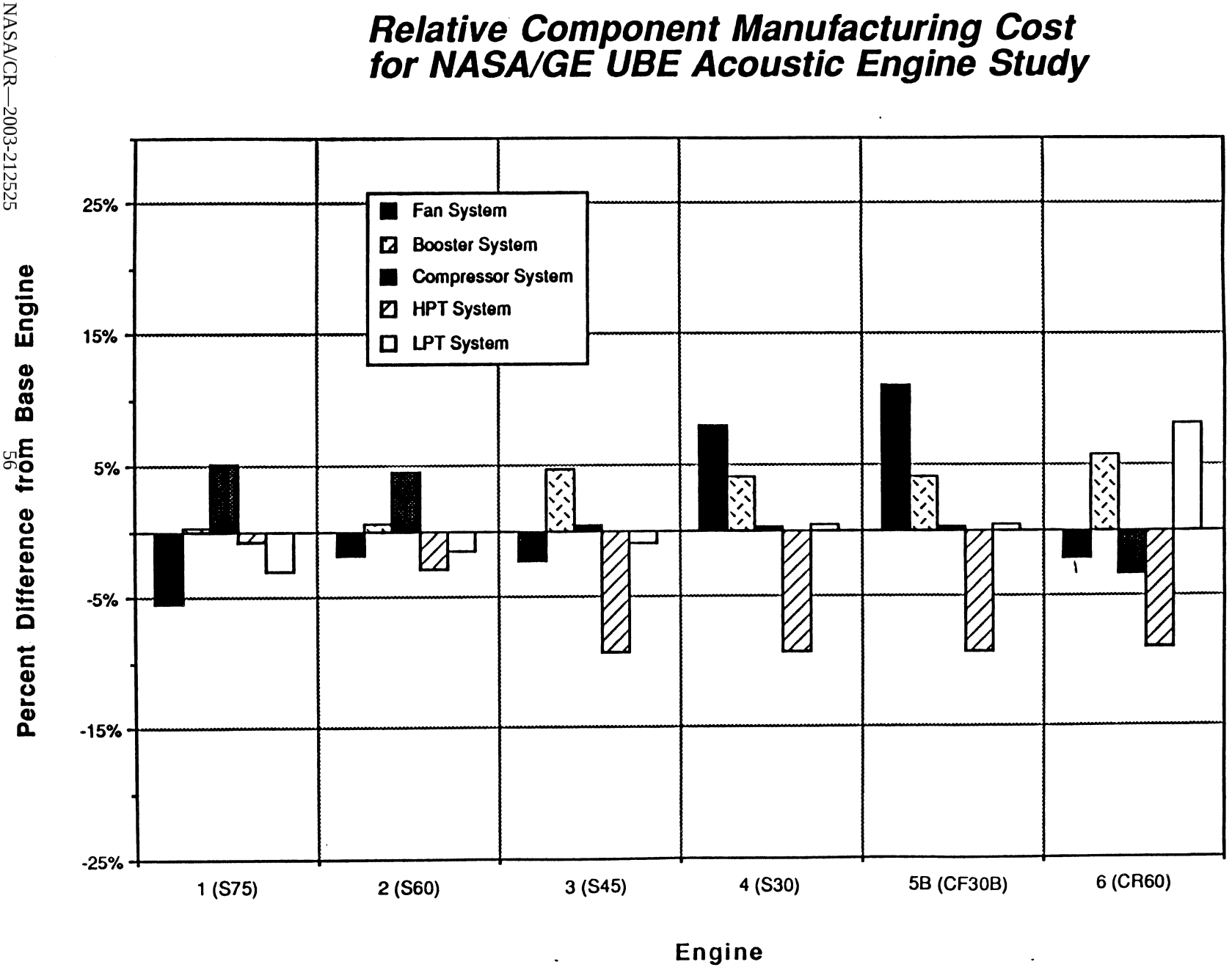

Figure 14 Relative Component Manufacturing Cost Breakdown

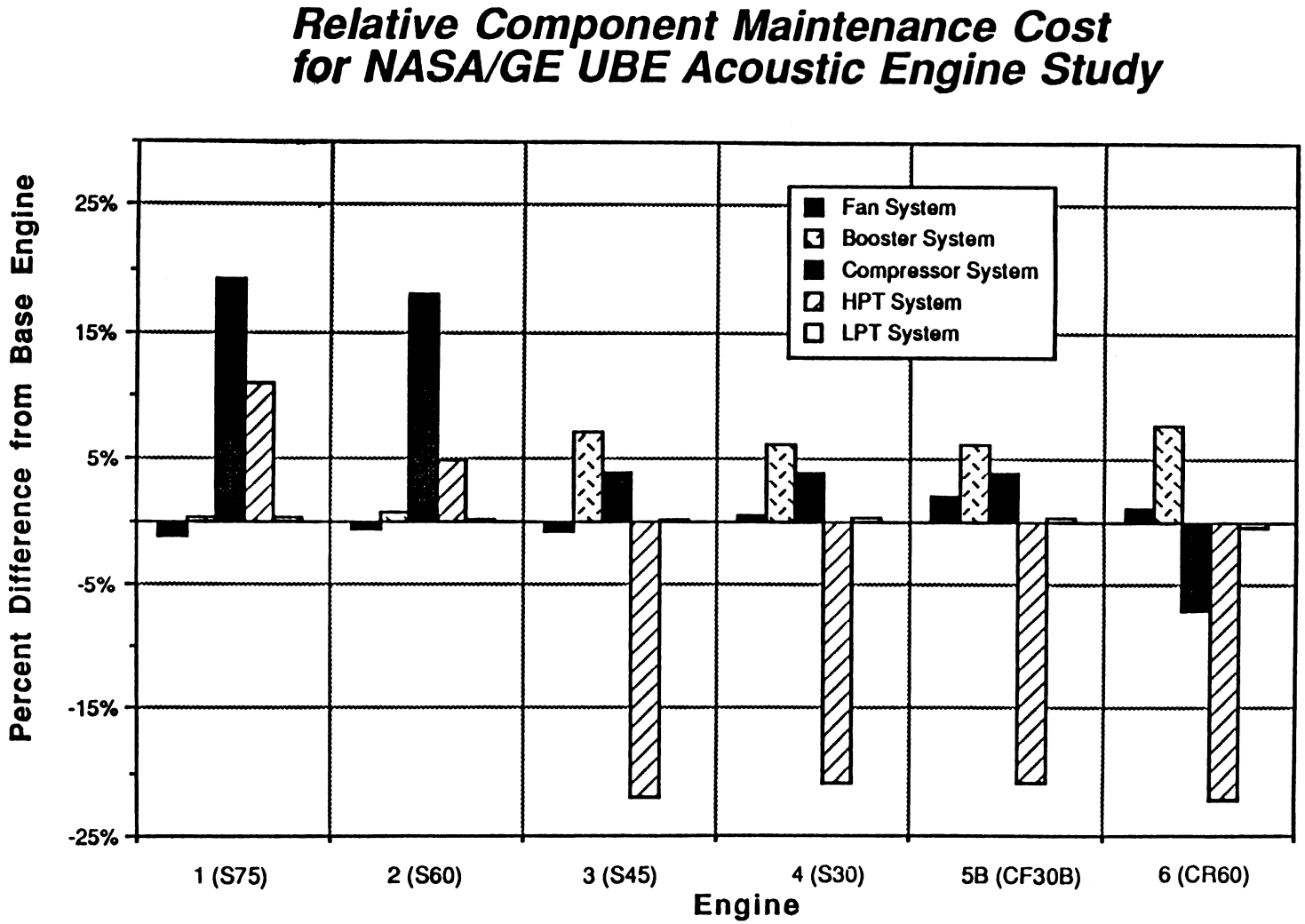

Figure 15 Relative Component Maintenance Cost Breakdown

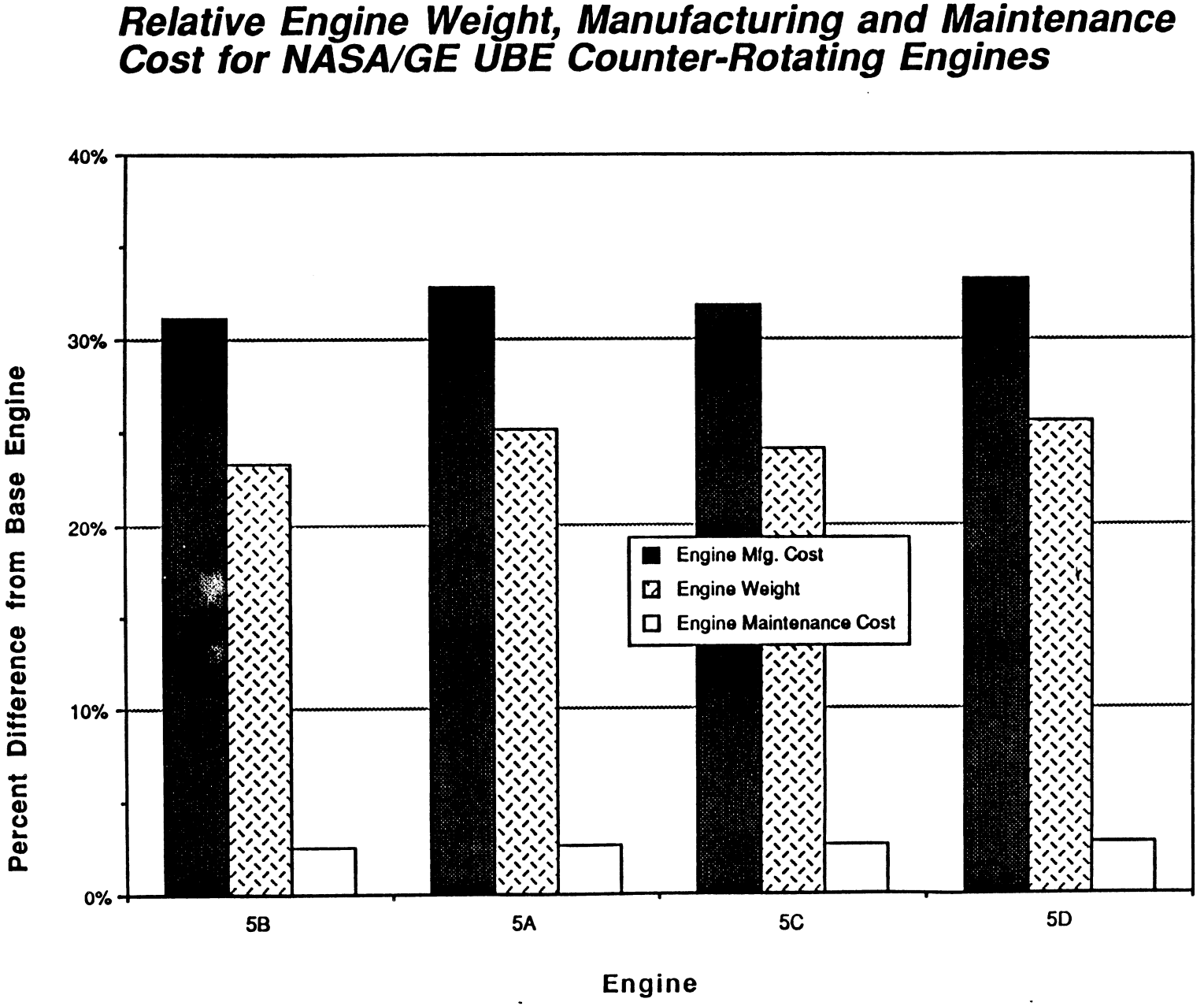

Figure 16 Relative Weight and Cost for Engine 5 Variations

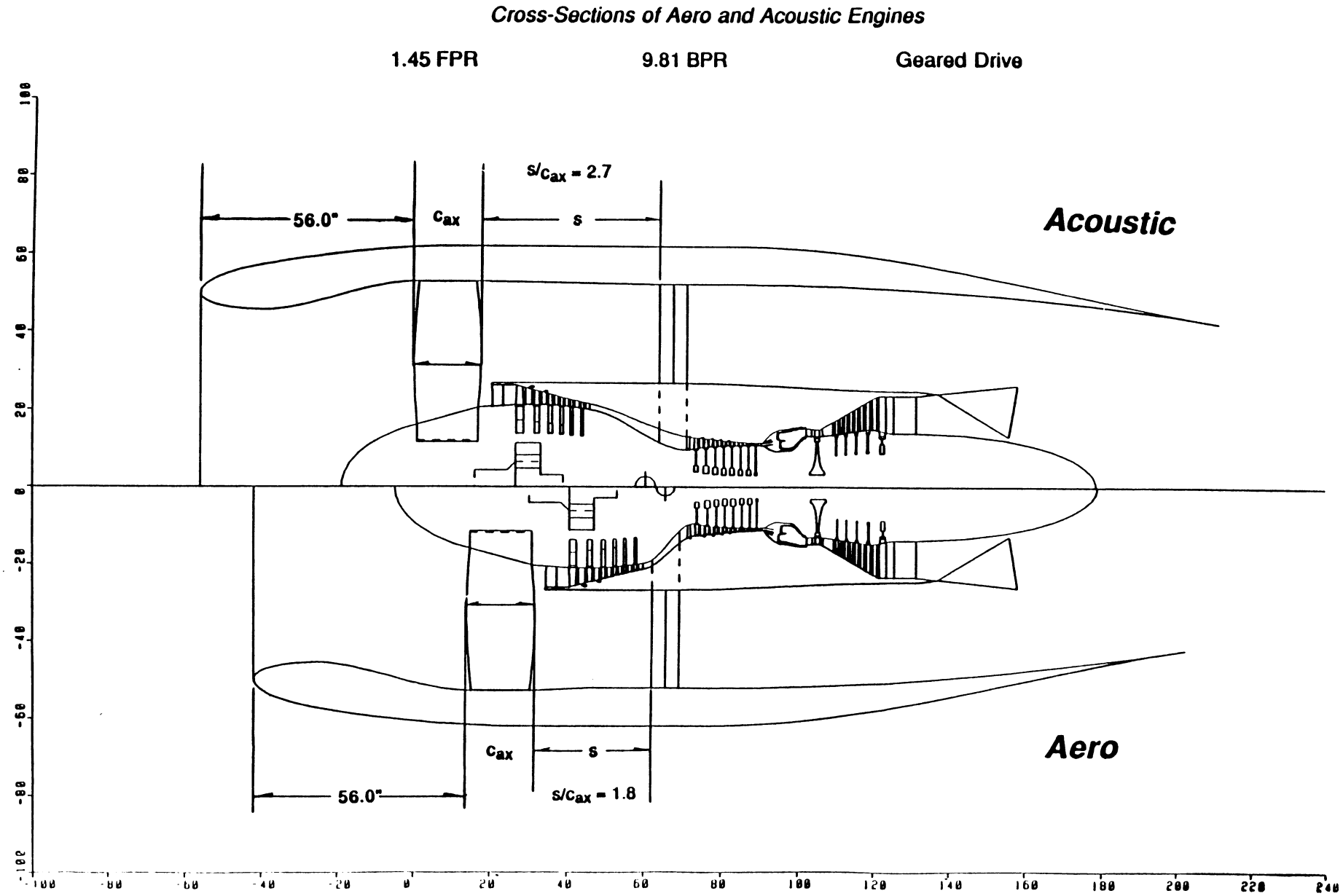

Figure 17 Engine 3 Cross-Section Modifications for Acoustic Changes

Relative Engine Weight, Manufacturing and Maintenance Cost Comparison for 1.45 FPR Geared Configuration

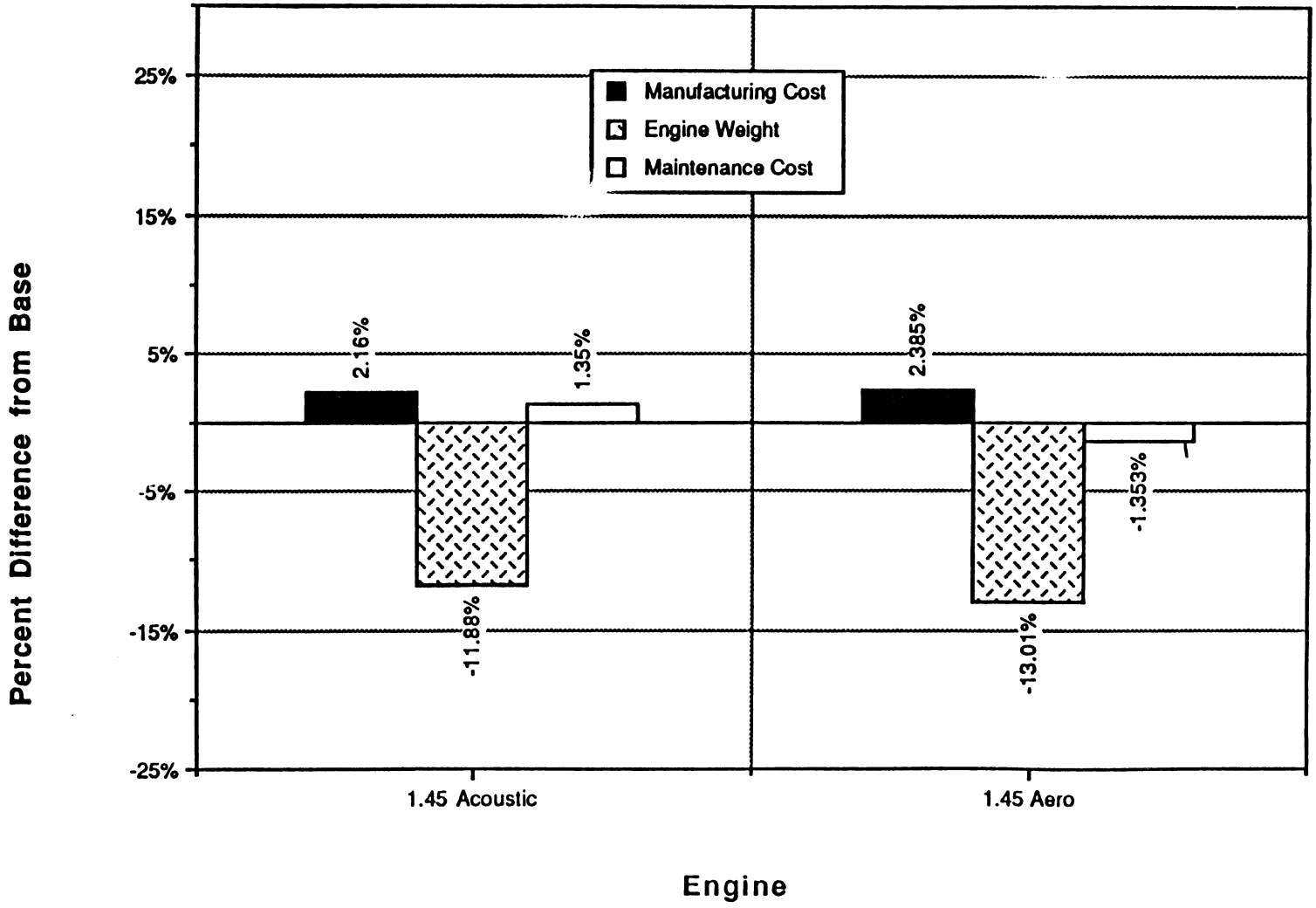

Figure 18 Impact of Acoustic Changes on Weight and Cost - Engine 3

Take-off

MTOGW 407,000 lbs

Thrust cutback point 984 ft

After cutback maintain a 4% gradient with AEO, All Engines Operating or level flight with OEI, One Engine Inoperative

Landing

Fixed weight and thrust

Mission

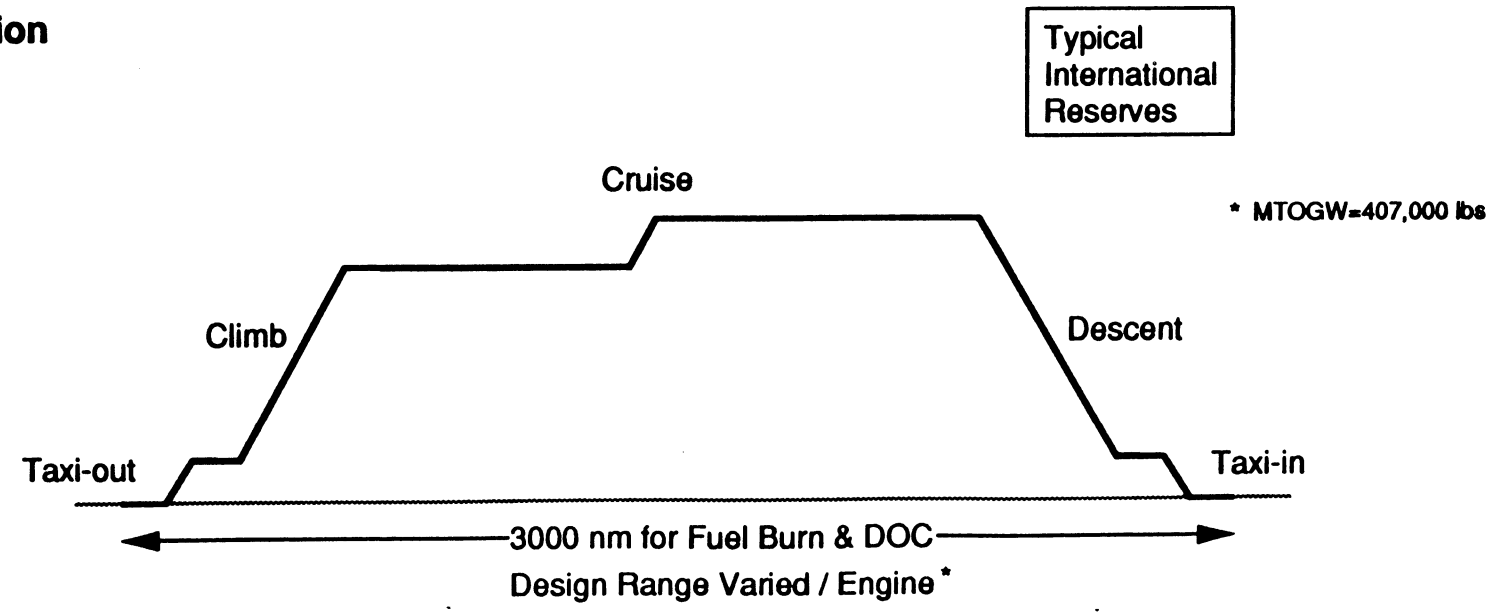

Figure 19 Engine/Aircraft Mission Profile Description

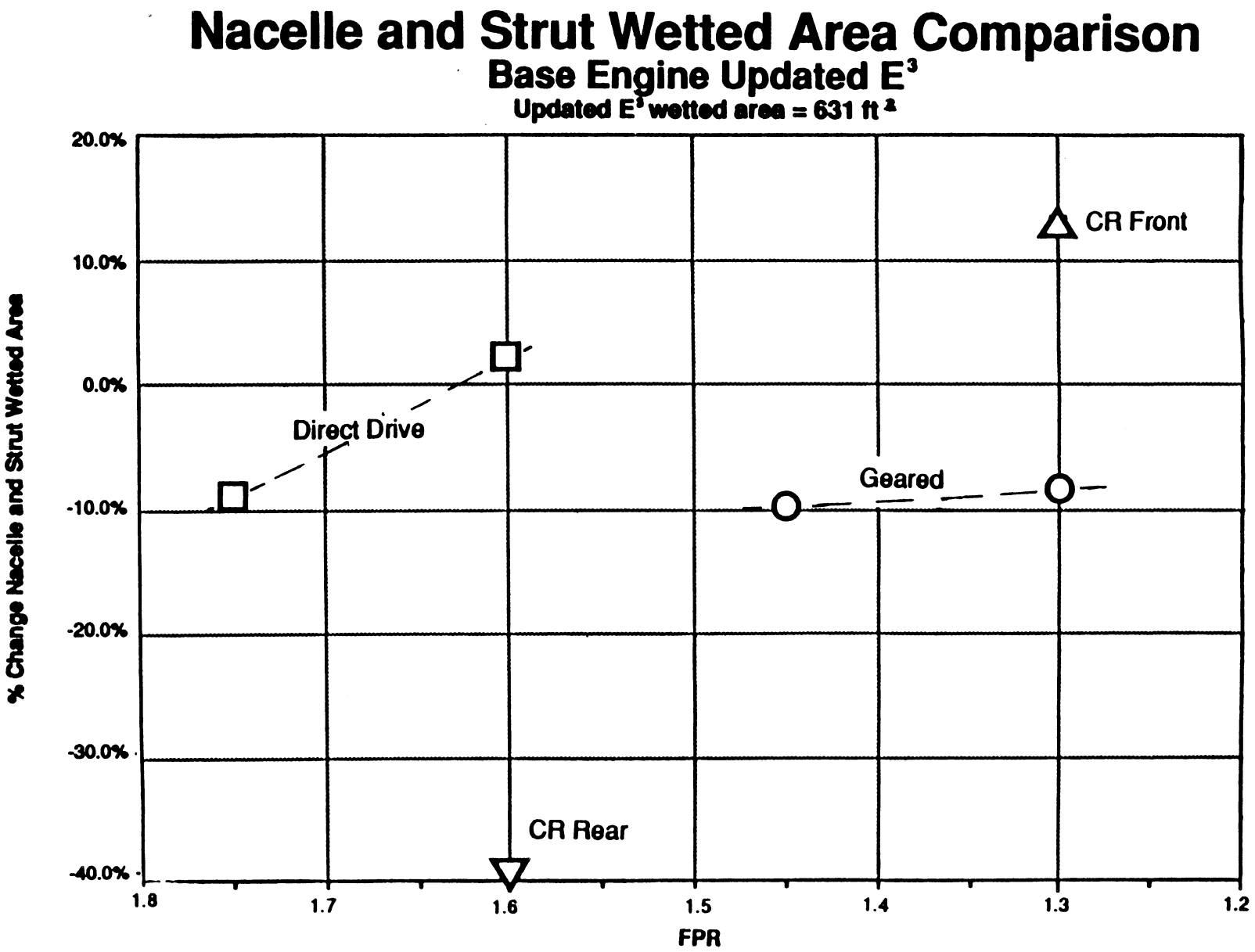

Figure 20 Nacelle plus Pylon Wetted Area Comparison

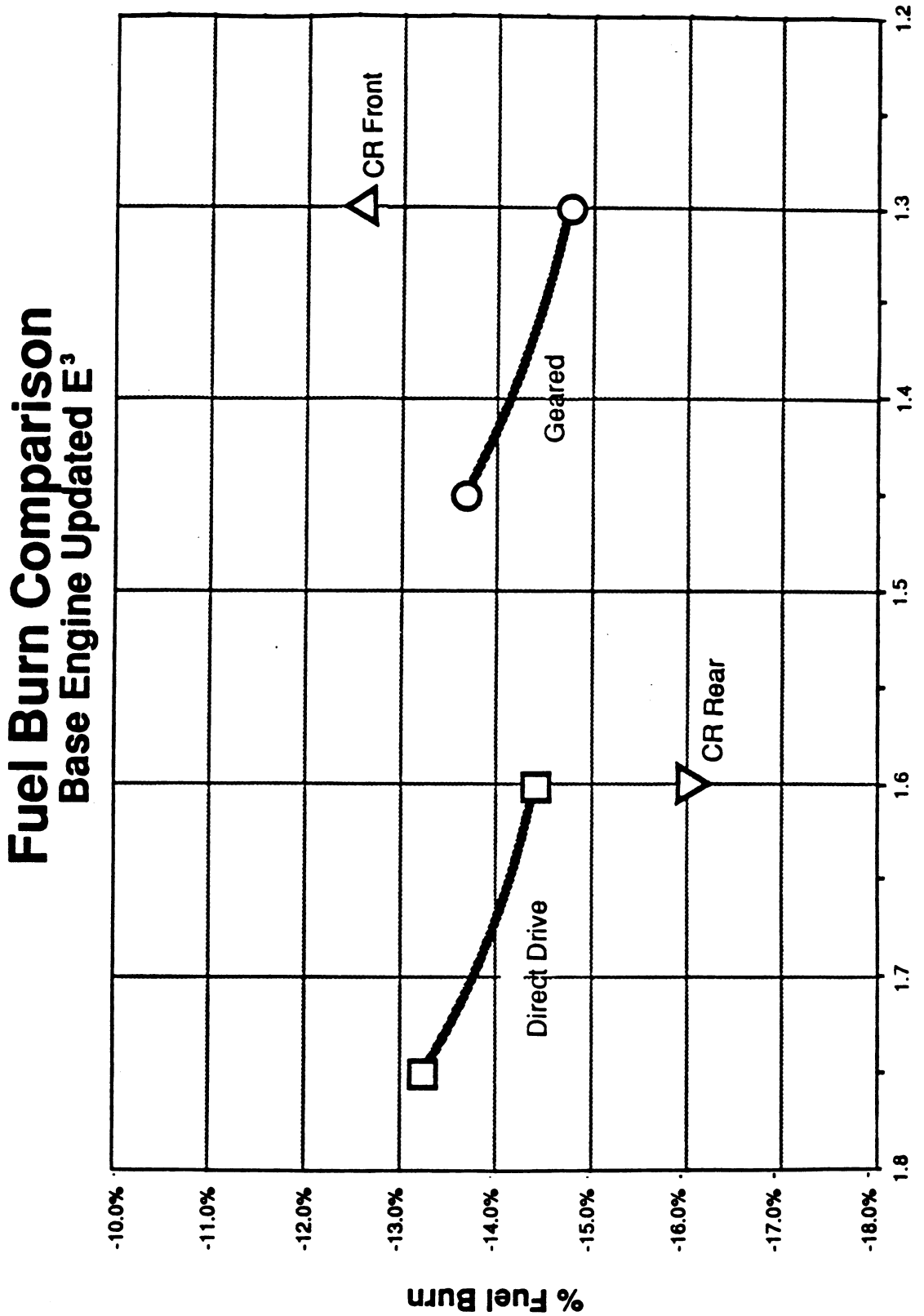

Figure 21 Advanced Engine Fuel Burn Improvement Comparison

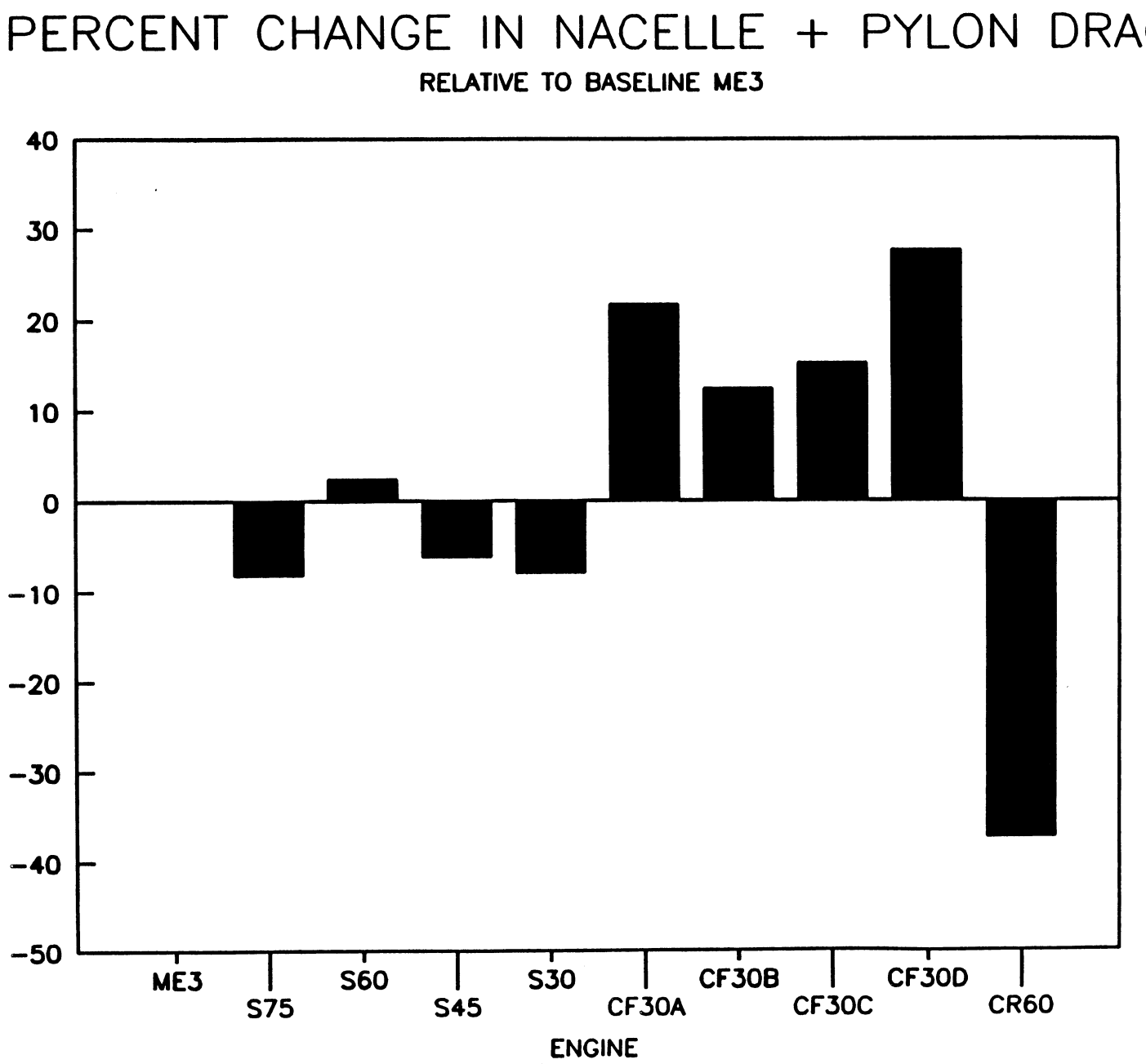

Figure 22 Advanced Engine Nacelle Drag Change Comparison

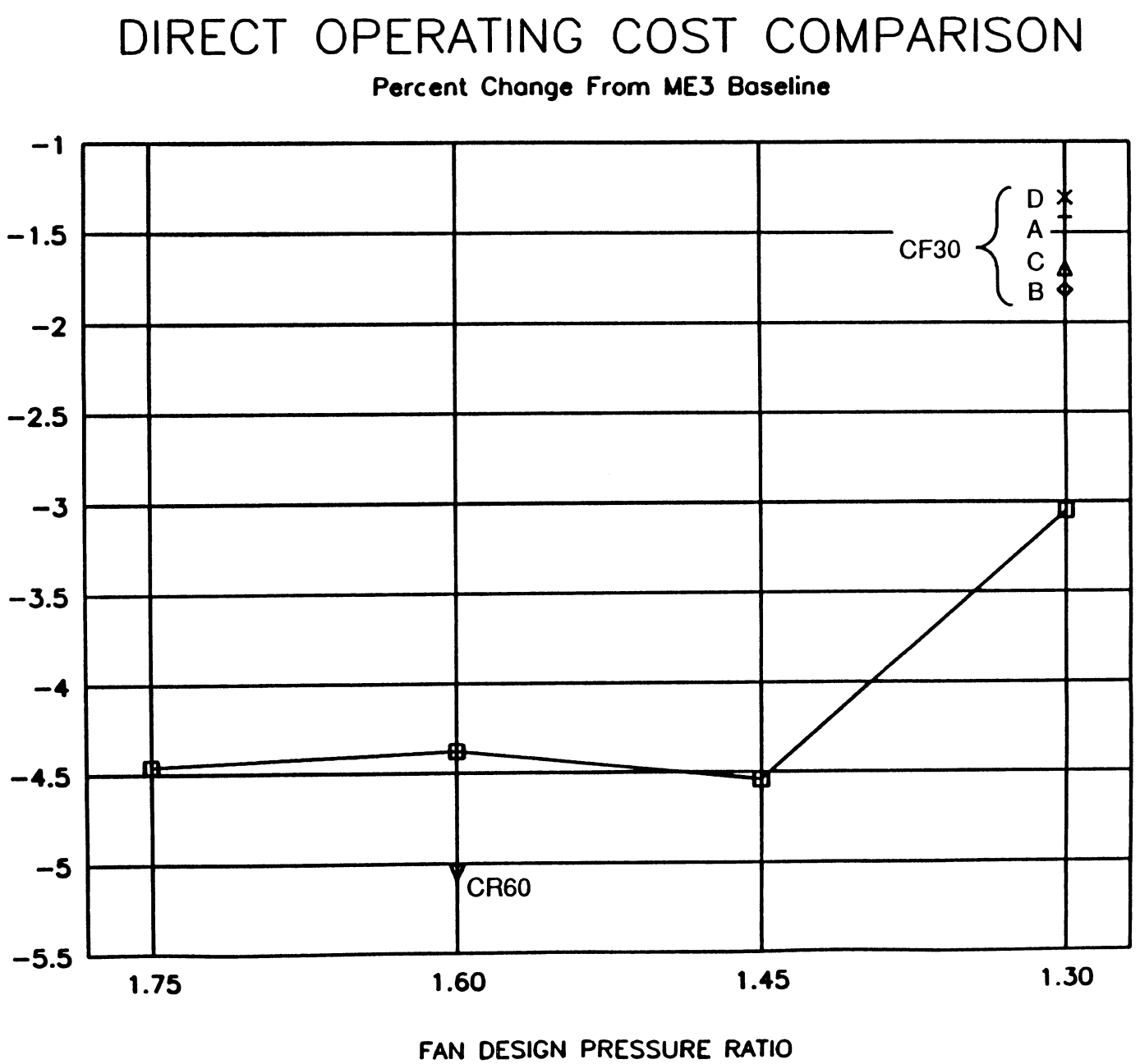

Figure 23 Advanced Engine Direct Operating Cost Change Comparison

AERO AND ECONOMIC PENALTY OF ACOUSTIC CHANGES
LONGER INTAKE AND WIDER AXIAL GAP
300NM MISSION FUEL $1.0/GAL

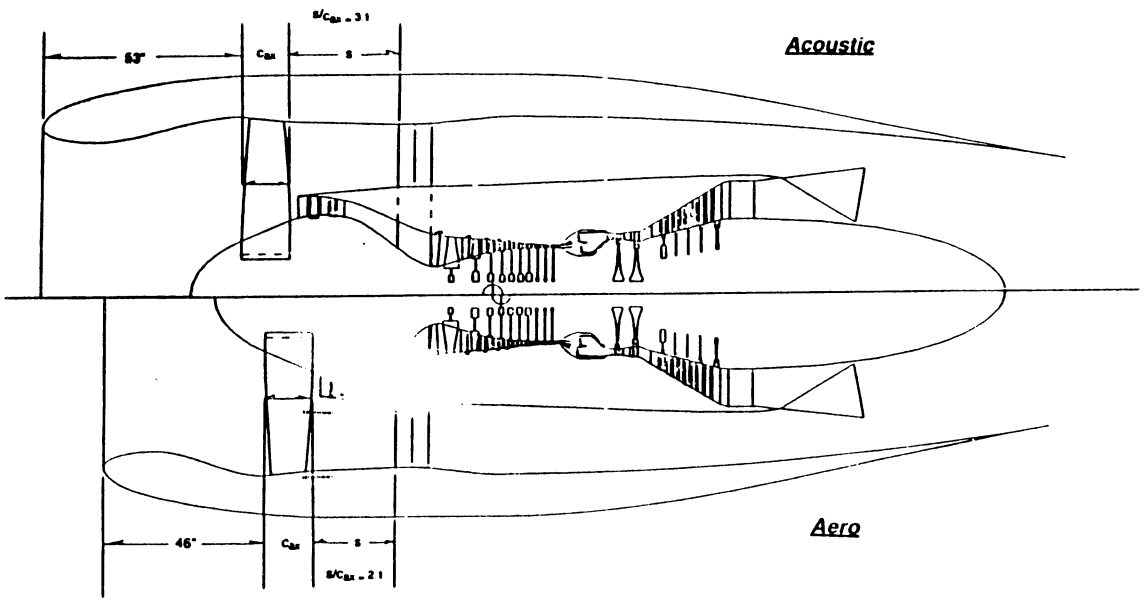

FPR	1.75	1.60	1.45	1.30
△ LENGTH INS	20	26	22.5	34
% △ WEIGHT	1.77	2.43	1.20	2.29
% △ COST	1.12	1.447	0.9	1.308
% △ DRAG	.220	0.328	0.222	0.524
% △ FUEL BURN	0.313	0.470	0.292	0.686
% △ DOC	0.197	0.274	0.089	0.328

Figure 24 Performance/Economic Penalties of Acoustic Changes

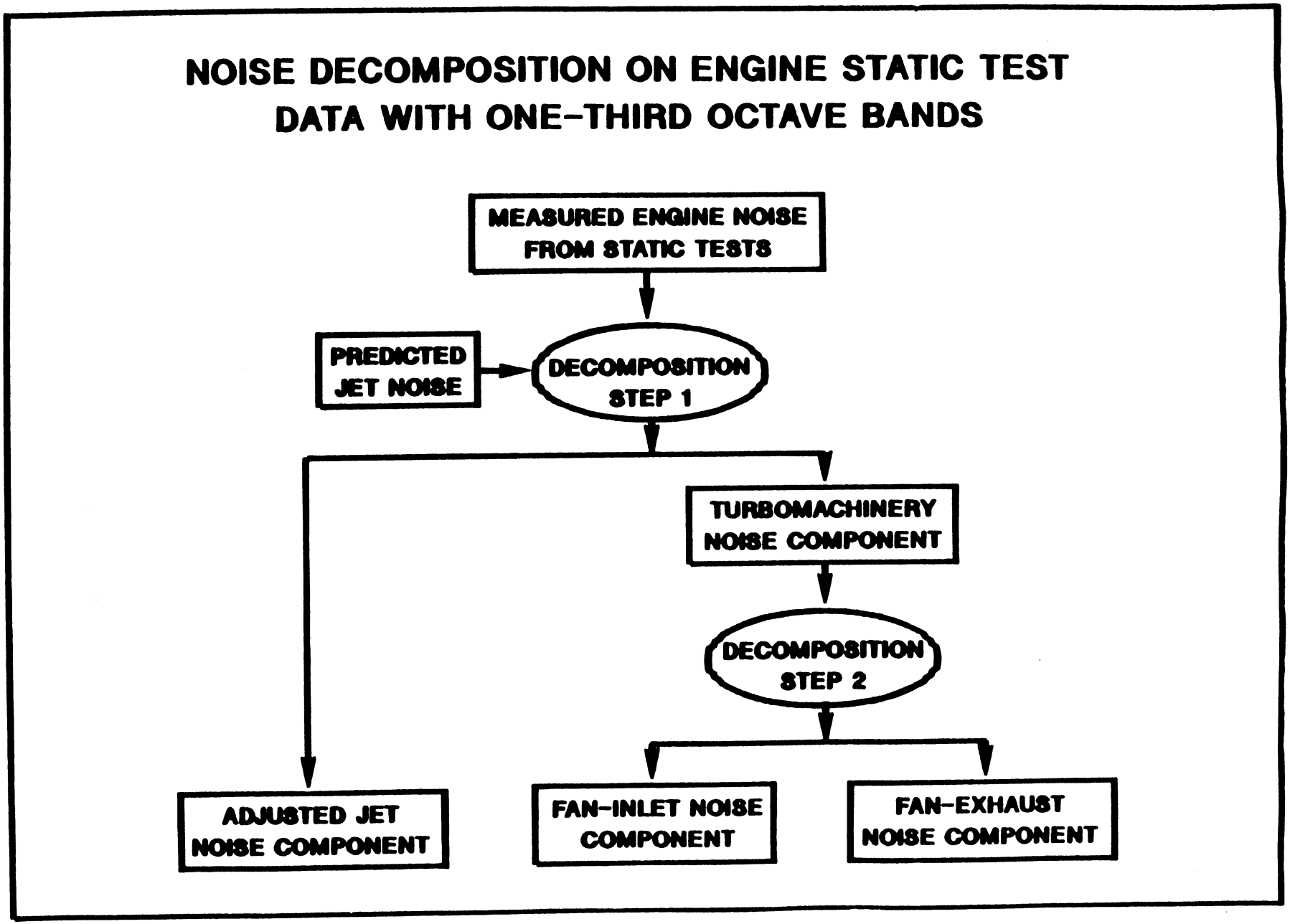

Figure 25 Engine Test Noise Data Component Decomposition Diagram

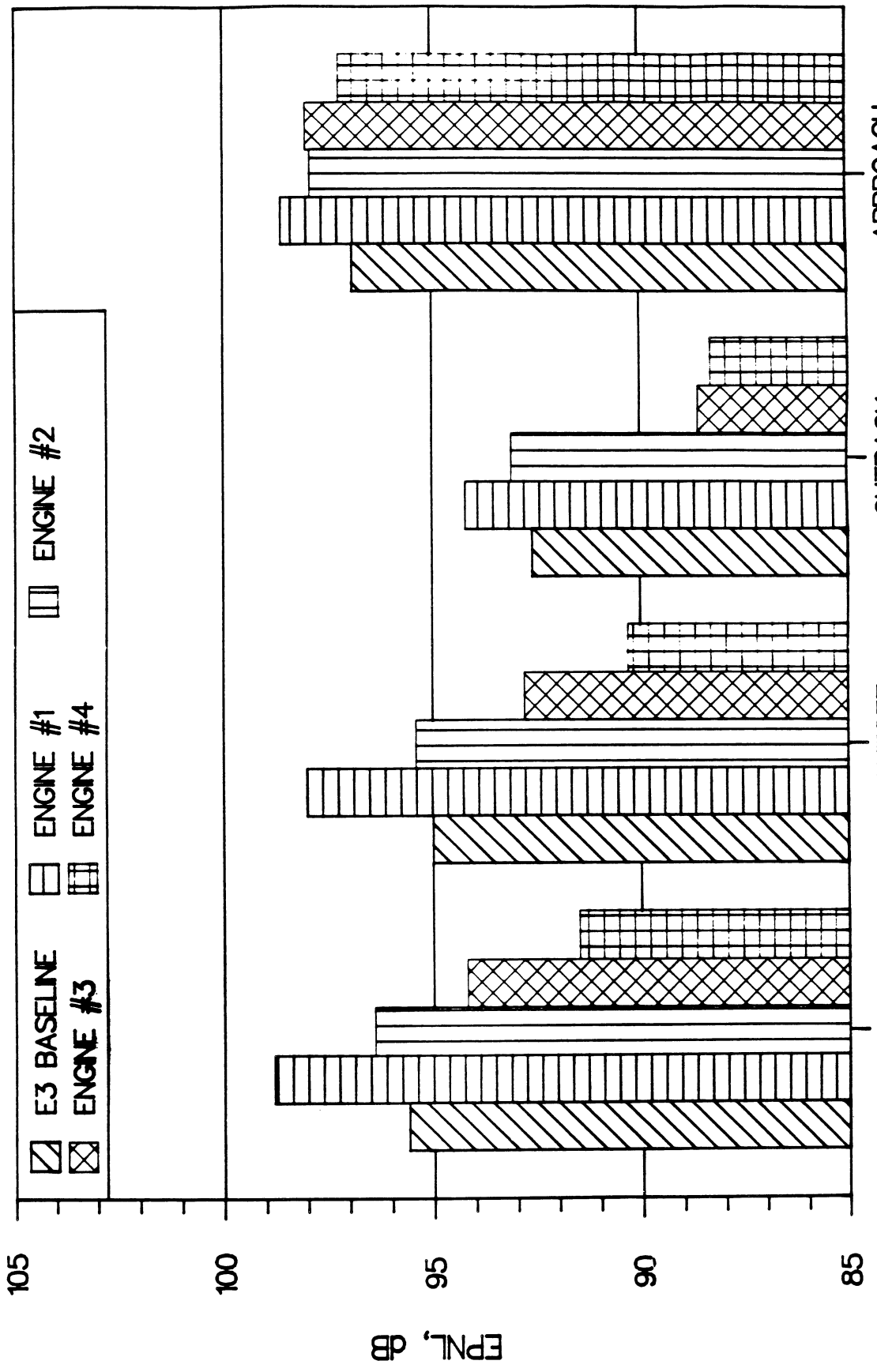

Figure 26 Single-Rotation Engine System Total Noise Comparisons

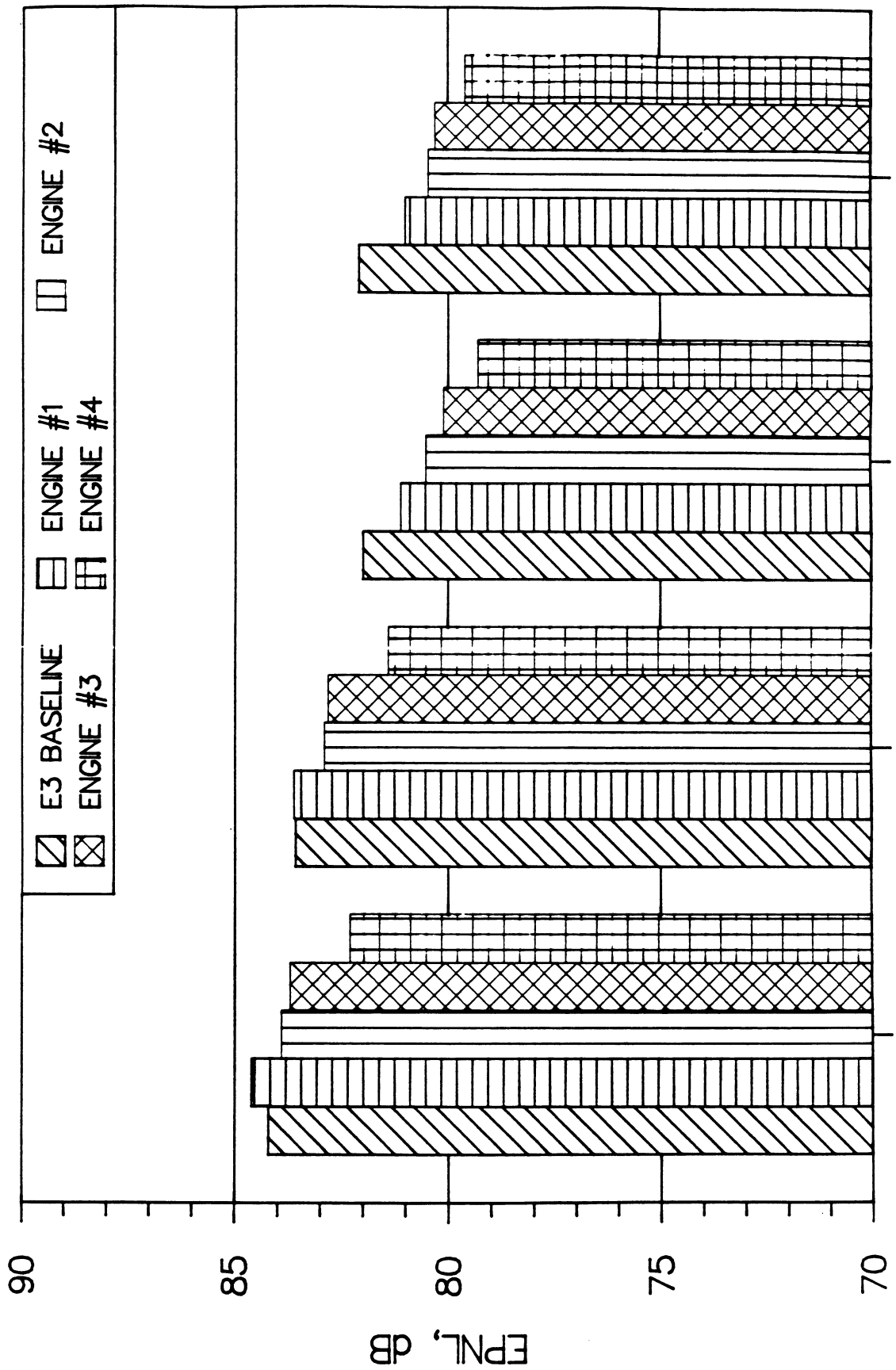

Figure 27 Single-Rotation Engine Combustion/Core Noise Comparisons

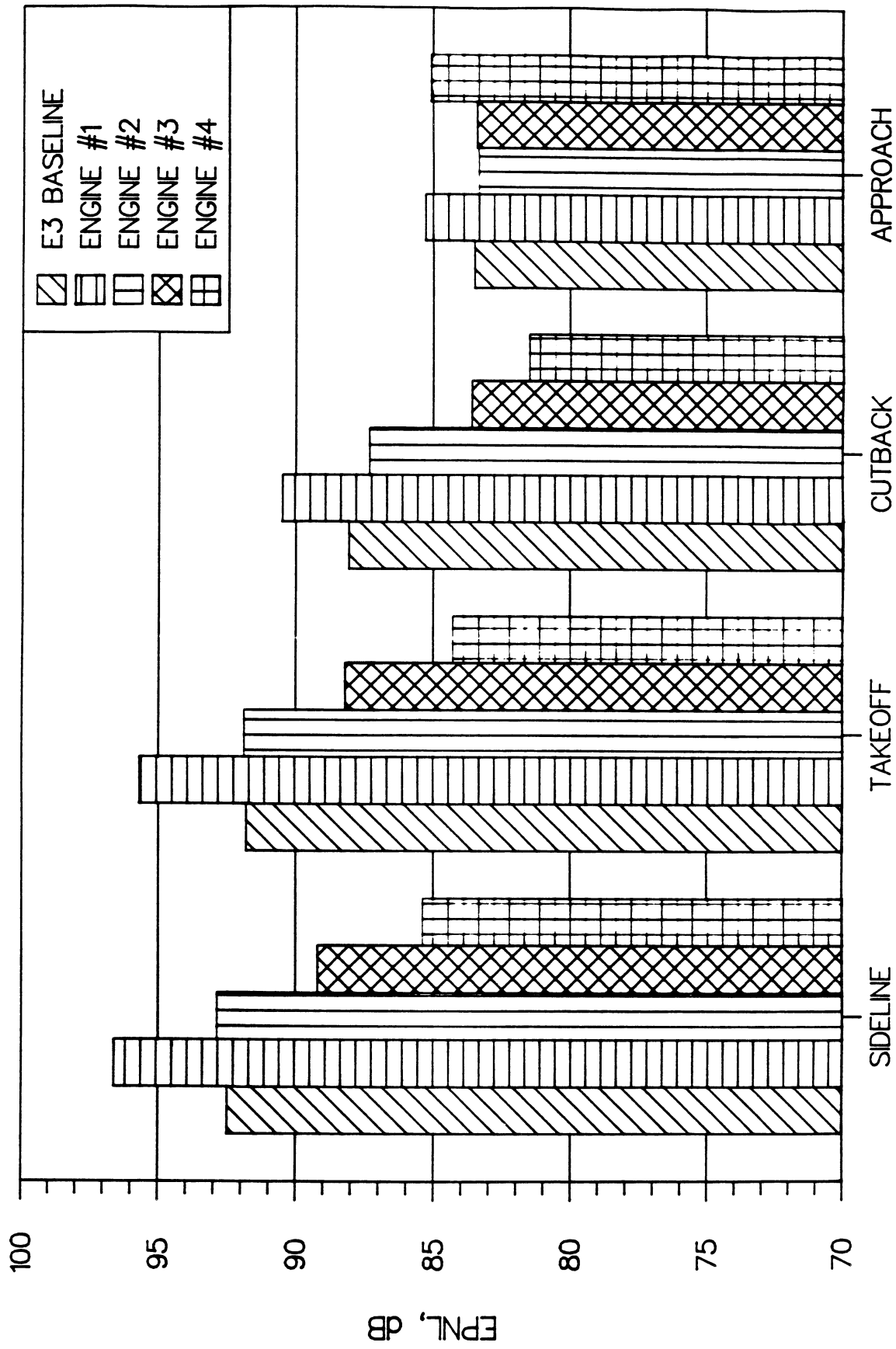

Figure 28 Single-Rotation Engine Jet Mixing Noise Comparisons

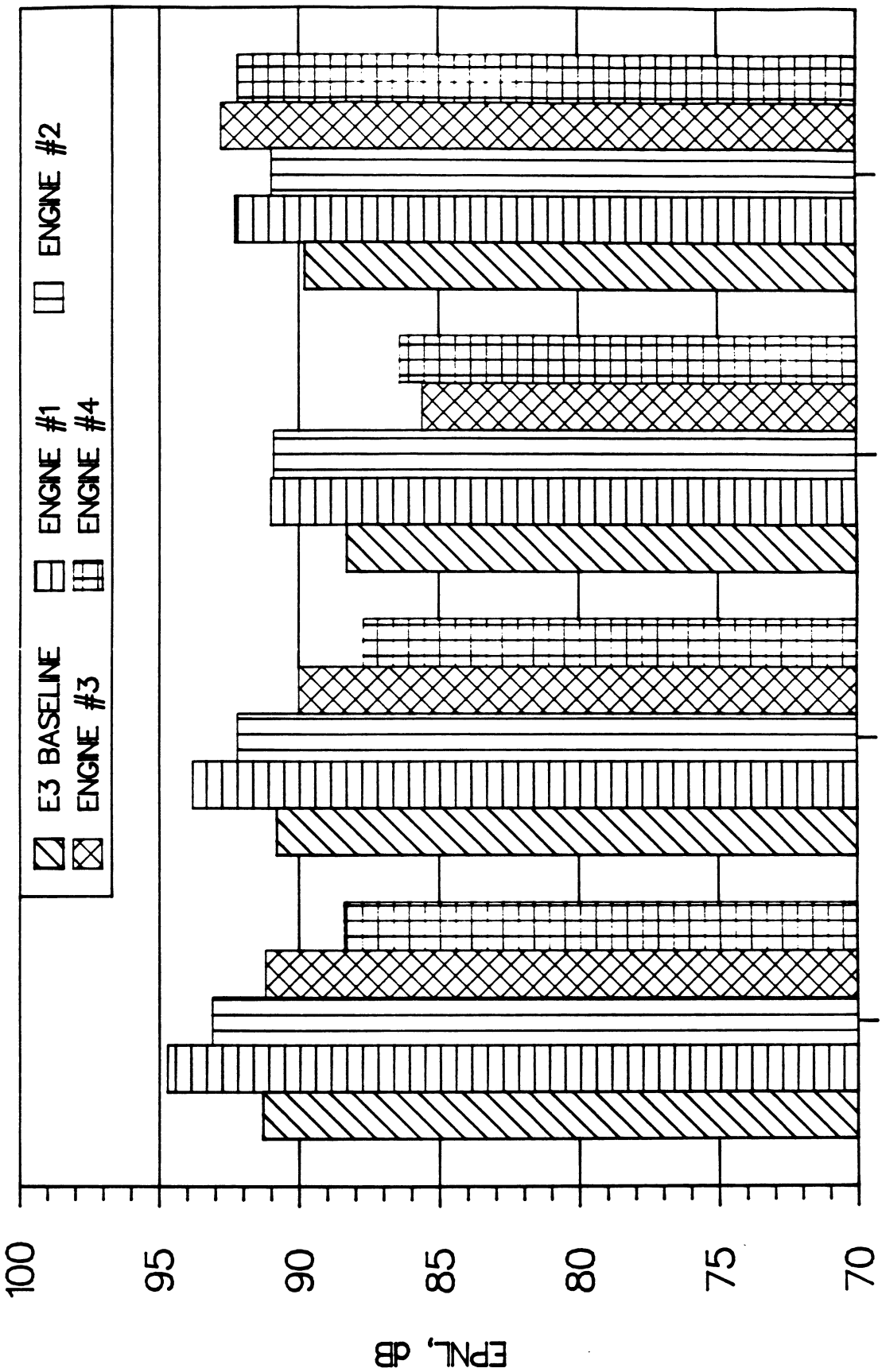

Figure 29 Single-Rotation Engine Fan Exhaust Noise Comparisons

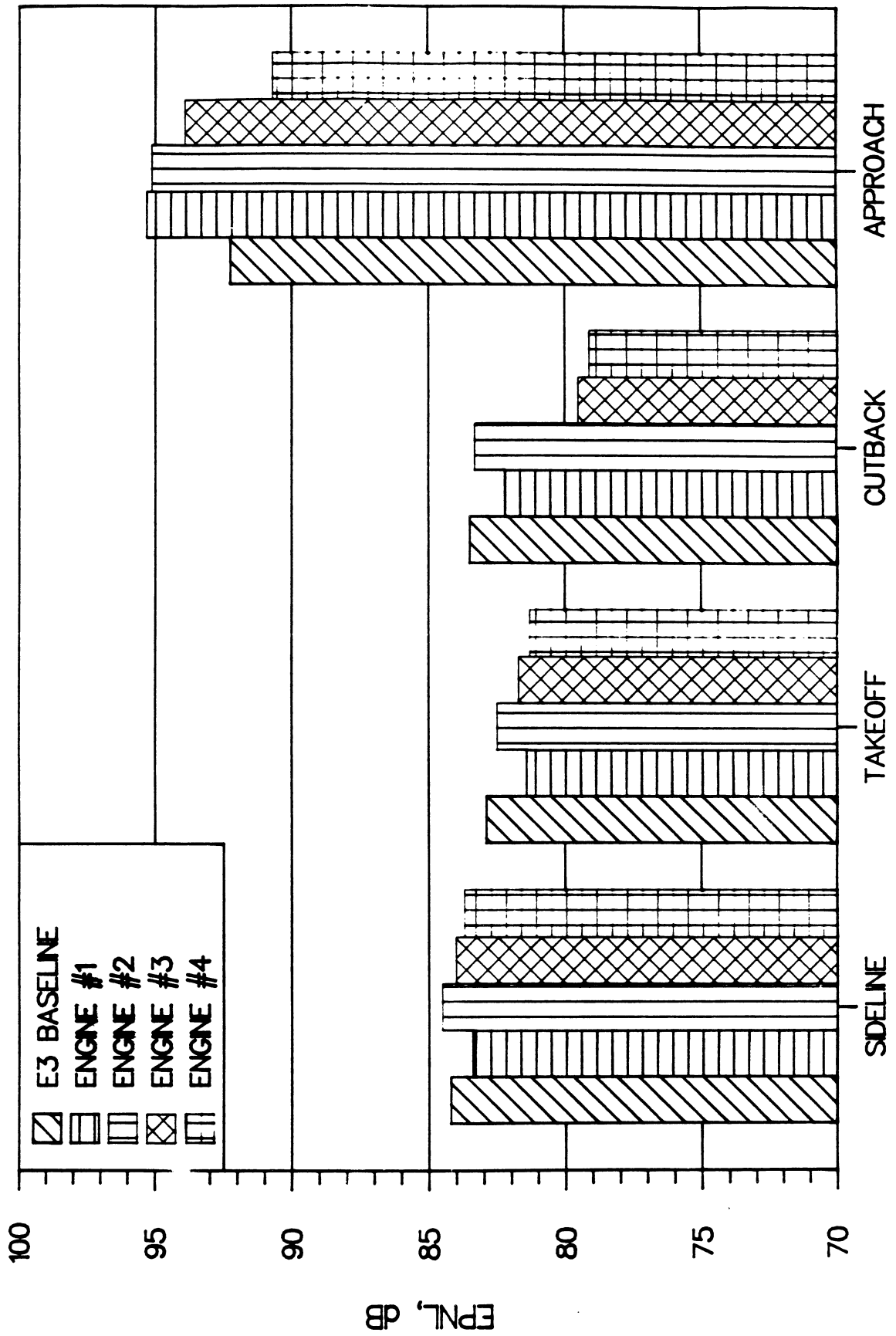

Figure 30 Single-Rotation Engine Fan Inlet Noise Comparisons

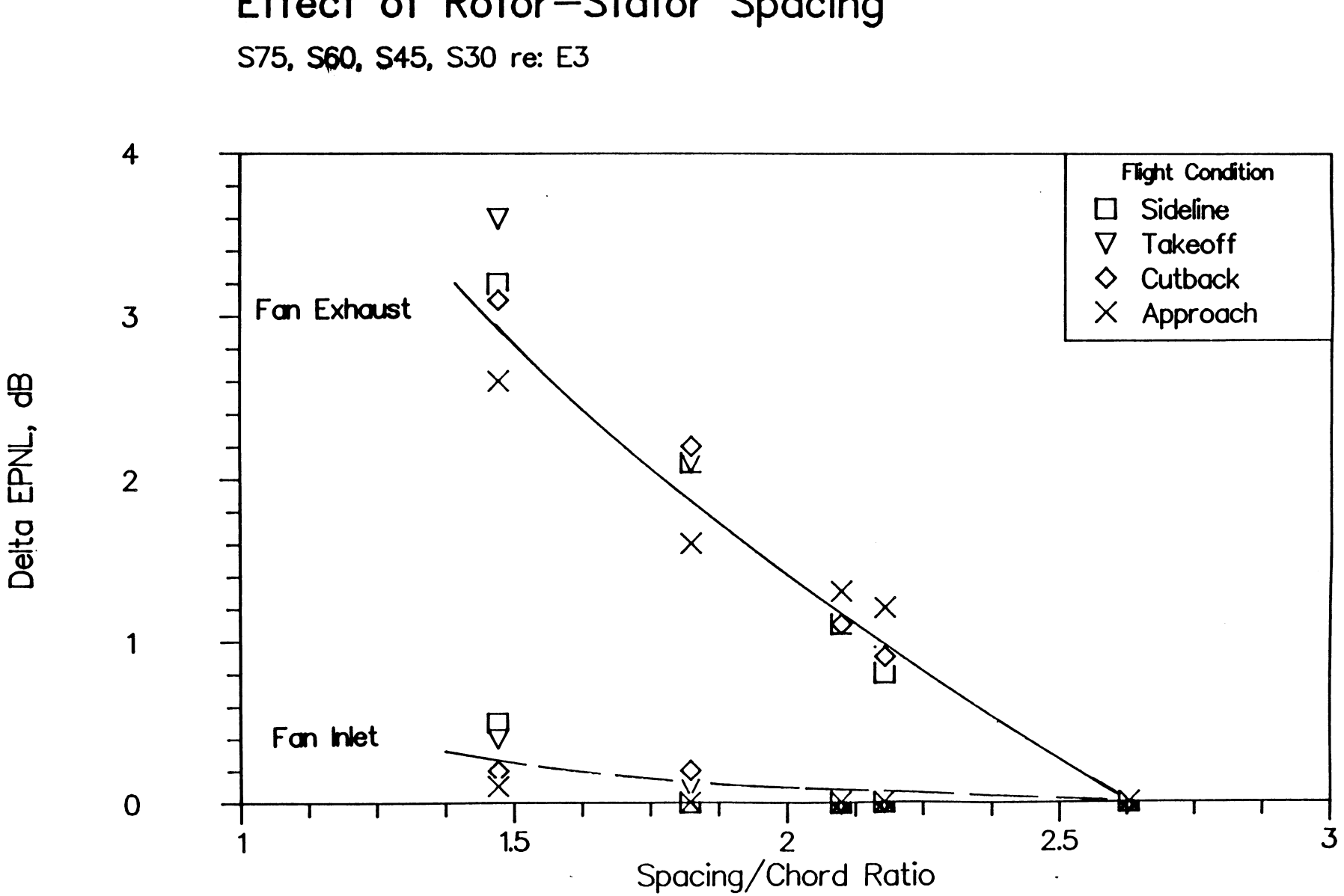

Figure 31 Effect of Rotor-Stator Axial Spacing on System EPNL

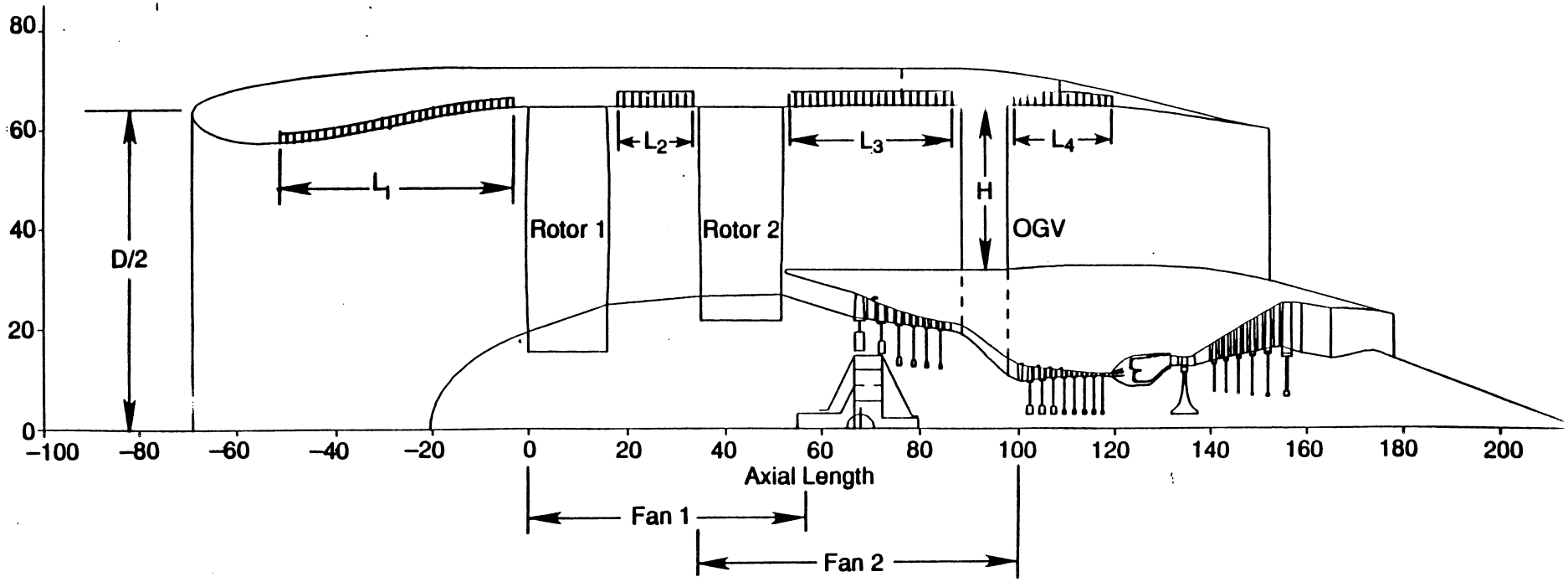

Fan 1:
$(L/D)_{IN} = (L_1)/D$
$(L/H)_{EX} = (L_3+L_4)/H$

Fan 2:
$(L/D)_{IN} = (L_1+L_2)/D$
$(L/H)_{EX} = (L_4)/H$

Figure 32 Counter-Rotating Ducted Fan Acoustic Model Schematic

CDF PRELIMINARY SYSTEM NOISE PROCESS

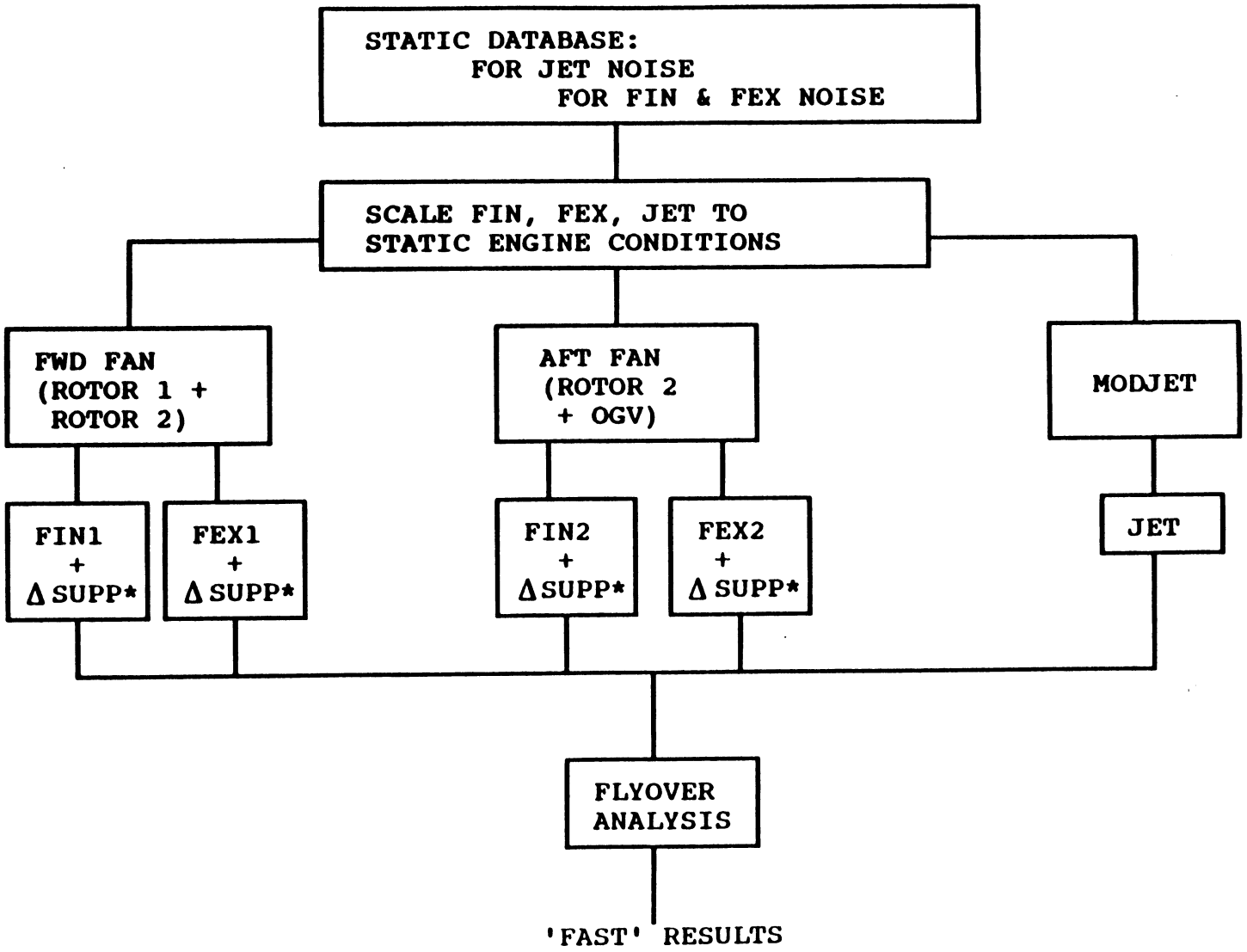

* ΔSUPP TO INCLUDE:
- TRANSMISSION LOSSES
- LINER SUPPRESSION

Figure 33 Counter-Rotating Ducted Fan Noise Synthesis Diagram

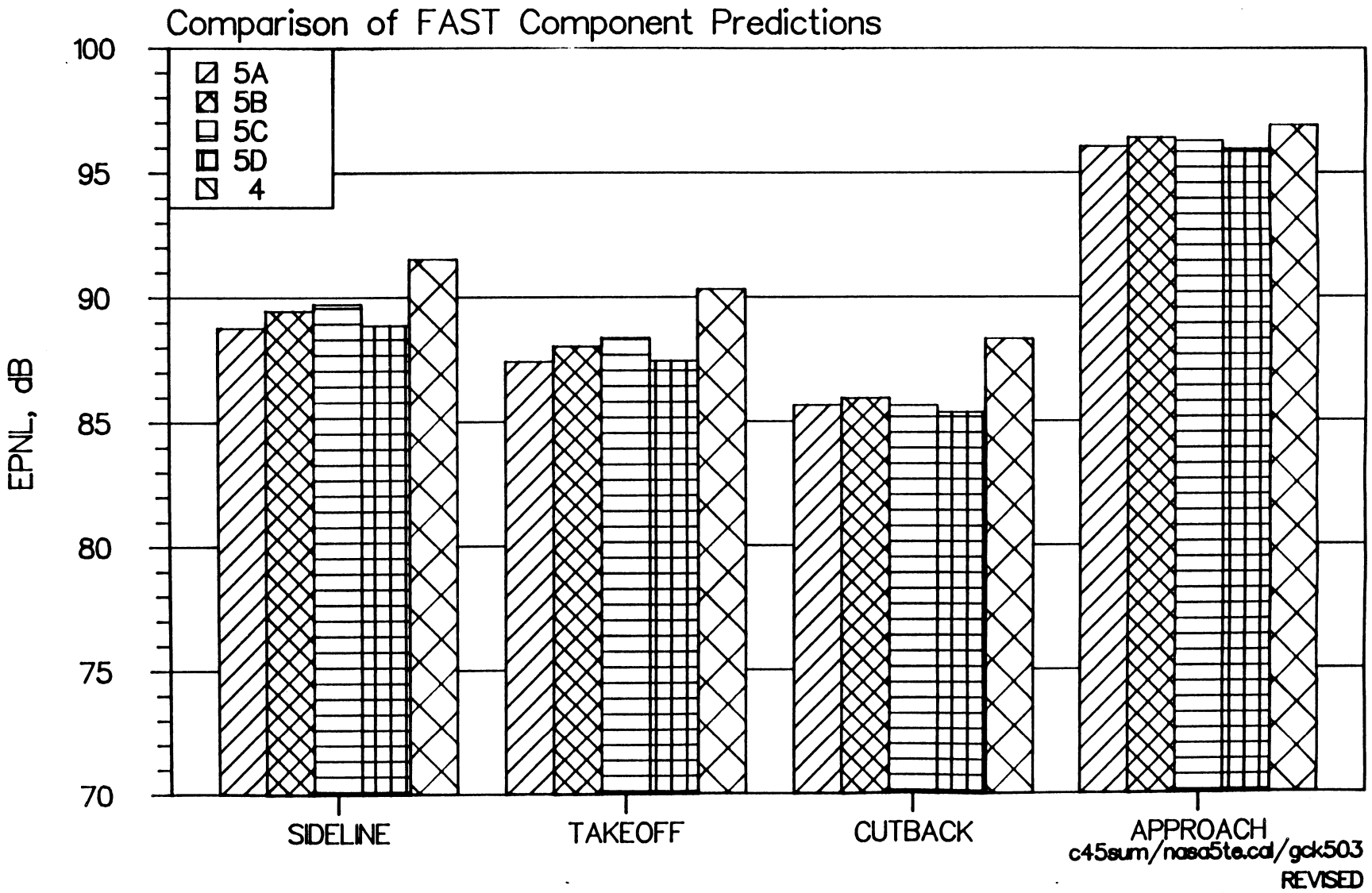

Figure 34 Front-Mounted, Geared CR Fan Engine 5 System Noise Results

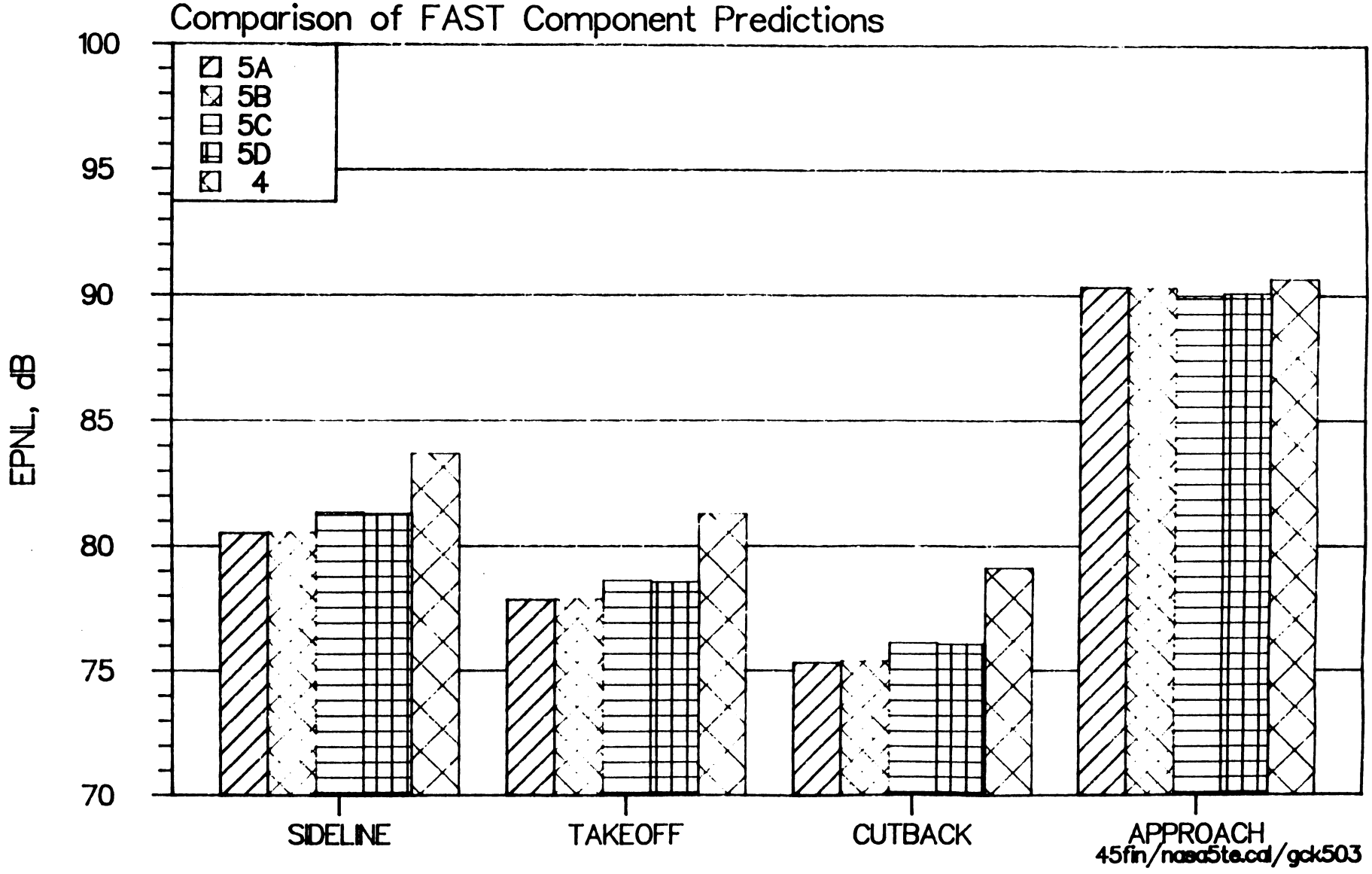

Figure 35 CR Engine 5 Fan Inlet Noise Component Comparisons

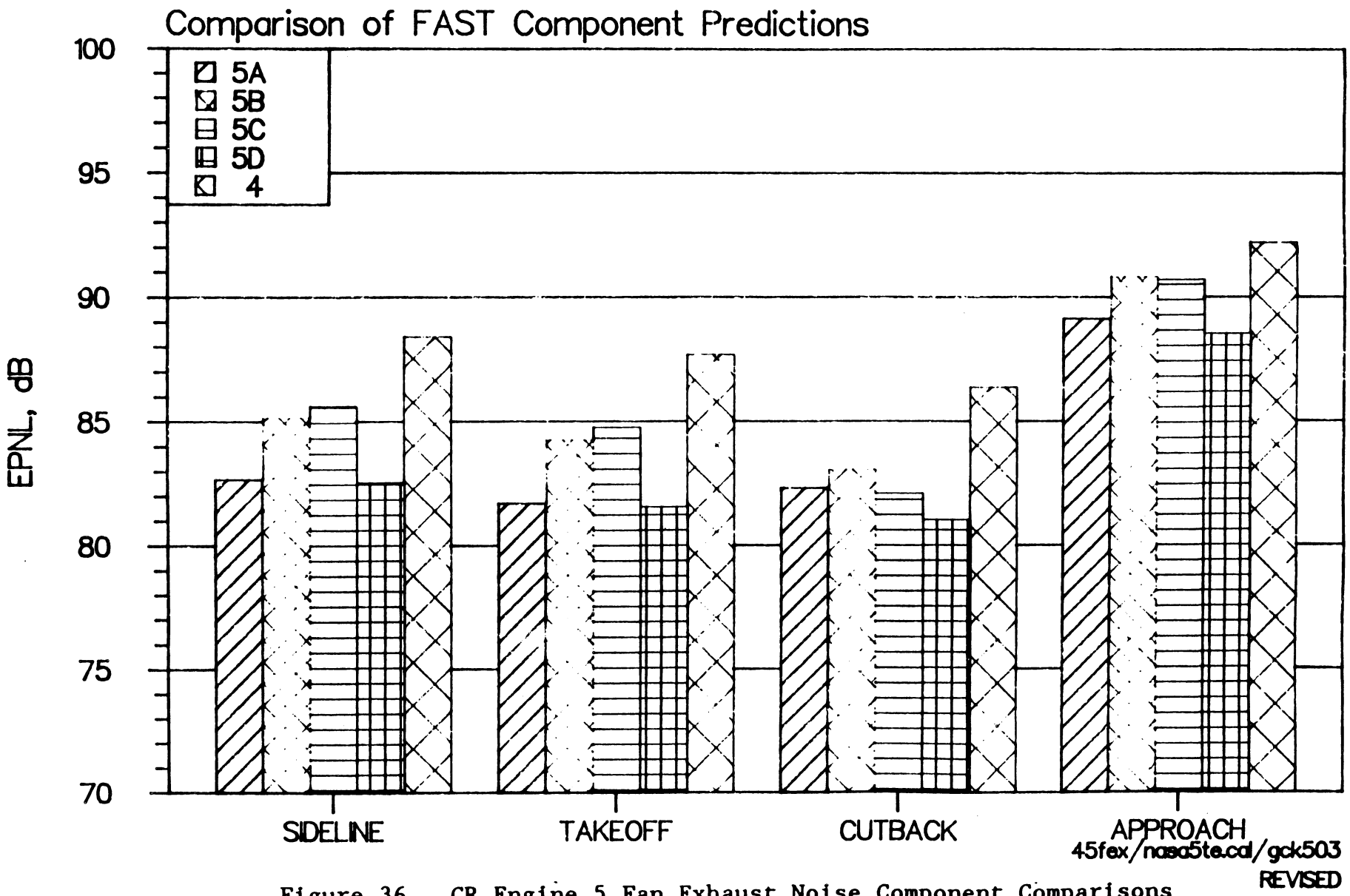

Figure 36 CR Engine 5 Fan Exhaust Noise Component Comparisons

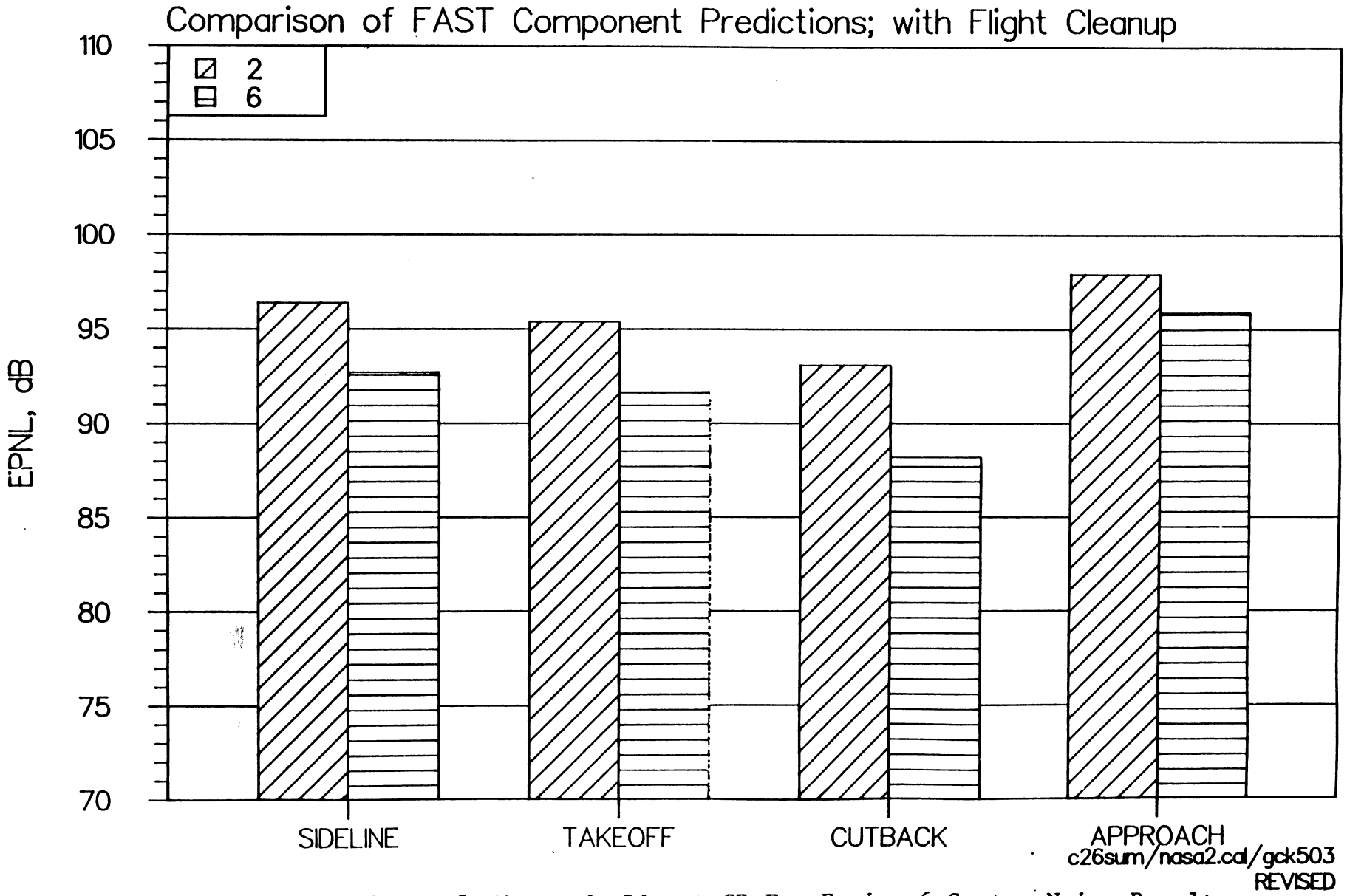

Figure 37 Aft-Mounted, Direct CR Fan Engine 6 System Noise Results

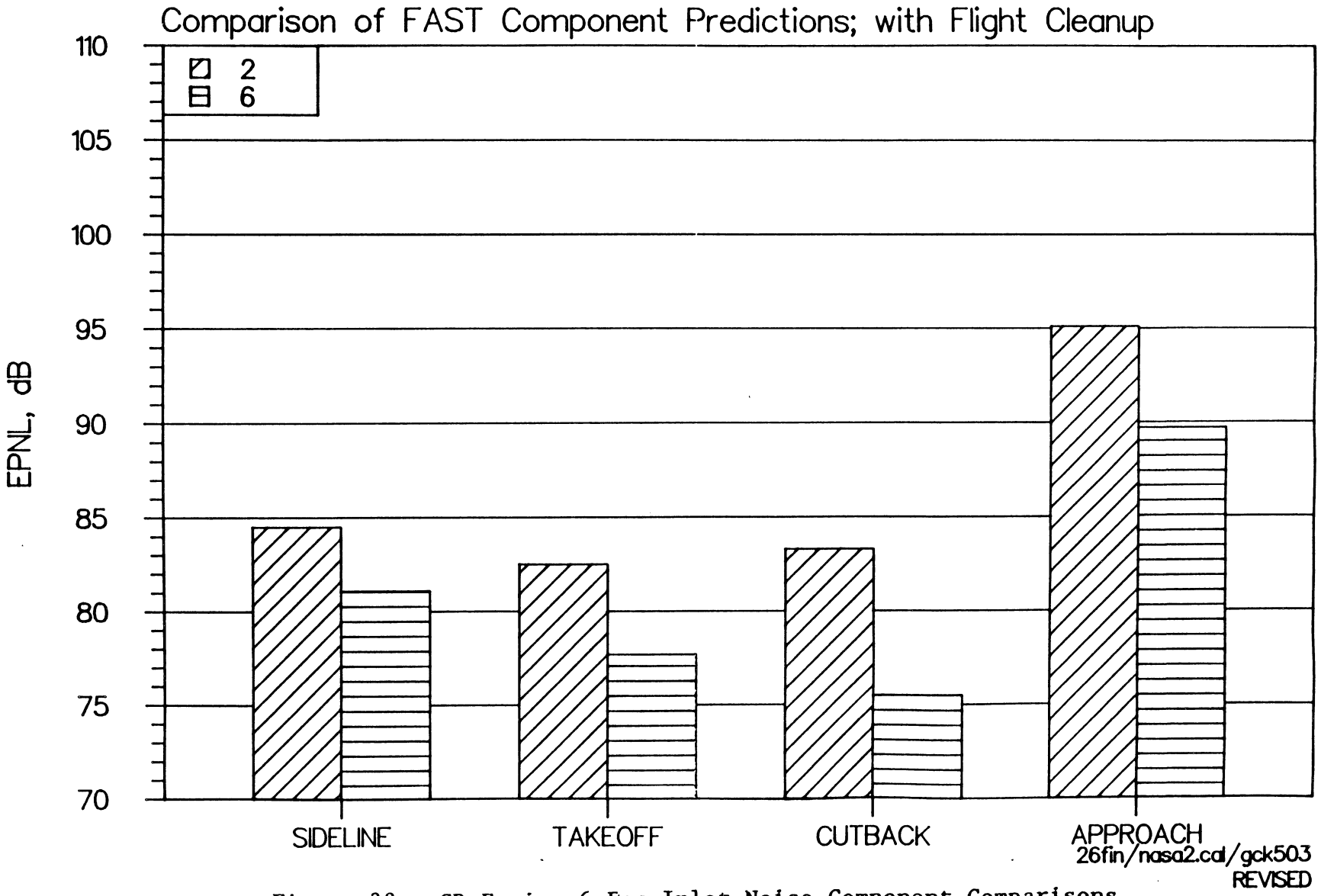

Figure 38 CR Engine 6 Fan Inlet Noise Component Comparisons

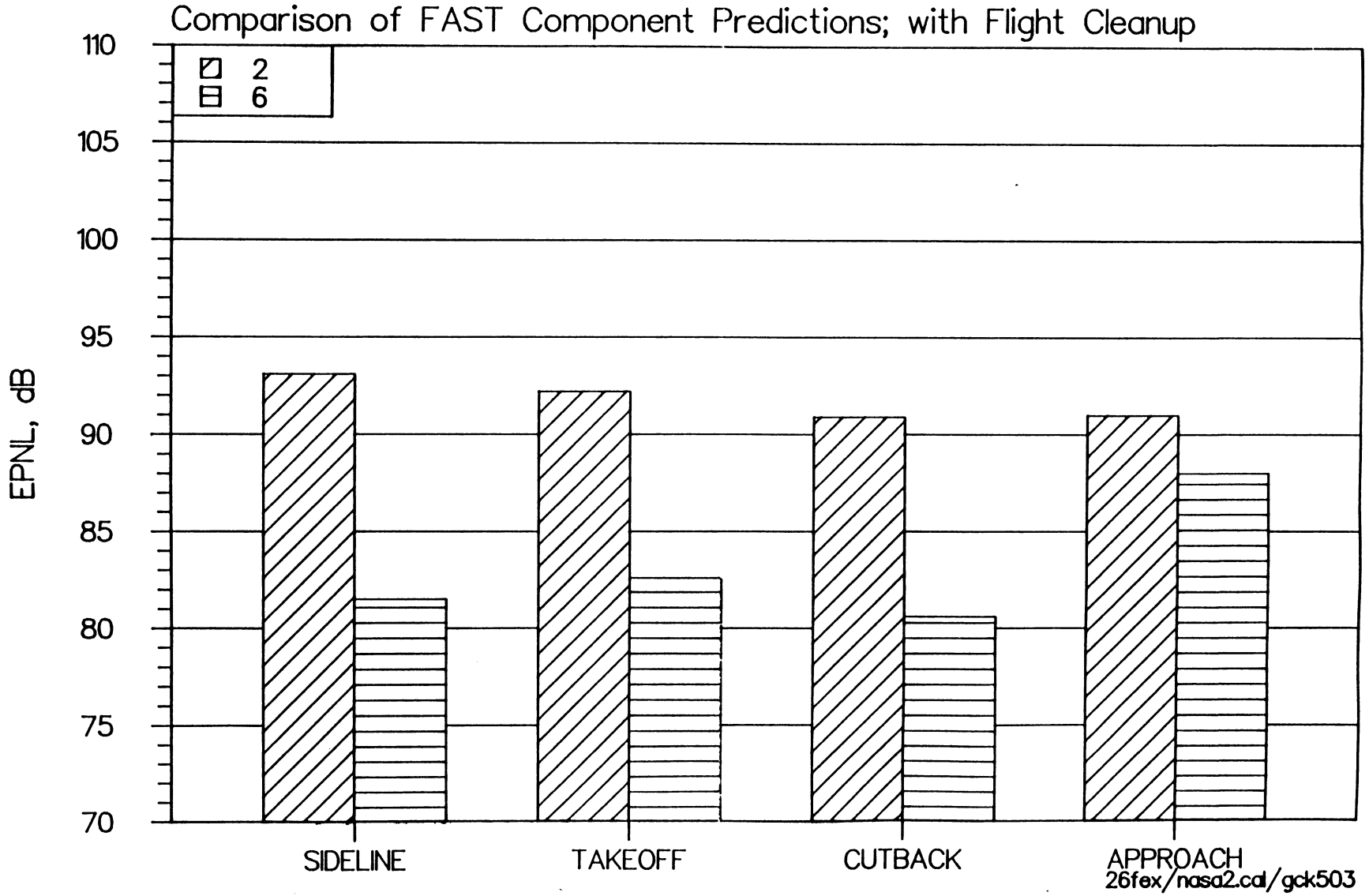

Figure 39 CR Engine 6 Fan Exhaust Noise Component Comparisons

SUMMARY – SIDELINE

150 FT ARC

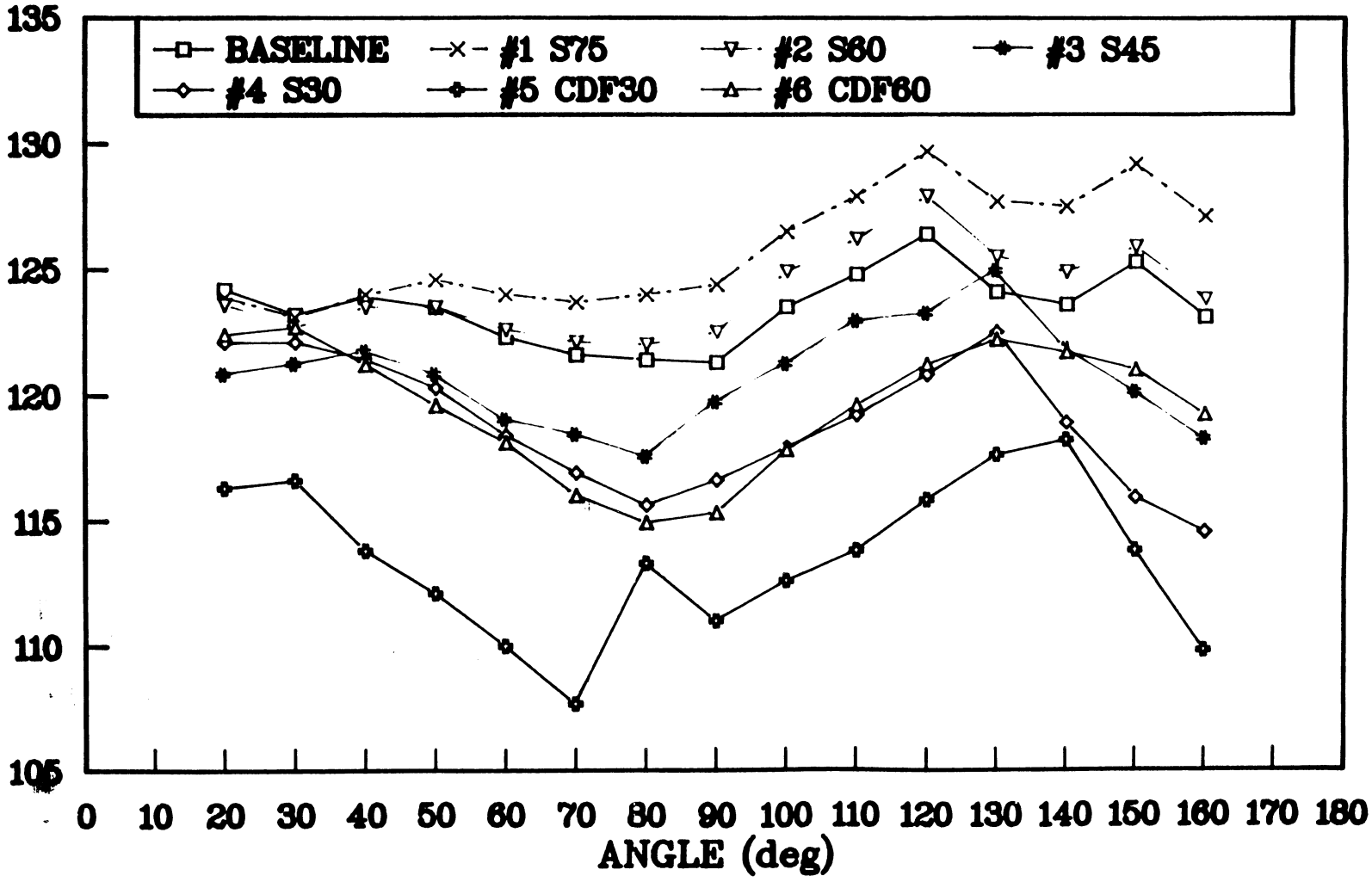

SUMMARY – APPROACH

150 FT ARC

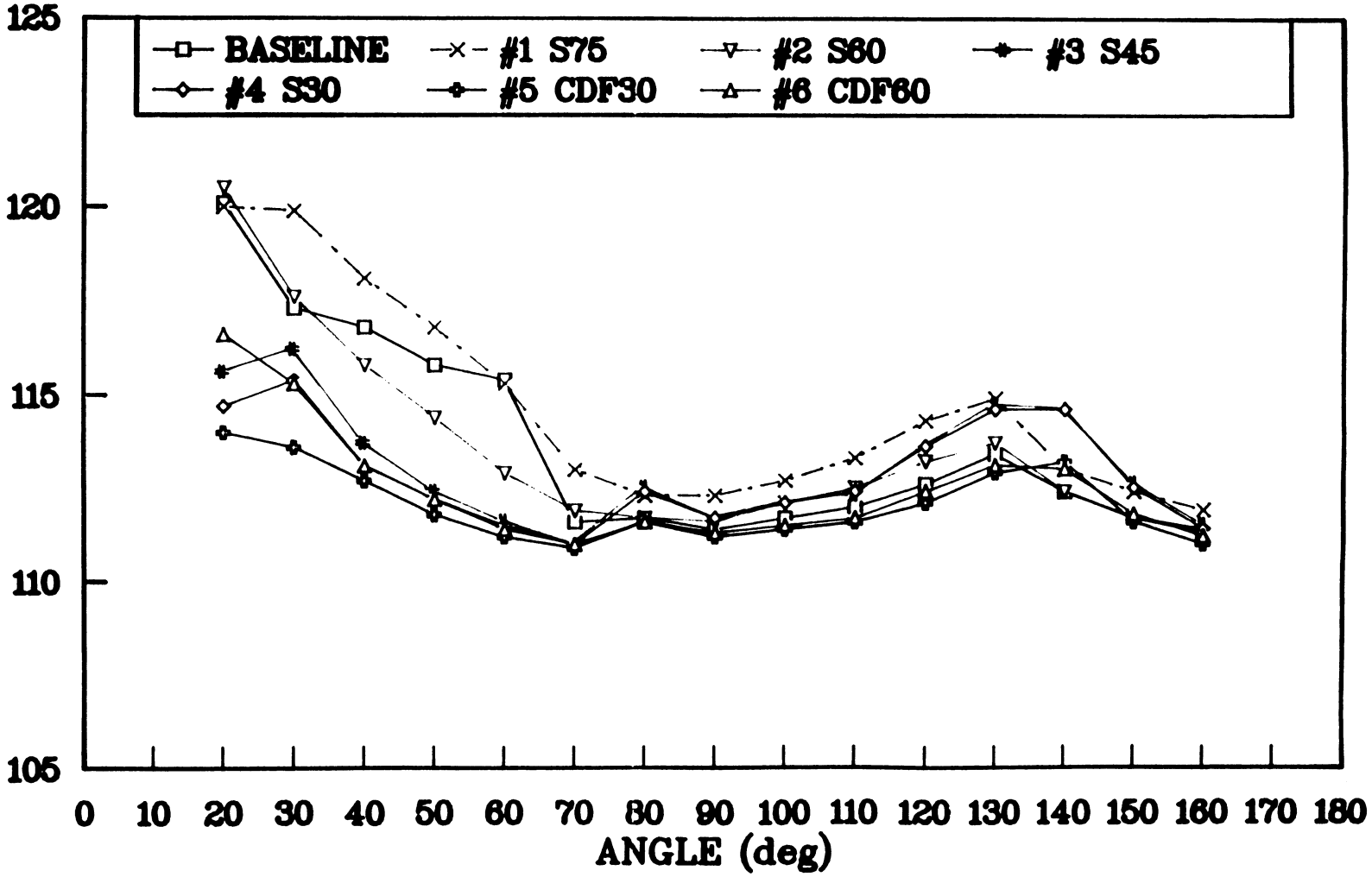

Figure 41 Approach PNLT Directivity Comparisons - All Engines

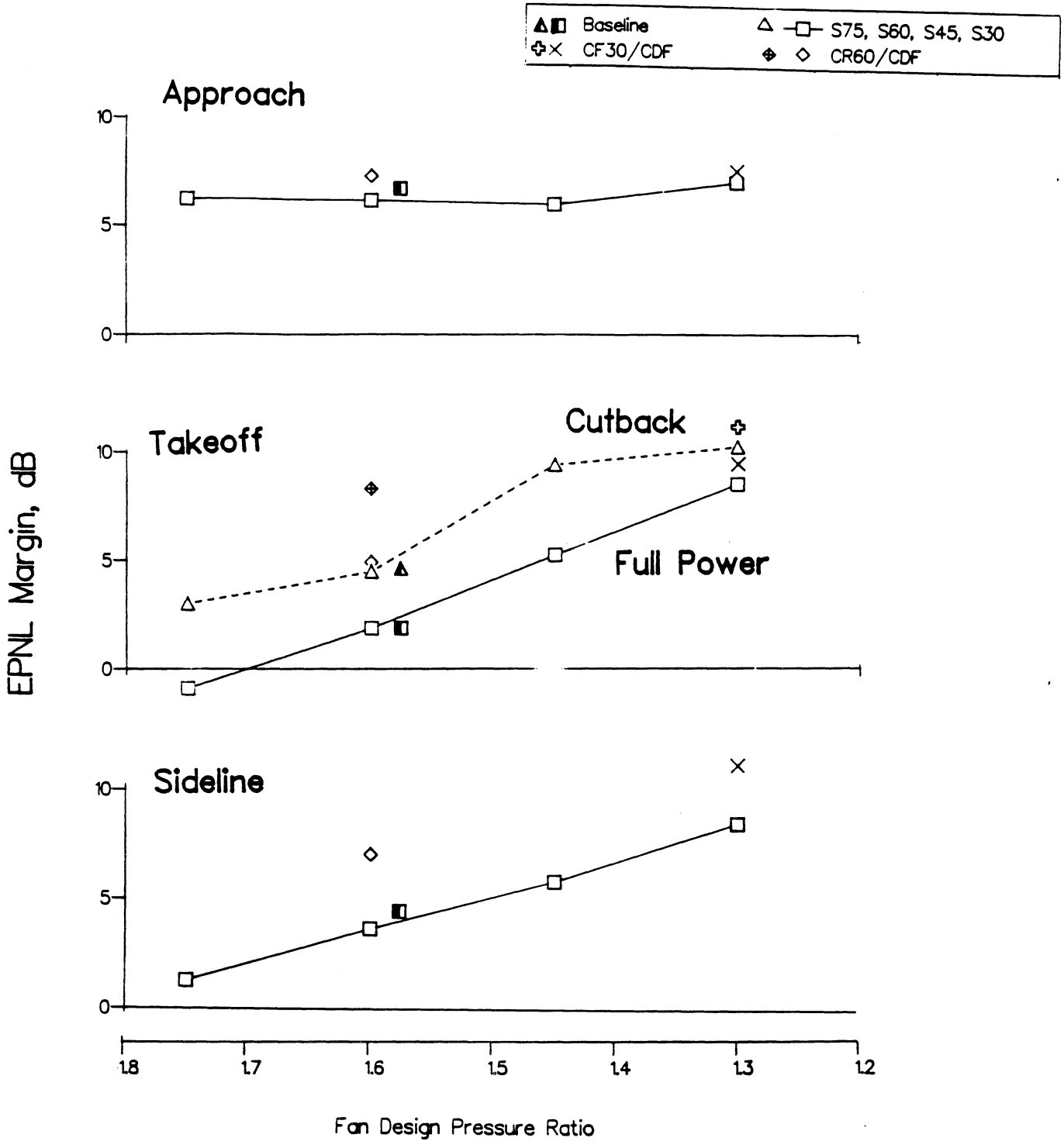

Figure 42 System EPNL Margins re: FAR36 Stage 3 - All Engines

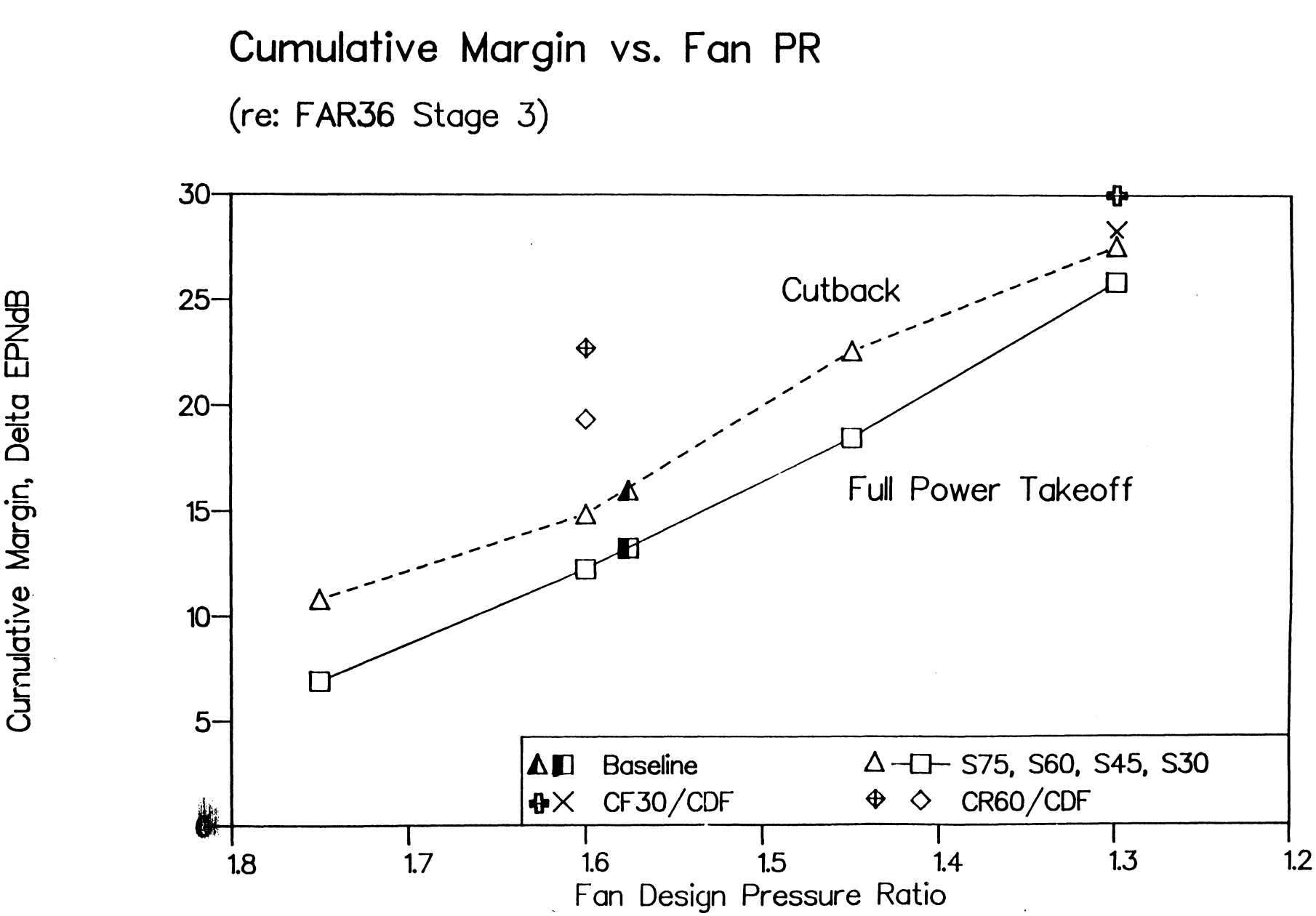

Figure 43 System Cummulative EPNL Margins re: Stage 3 - All Engines

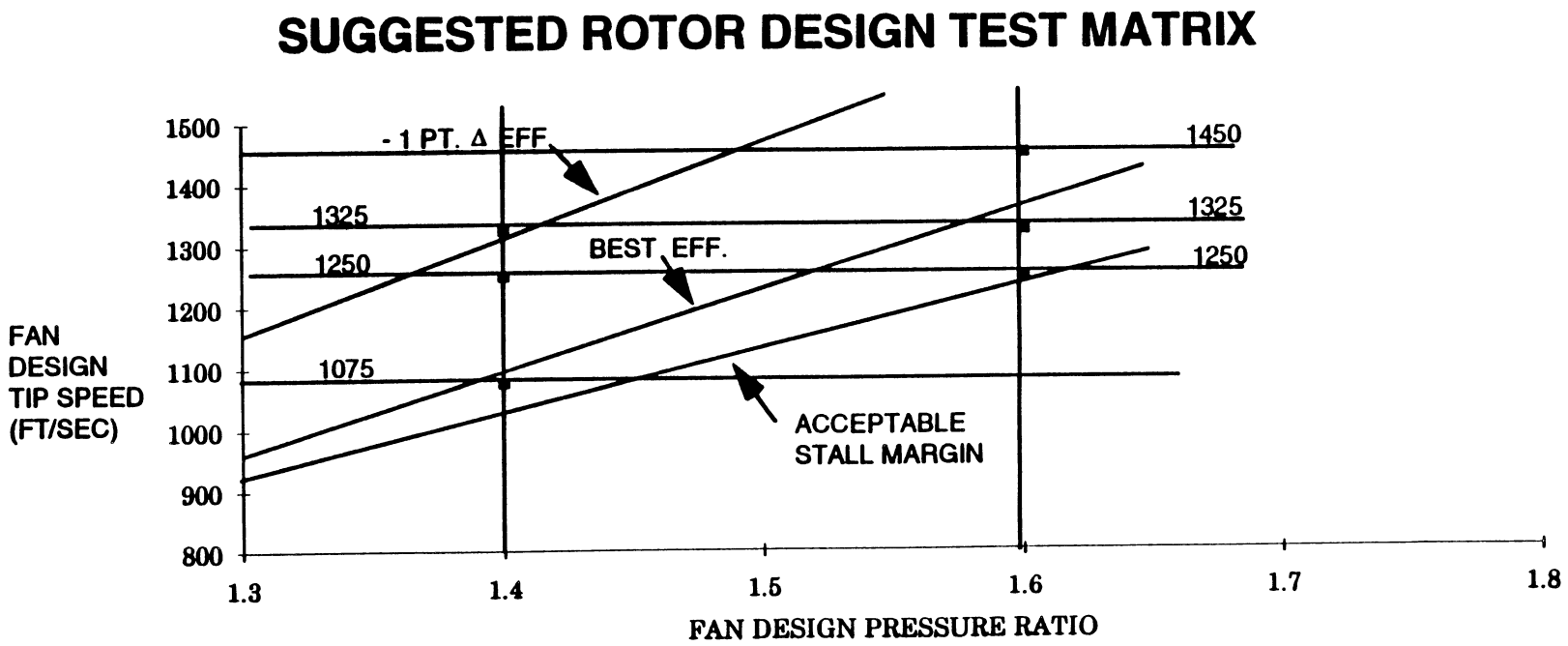

Figure 44 Suggested Scale Model Fan Test Configuration Matrix

APPENDIX A

ENGINE NOISE SOURCE COMPONENT CONTRIBUTIONS

This appendix contains the calculated engine noise source component contributions to the total system noise for each of the single-rotation engines studied. The counter-rotation engine components are given in the main body of the report for the components that are different, i.e., the fan inlet and exhaust components. For each engine, the component contributions to system EPNL are given in bar-graph form for Sideline, Full-power Takeoff, Cutback and Approach conditions. This is followed by two tone-corrected Perceived Noise Level (PNLT) directivity pattern plots, showing the component contributions to the total engine noise. The first PNLT plot is for the sideline condition, and the second is for the approach condition, representing the two extremes in power setting. The graphs and plots are given in order for the baseline EEE engine, Engine 1, Engine 2, Engine 3, and Engine 4, respectively. Nomenclature for the component EPNL labels in the figures is given below.

AFN	Airframe noise component level
COM	Combustor noise component level
FEX	Fan exhaust noise component level
FIN	Fan inlet noise component level
JET	Jet exhaust noise component level (either CNJ or SFJ)
CNJ	Conical nozzle (mixed flow) jet noise component level
SFJ	Separate flow jet noise component level

Directivity Patterns

- 150 ft arc
- Single – engine
- Component contributions
- Sideline and approach

A.	Baseline ME^3	–	FPR = 1.58,	U_T = 1272 ft/sec
B.	Engine 1 (S75)	–	FPR = 1.75,	U_T = 1480 ft/sec
C.	Engine 2 (S60)	–	FPR = 1.60,	U_T = 1354 ft/sec
D.	Engine 3 (S45)	–	FPR = 1.45,	U_T = 1030 ft/sec
E.	Engine 4 (S30)	–	FPR = 1.30,	UT = 984 ft/sec

FIGURE A-1

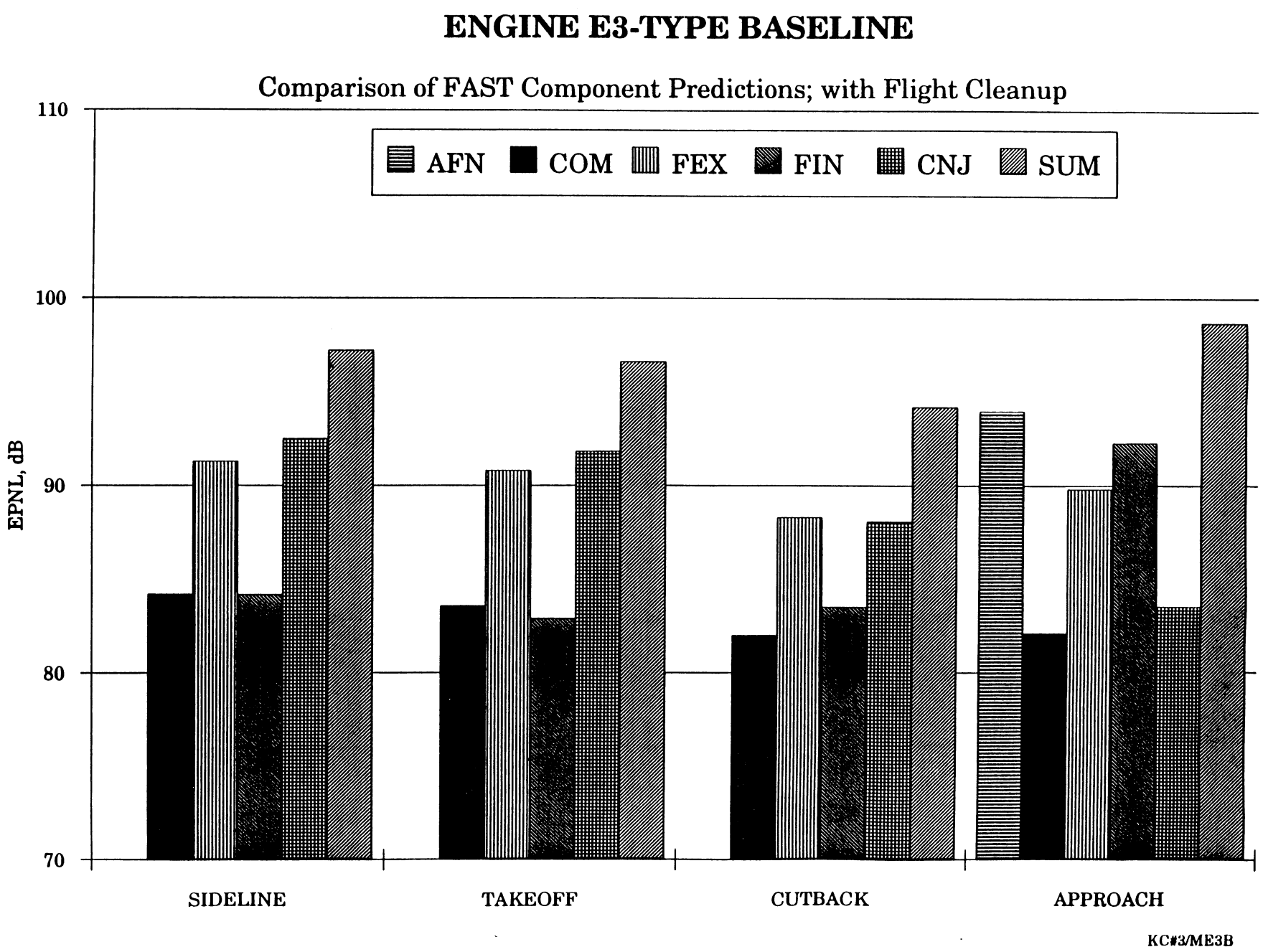
ENGINE E3-TYPE BASELINE
Comparison of FAST Component Predictions; with Flight Cleanup
AFN
COM
FEX
FIN
CNJ
SUM
EPNL, dB
110
100
90
80
70
SIDELINE
TAKEOFF
CUTBACK
APPROACH
KC#3/ME3B

FIGURE A-2

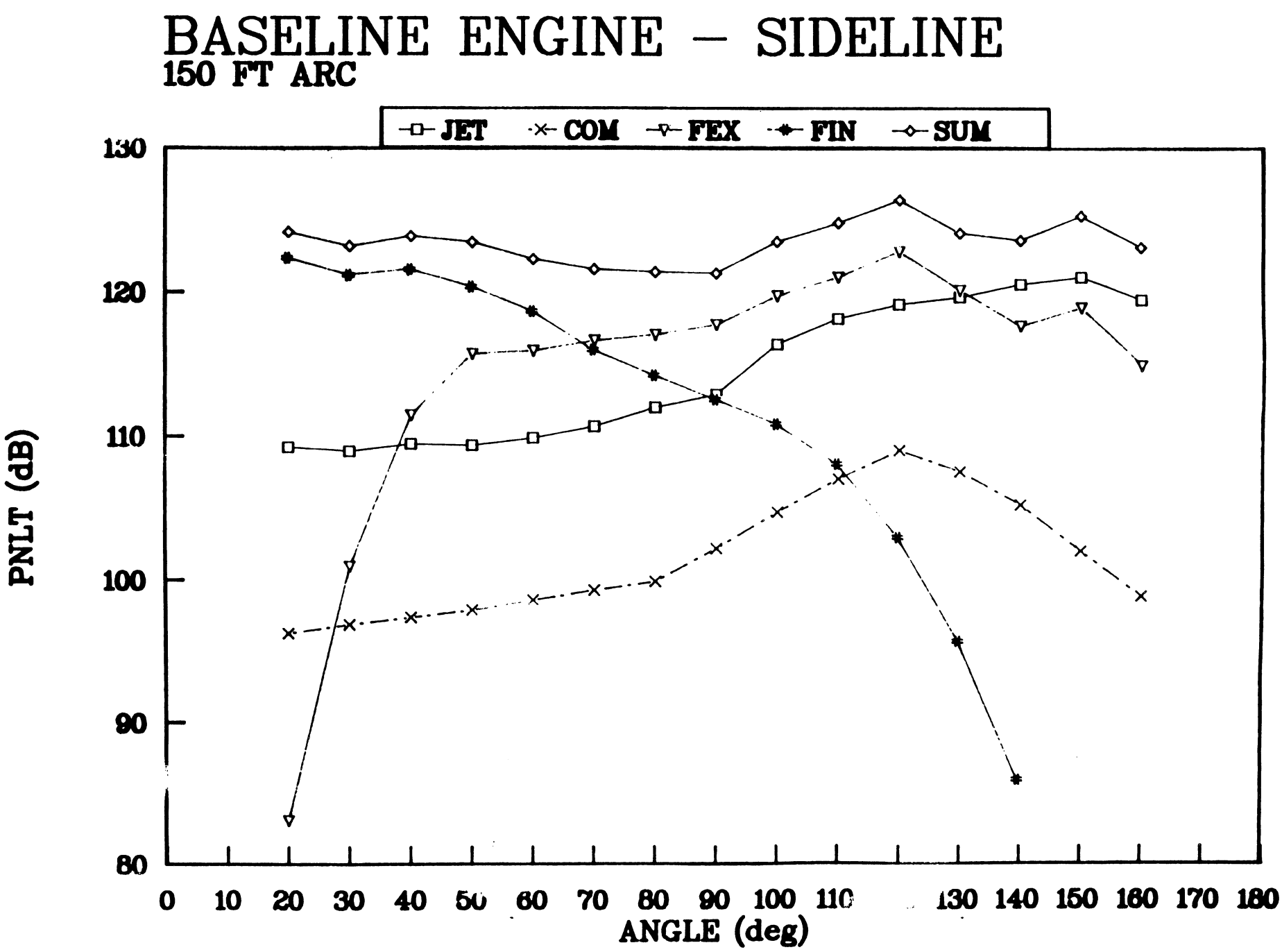
BASELINE ENGINE – SIDELINE
150 FT ARC
JET
COM
FEX
FIN
SUM
PNLT (dB)
130
120
110
100
90
80
0
10
20
30
40
50
60
70
80
90
100
110
130
140
150
160
170
180
ANGLE (deg)

FIGURE A-3

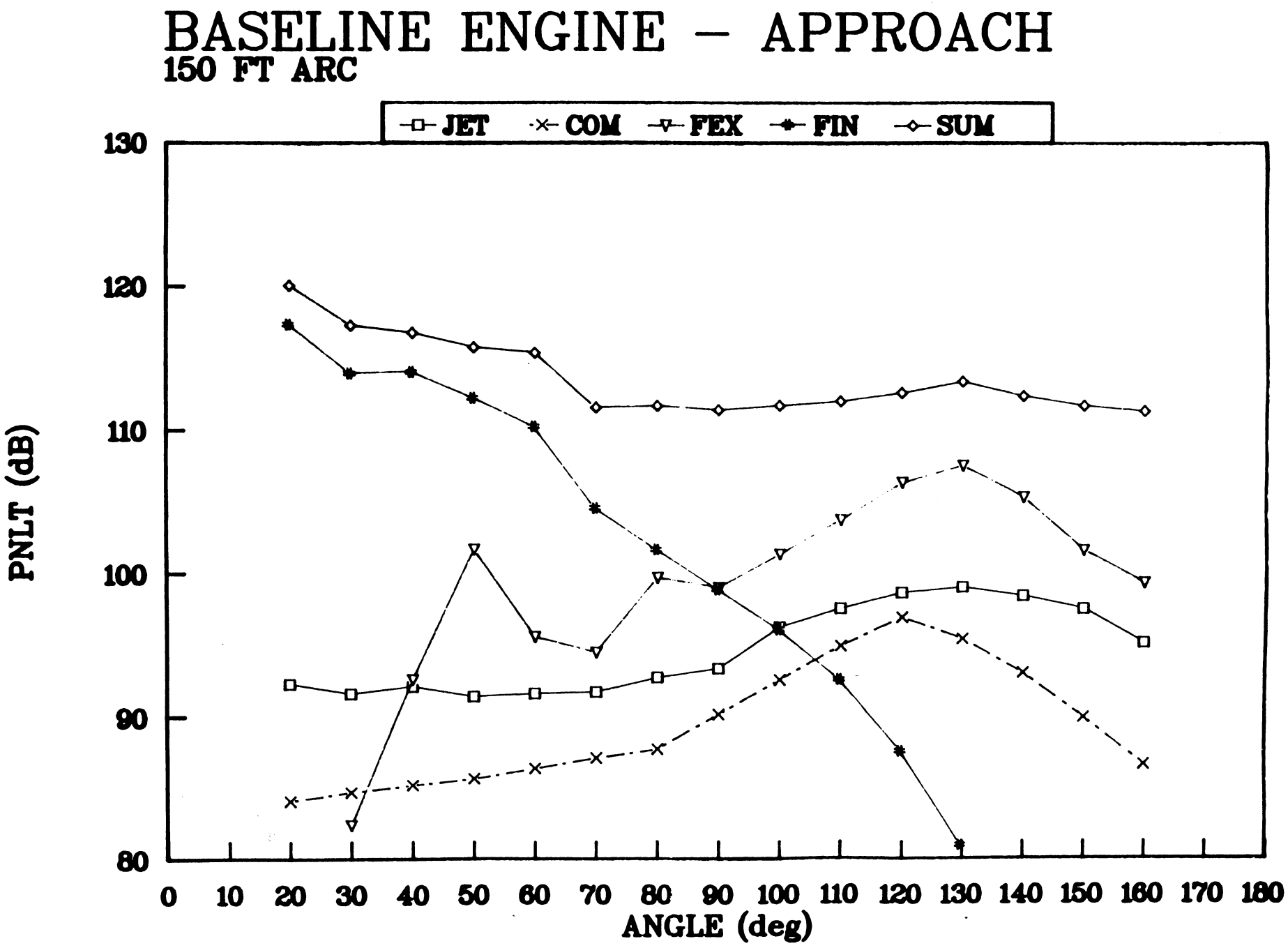
BASELINE ENGINE – APPROACH
150 FT ARC
JET
COM
FEX
FIN
SUM
PNLT (dB)
130
120
110
100
90
80
0
10
20
30
40
50
60
70
80
90
100
110
120
130
140
150
160
170
180
ANGLE (deg)

FIGURE A-4

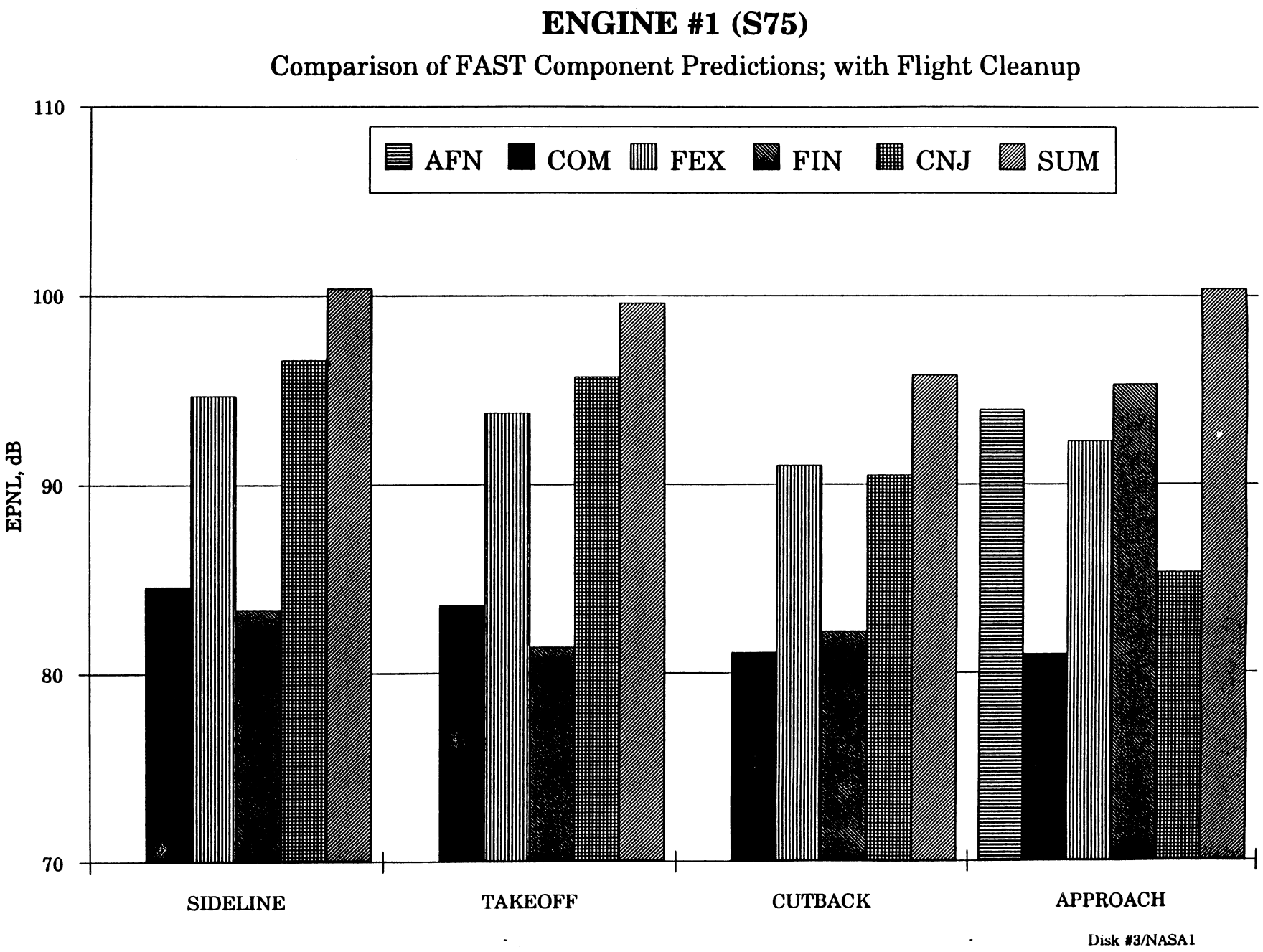
ENGINE #1 (S75)
Comparison of FAST Component Predictions; with Flight Cleanup
AFN
COM
FEX
FIN
CNJ
SUM
EPNL, dB
110
100
90
80
70
SIDELINE
TAKEOFF
CUTBACK
APPROACH
Disk #3/NASA1

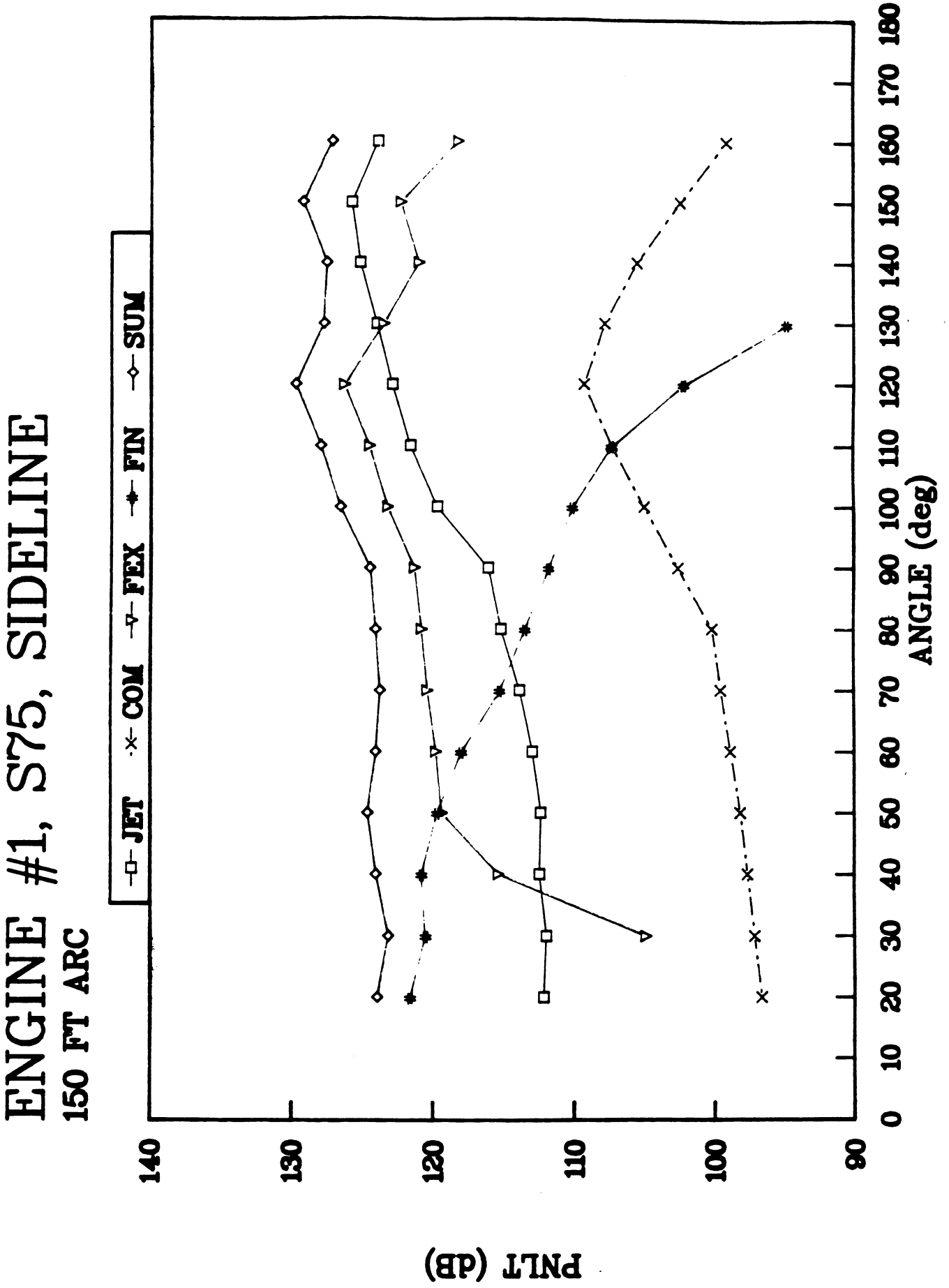
ENGINE #1, S75, SIDELINE
150 FT ARC
JET
COM
FEX
FIN
SUM
PNLT (dB)
ANGLE (deg)
140
130
120
110
100
90
0
10
20
30
40
50
60
70
80
90
100
110
120
130
140
150
160
170
180

FIGURE A-5

FIGURE A-6

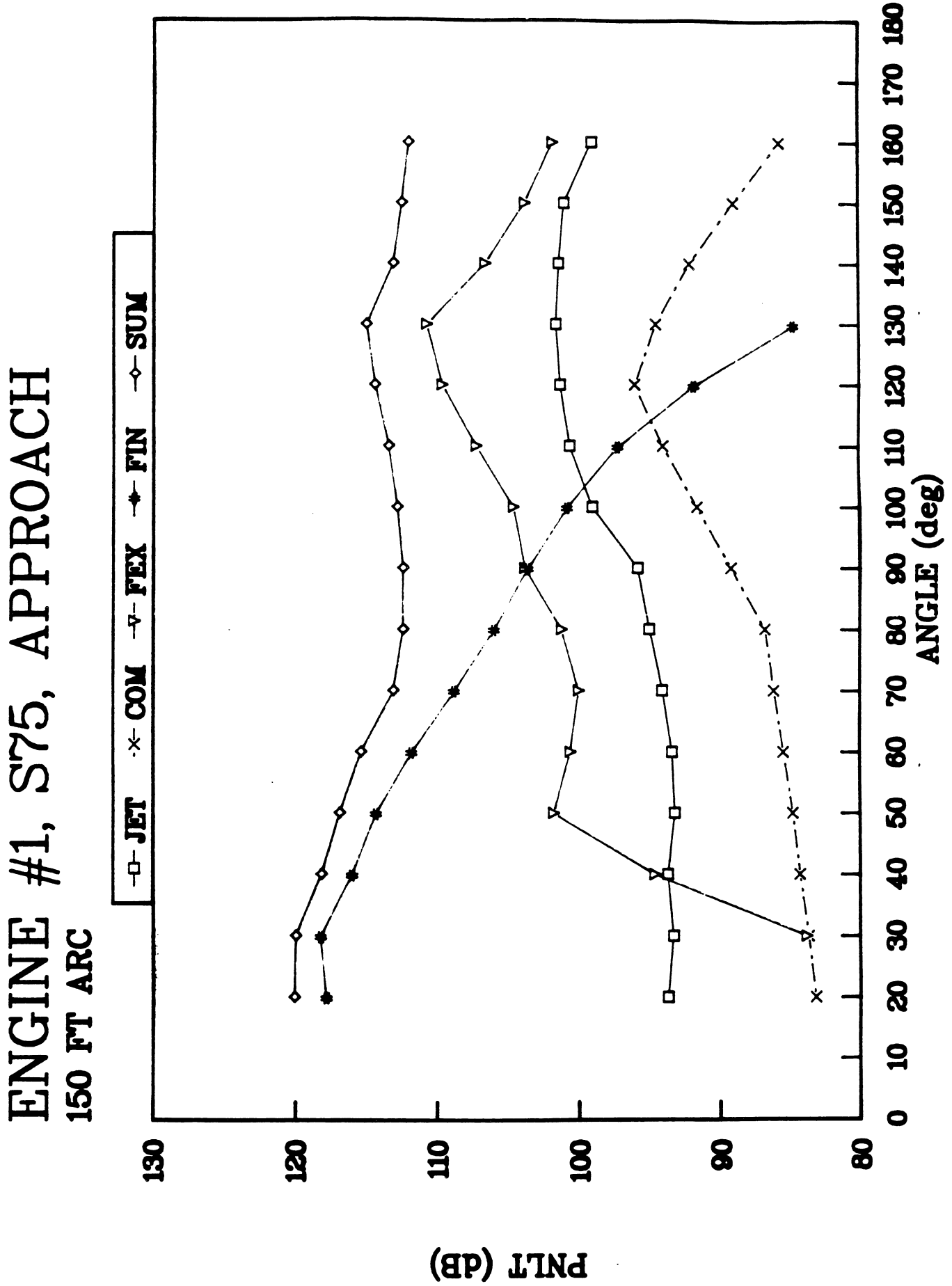
ENGINE #1, S75, APPROACH
150 FT ARC
JET
COM
FEX
FIN
SUM
PNLT (dB)
ANGLE (deg)
130
120
110
100
90
80
0
10
20
30
40
50
60
70
80
90
100
110
120
130
140
150
160
170
180

FIGURE A-7

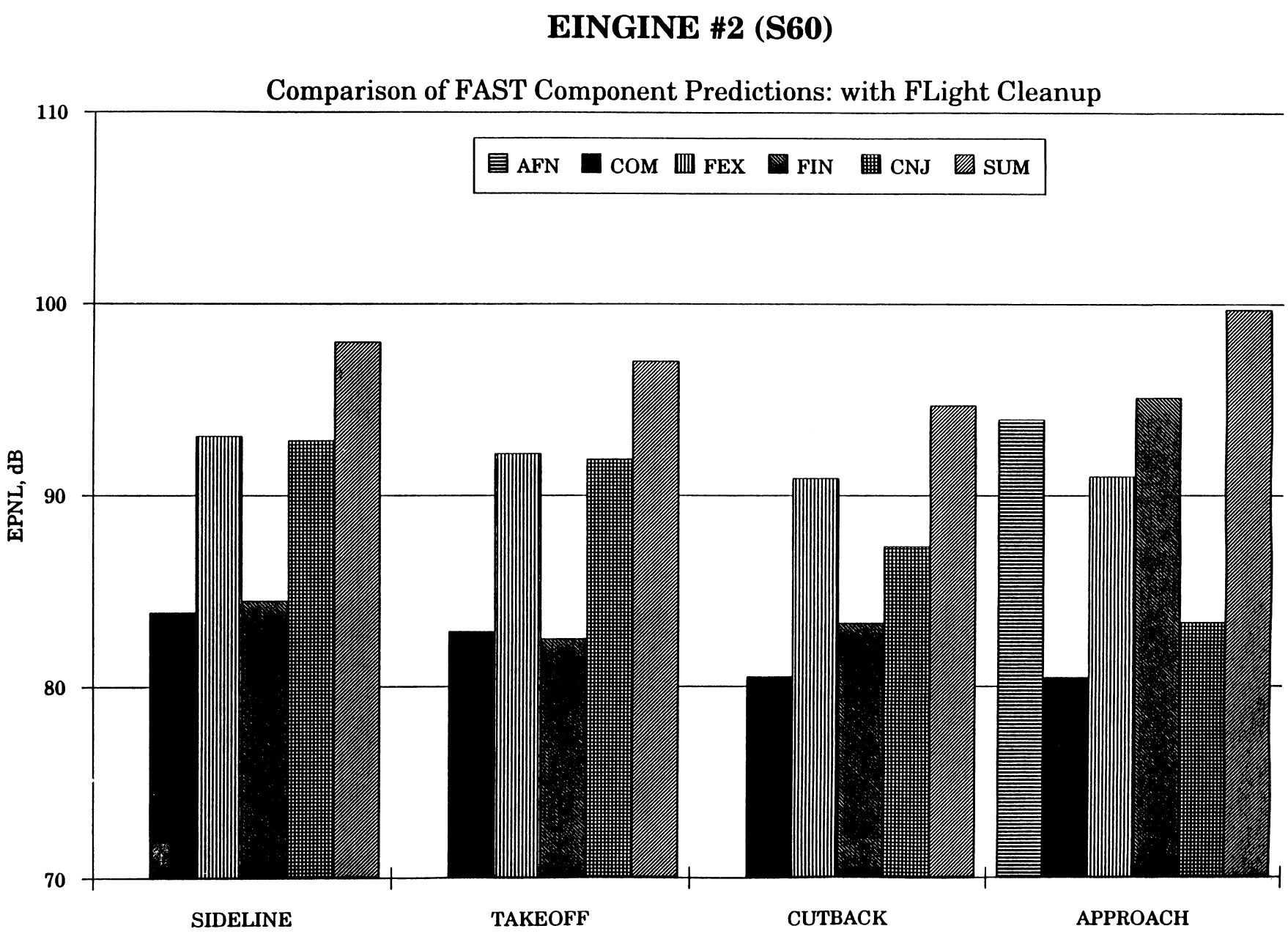
EINGINE #2 (S60)
Comparison of FAST Component Predictions: with FLight Cleanup
AFN
COM
FEX
FIN
CNJ
SUM
EPNL, dB
110
100
90
80
70
SIDELINE
TAKEOFF
CUTBACK
APPROACH

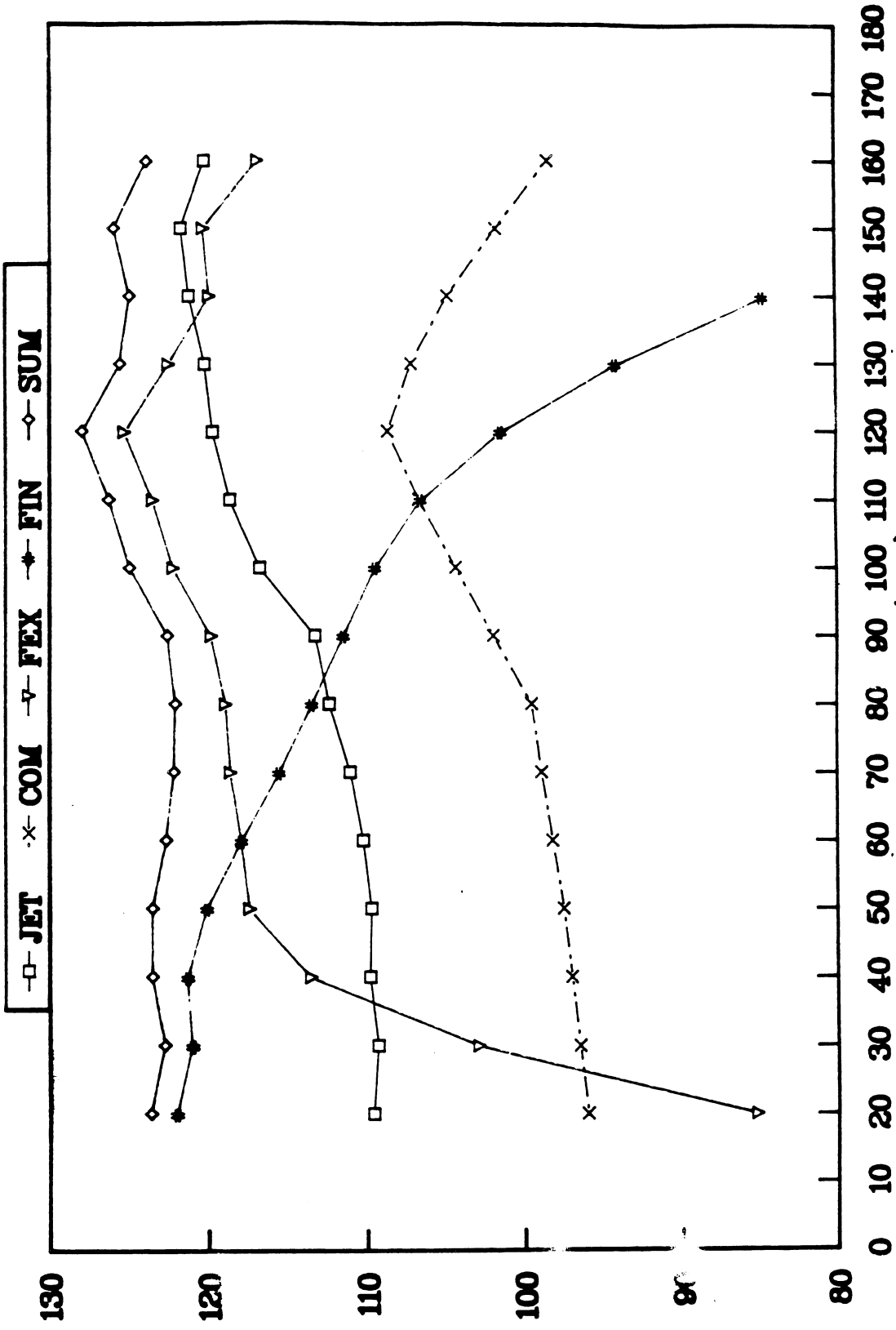
ENGINE #2, S60, SIDELINE
150 FT ARC
JET
COM
FEX
FIN
SUM
PNLT (dB)
ANGLE (deg)
130
120
110
100
80
0
10
20
30
40
50
60
70
80
90
100
110
120
130
140
150
160
170
180

FIGURE A-8

FIGURE A-9

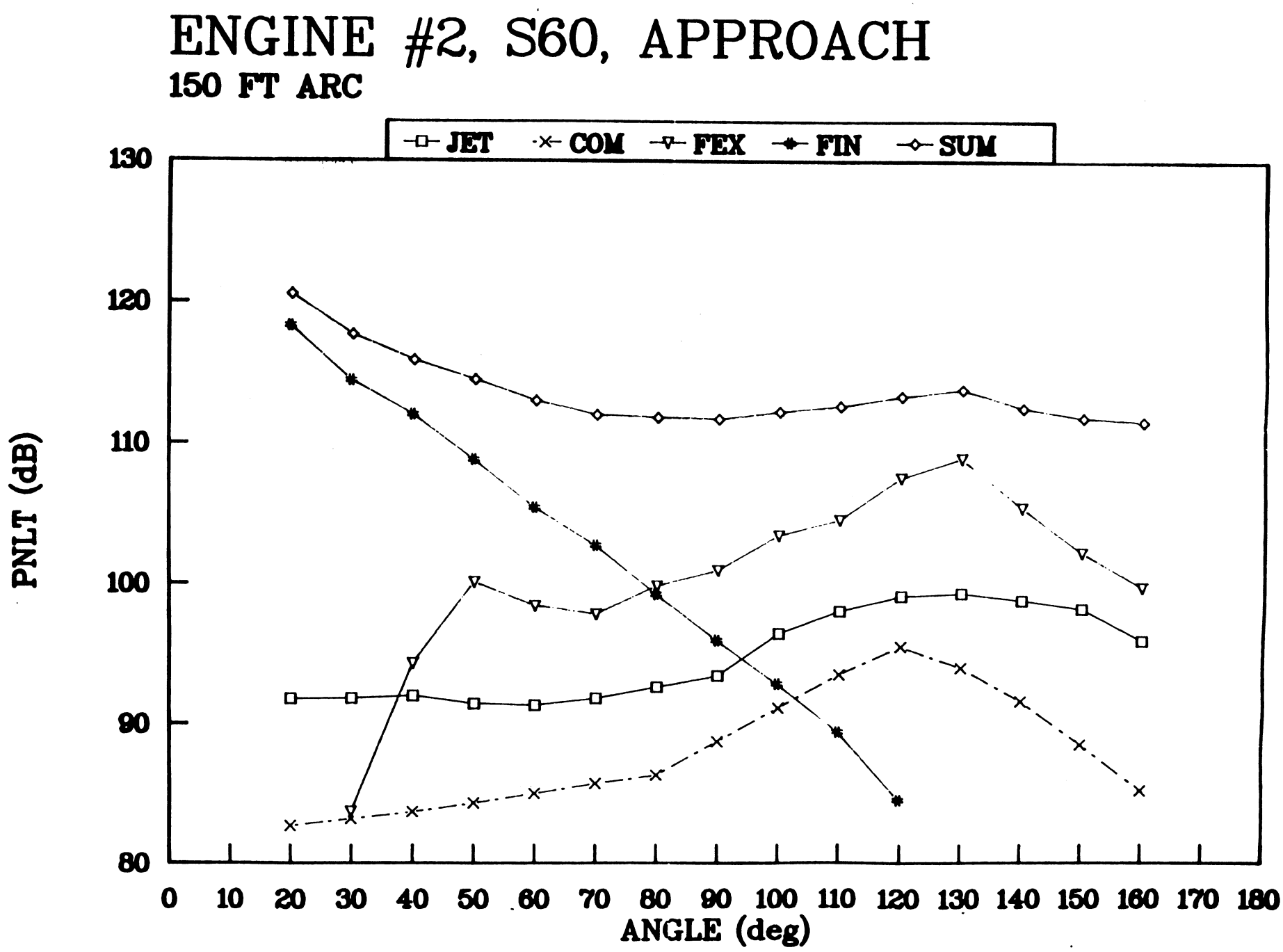
ENGINE #2, S60, APPROACH
150 FT ARC
JET
COM
FEX
FIN
SUM
PNLT (dB)
130
120
110
100
90
80
0
10
20
30
40
50
60
70
80
90
100
110
120
130
140
150
160
170
180
ANGLE (deg)

FIGURE A-10

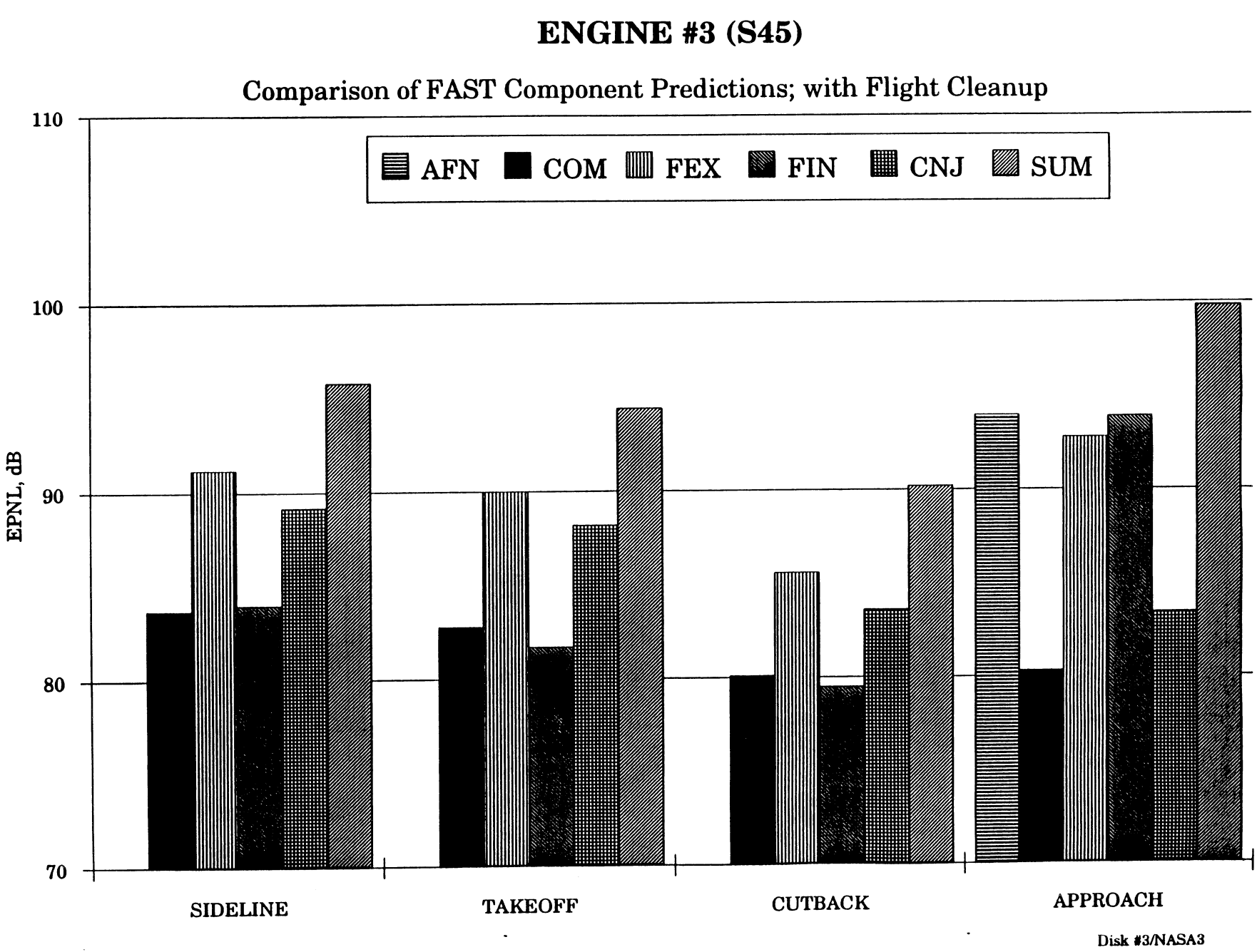
ENGINE #3 (S45)
Comparison of FAST Component Predictions; with Flight Cleanup
AFN
COM
FEX
FIN
CNJ
SUM
EPNL, dB
110
100
90
80
70
SIDELINE
TAKEOFF
CUTBACK
APPROACH
Disk #3/NASA3

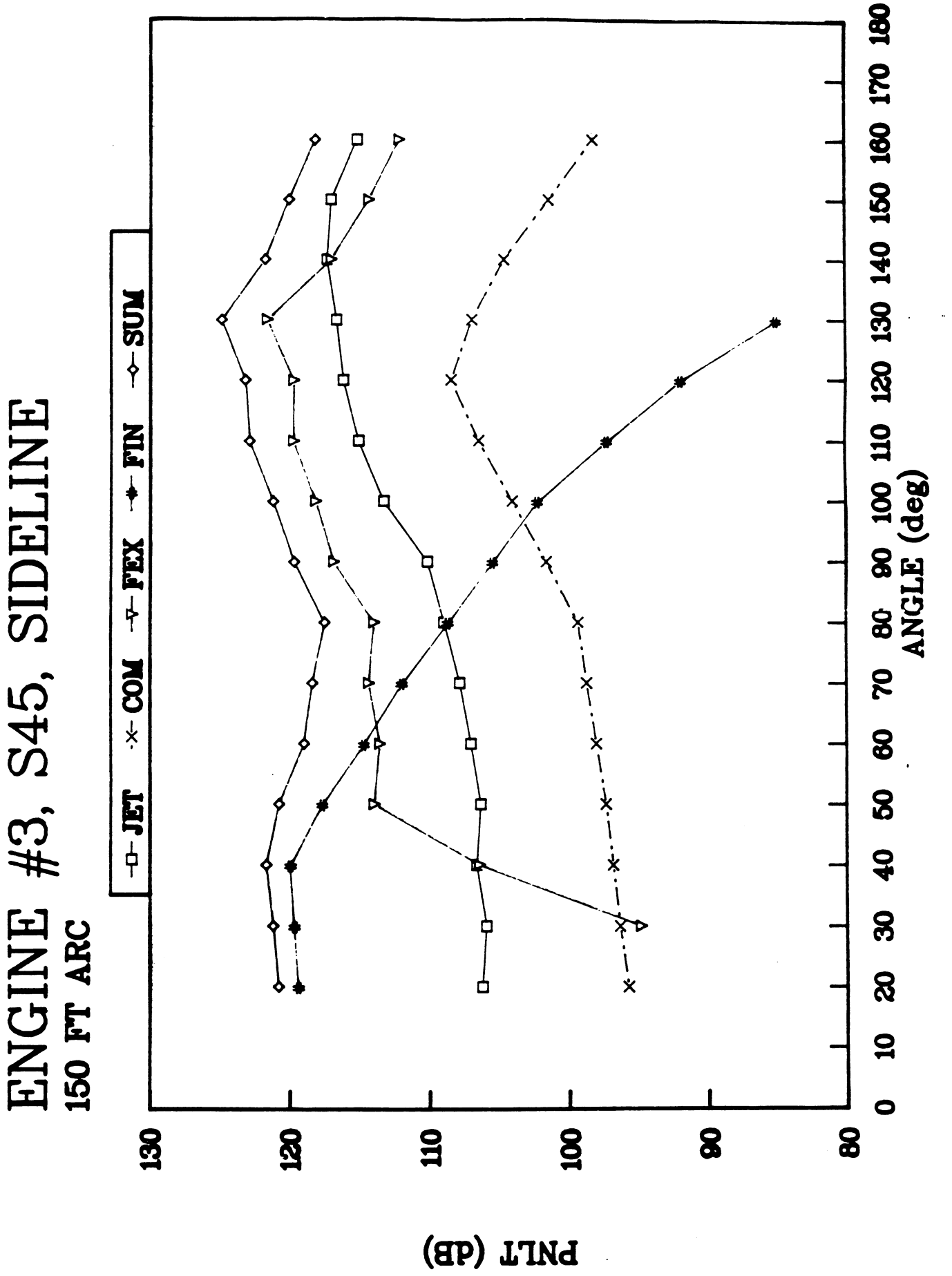
ENGINE #3, S45, SIDELINE
150 FT ARC
JET
COM
FEX
FIN
SUM
PNLT (dB)
ANGLE (deg)
130
120
110
100
90
80
0
10
20
30
40
50
60
70
80
90
100
110
120
130
140
150
160
170
180

FIGURE A-11

FIGURE A-12

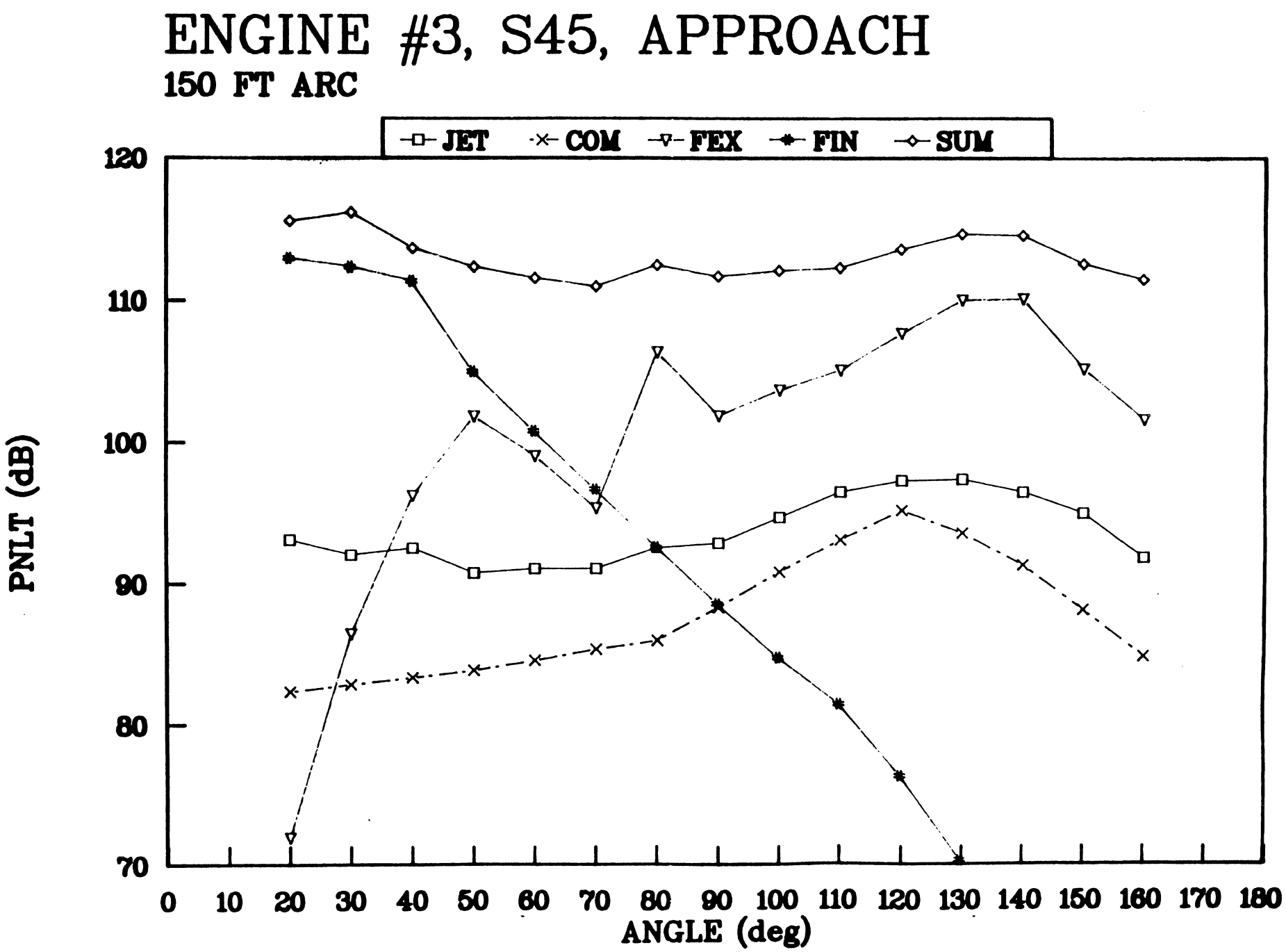
ENGINE #3, S45, APPROACH
150 FT ARC
JET
COM
FEX
FIN
SUM
PNLT (dB)
120
110
100
90
80
70
0
10
20
30
40
50
60
70
80
90
100
110
120
130
140
150
160
170
180
ANGLE (deg)

FIGURE A-13

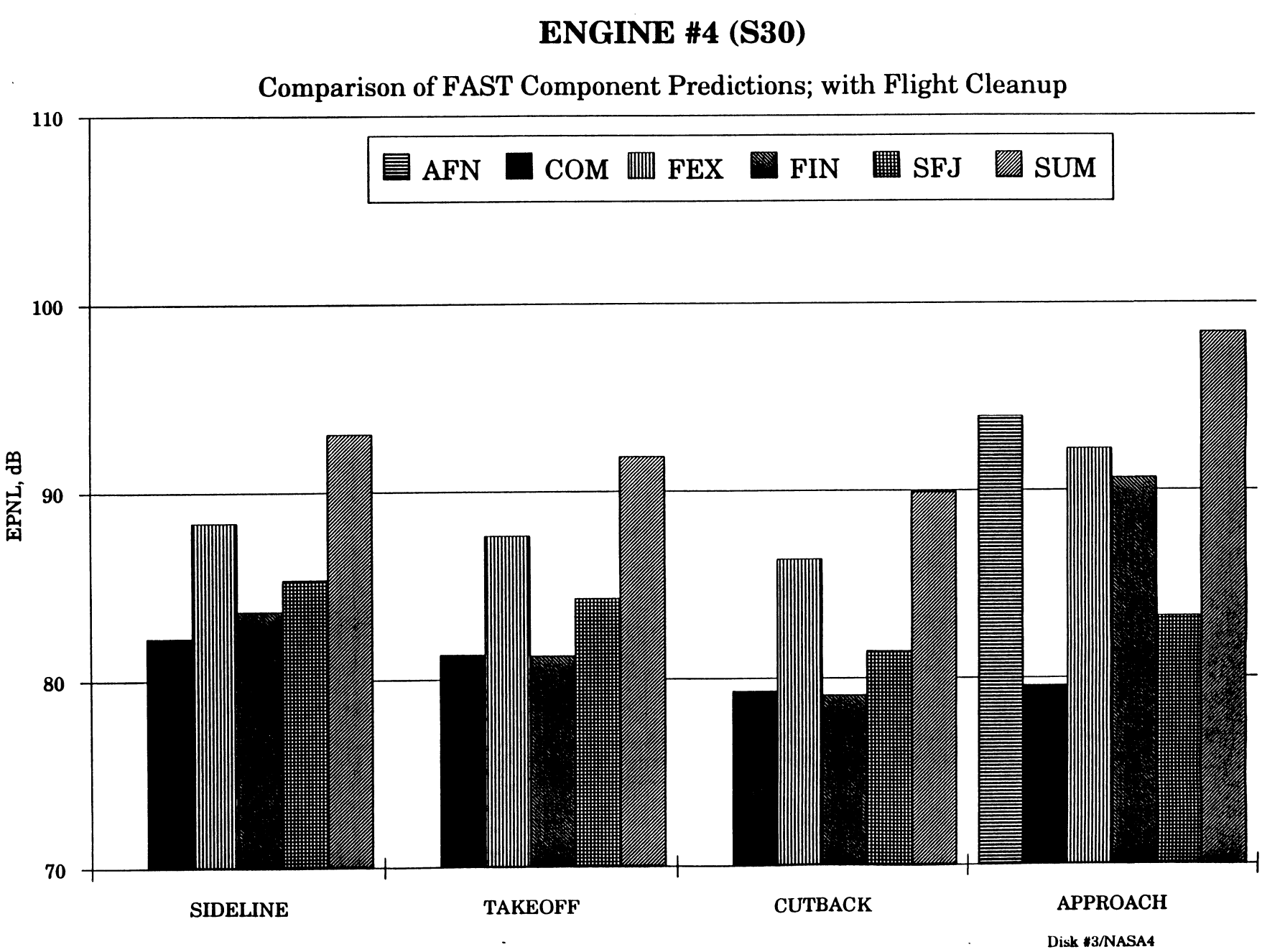
ENGINE #4 (S30)
Comparison of FAST Component Predictions; with Flight Cleanup
AFN
COM
FEX
FIN
SFJ
SUM
EPNL, dB
110
100
90
80
70
SIDELINE
TAKEOFF
CUTBACK
APPROACH
Disk #3/NASA4

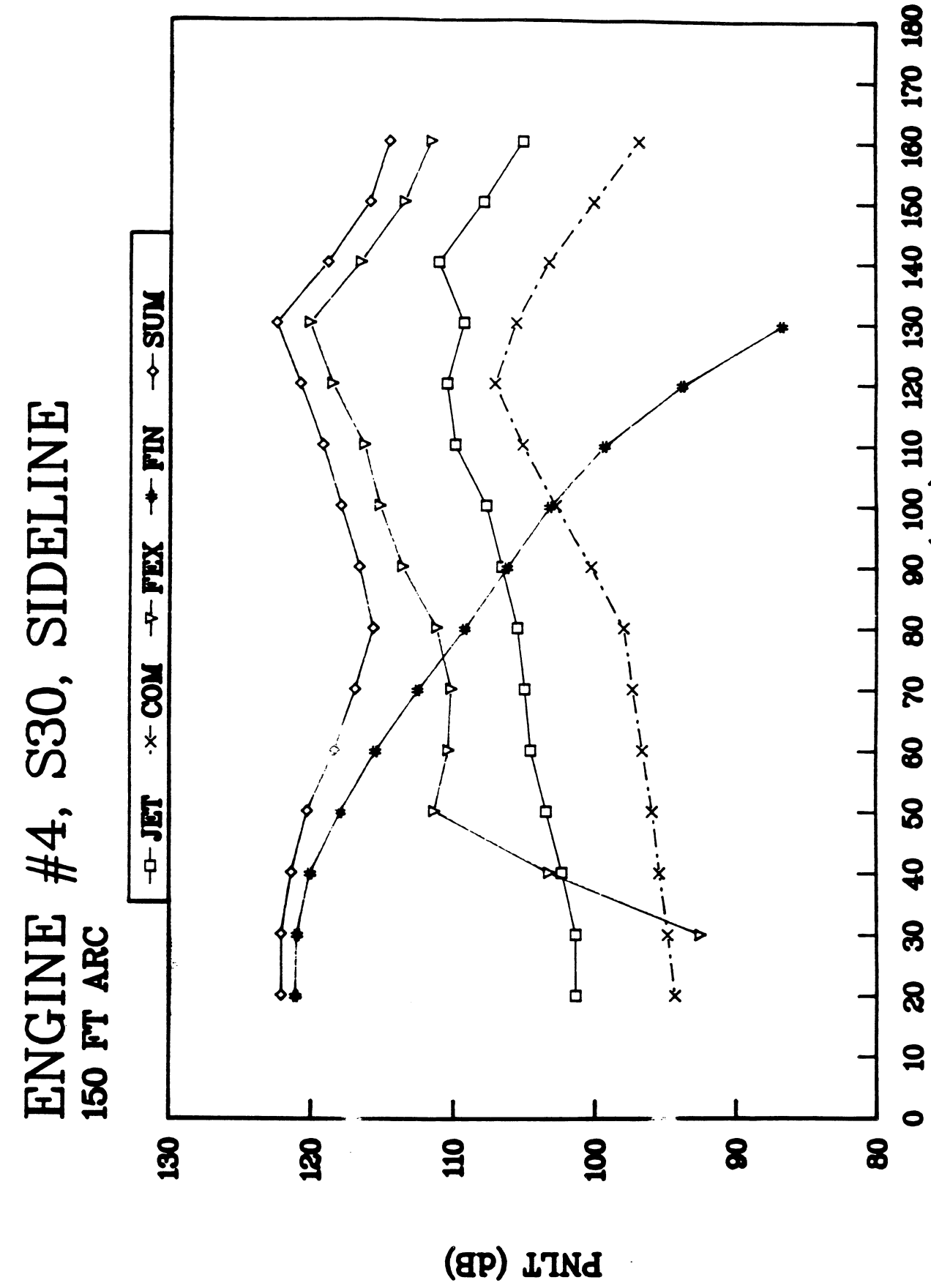
ENGINE #4, S30, SIDELINE
150 FT ARC
JET
COM
FEX
FIN
SUM
PNLT (dB)
ANGLE (deg)
130
120
110
100
90
80
0
10
20
30
40
50
60
70
80
90
100
110
120
130
140
150
160
170
180

FIGURE A-14

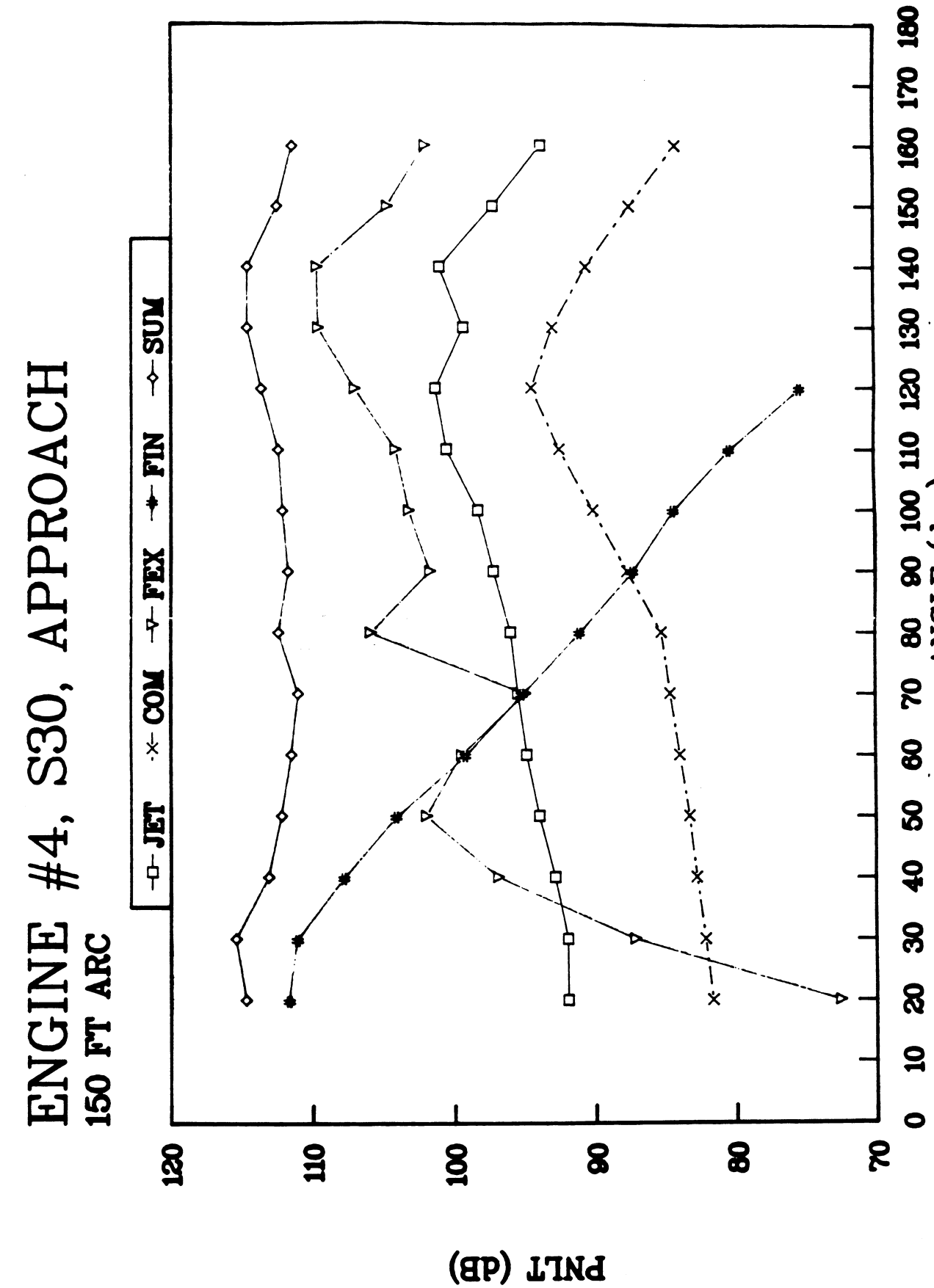
ENGINE #4, S30, APPROACH
150 FT ARC
JET
COM
FEX
FIN
SUM
PNLT (dB)
ANGLE (deg)
120
110
100
90
80
70
0
10
20
30
40
50
60
70
80
90
100
110
120
130
140
150
160
170
180

FIGURE A-15

REPORT DOCUMENTATION PAGE

Form Approved
OMB No. 0704-0188

1. AGENCY USE ONLY (*Leave blank*)	2. REPORT DATE	3. REPORT TYPE AND DATES COVERED
	October 2003	Final Contractor Report

4. TITLE AND SUBTITLE

Ultra-High Bypass Engine Aeroacoustic Study

5. FUNDING NUMBERS

WBS–22–781–30–12
NAS3–25269, Task Order 4

6. AUTHOR(S)

Philip R. Gliebe and Bangalore A. Janardan

7. PERFORMING ORGANIZATION NAME(S) AND ADDRESS(ES)

GE Aircraft Engines
Advanced Engineering Programs Department
1 Neumann Way, Mail Drop A304
Cincinnati, Ohio 45215

8. PERFORMING ORGANIZATION REPORT NUMBER

E–14087

9. SPONSORING/MONITORING AGENCY NAME(S) AND ADDRESS(ES)

National Aeronautics and Space Administration
Washington, DC 20546–0001

10. SPONSORING/MONITORING AGENCY REPORT NUMBER

NASA CR—2003-212525

11. SUPPLEMENTARY NOTES

Project Manager, James H. Dittmar (retired). Responsible person, Dennis Huff, Structures and Acoustics Division, NASA Glenn Research Center, organization code 5940, 216–433–3913.

12a. DISTRIBUTION/AVAILABILITY STATEMENT

Unclassified - Unlimited
Subject Category: 07 Distribution: Nonstandard

Available electronically at http://gltrs.grc.nasa.gov

This publication is available from the NASA Center for AeroSpace Information, 301–621–0390.

12b. DISTRIBUTION CODE

13. ABSTRACT ***(Maximum 200 words)***

A system study was carried out to identify potential advanced aircraft engine concepts and cycles which could be capable of achieving a 5 to 10 EPNdB reduction in community noise level relative to current FAR36 Stage 3 limits for a typical large-capacity commercial transport aircraft. The study was directed toward large twin-engine aircraft applications in the 400,000 to 500,000 pound take-off gross weight class. Four single rotation fan engine designs with fan pressure ratios from 1.3 to 1.75, and two counter-rotating fan engine configurations were studied. Several engine configurations were identified which, with further technology development, could achieve the objective of 5 to 10 EPNdB noise reduction. Optimum design fan pressure ratio is concluded to be in the range of 1.4 to 1.55 for best noise reduction with acceptable weight and Direct Operating Cost (DOC) penalties.

14. SUBJECT TERMS

Engine noise reduction; Turbofan engines; Ultra high bypass ratio; Fans; Aerodynamics; Aeroacoustics

15. NUMBER OF PAGES

110

16. PRICE CODE

17. SECURITY CLASSIFICATION OF REPORT	18. SECURITY CLASSIFICATION OF THIS PAGE	19. SECURITY CLASSIFICATION OF ABSTRACT	20. LIMITATION OF ABSTRACT
Unclassified	Unclassified	Unclassified	